Doctor of Philosophy Degree in Pharmacy

Pharmacological mechanism underlying anti-inflammatory, anti-nociceptive and neuroprotective activities of anomalin and capillarisin

August 2013

College of Pharmacy

Seoul National University

Salman Khan

ABSTRACT

In our continuous search for novel anti-inflammatory and analgesic agents from traditional medicinal plants, *Saposhnikovia divaricata*, *Sesli resinosum*, *Leonurus japonicus* and *Artemisia capillaris* have been focused of our investigations. Anomalin, calipteryxin, (3´*S*,4´*S*)-3´, 4´-disenecioyloxy-3´,4´-dihydroseselin), 15, 16-epoxy-3α-hydroxylabda-8,13(16),14-trien-7-one and capillarisin are considered to exhibit anti-inflammatory activity. Based on significant anti-inflammatory effects, anomalin and capillarisin were studied in detail. To clarify the cellular signaling mechanisms underlying the anti-inflammatory action of anomalin and capillarisin, the effect of both the compounds were investigated on the production of inflammatory molecules in LPS-stimulated murin macrophages. Anomalin and capillarisin dose-dependently inhibited inducible nitric oxide synthase (iNOS) and cyclooxygenase-2 (COX-2) mRNA and protein expression levels in LPS-stimulated RAW 264.7 macrophages. Molecular analysis using quantitative real time polymerase chain reaction (qRT-PCR) revealed that several pro-inflammatory cytokines were reduced by anomalin and capillarisin, and this reduction correlated with the down-regulation of the NF-κB signaling pathway. Additionally, MAPKs and Akt pathways were also focused under investigation. The time course experimental results showed that both the compounds exhibited remarkable inhibitory effects on the activation of Akt and MAPKs proteins.

Due to the considerable anti-inflammatory effects of anomalin and capillarisin, CFA- and carrageenan-induced acute and chronic pain models were next focused. The animal models for anti-hyperalgesic and anti-allodynic effects revealed that anomalin and capillarisin significantly inhibited CFA- and carrageenan-induced pain by using Randall Selitto and Von Frey filaments. Another set of experiments observed that anomalin and capillarisin inhibited CFA- and

carrageenan-induced paw edema in acute and chronic models, and it did not cause any apparent toxicity. To elucidate the molecular mechanism underlying the anti-nociceptive effect of anomalin and capillarisin, various pain signaling pathways (NF-κB, CREB, and MAPKs/AP-1) that are involved were examined. Intraperitoneal pre-treatment of anomalin and capillarisin exhibited potent inhibitory effects on direct mediators of hyperalgesia (iNOS, COX-2 and MAPKs proteins). The release of CFA-induced plasma nitrite and paw tissue hyperalgesic cytokine (TNF-α) was reduced remarkably. Another signaling molecule, adenosine 5'-triphosphate (ATP) in plasma and substance P (SP) in paw tissue were markedly suppressed by anomalin and capillarisin. Moreover, *in vitro* experiment demonstrated that anomalin and capillarisin exhibited promising neuroprotective and anti-neuroinflammatory effects against sodium nitroprussid (SNP)-induced N2a neuroblastoma cells. Anomalin and capillarisin were observed remarkable inhibitory activity against STZ-induced type I diabetic animal neuropathic pain model. Hence, these results clearly demonstrated that anomalin and capillarisin showed substantial anti-inflammatory and analgesic effects in a consistent manner and their mechanisms involve the inhibition of the NF-κB, CREB, and MAPKs/AP-1 signaling pathways. Thus, the present study showed that anomalin and capillarisin could be developed for the management of acute and chronic inflammatory pain.

Keywords: Anomalin, Calipteryxin, (3´*S*,4´*S*)-3´,4´-Disenecioyloxy-3´,4´-dihydroseselin), 15,16-Epoxy-3α-hydroxylabda-8,13(16),14-trien-7-one, Capillarisin, Anti-inflammatory, Anti-nociceptive, Pain, Neuropathic, NF-κB, MAPKs, CFA, Carrageenan, STZ, Type I diabetes, RAW 264.7 cells, N2a cells.

Student Number: 2009-30772

CONTENTS

LIST OF FIGURES

LIST OF TABLES

PART I

Introduction

A. BACKGROUND

1. Inflammation

Inflammation can be defined as a complex body defense mechanism to respond to perilous endogenous or exogenous stimuli [1]. From a very early stage in phylogenesis, inflammation is associated with the host defense against infectious agents or injury. A variety of exogenous and endogenous mediators are capable of inducing inflammatory responses, such as microbial agents, toxins and pH changes. It leads to alters in tissue homeostasis, immune-cell activation and migration, and secretion of pro-inflammatory cytokines and mediators in a spatio-temporally coordinated manner [2]. Study on the molecular mechanisms of the inflammatory signaling has identified various mediators (enzymes, and cytokines), and protein kinases that play as fundamental signaling components, which represent potential therapeutic targets [3]. With regard to inflammation, the traditional features of this condition do not apply to the diseases in question. In previous reports, inflammation is expressed as the principal response of the body invoked to deal with injuries, and the hallmarks of which include typical symptoms (swelling, redness, pain and fever) [4]. This often short-term adaptive inflammatory response is an essential component of tissue repair and involves integration of several complex signals in distinct cells and organs **Fig. 1**.

Acute inflammation is typically suppressed after exclusion of pathogens and cellular debris [5]. However, in various diseases, such as rheumatoid arthritis, inflammatory bowel disease and bronchial asthma, a chronic inflammatory state is maintained, leading to local and systemic venomous effects on host cells and tissues. Generally, defects linked with

inflammation are observed in atherosclerosis, Alzheimer's disease, ischemic heart, brain diseases and cancer [1]. However, the long term consequences of prolonged inflammation are often not beneficial.

Chronic inflammation is generally treated by a variety of approaches [1]. Traditional and conventional treatments include fast-acting symptomatic agents (non-steroidal anti-inflammatory drugs (NSAIDs), glucocorticoids), slow-acting disease-modifying anti-rheumatic drugs (low-dose methotrexate), and cytostatic agents (azathioprine, cyclophosphamide and high-dose methotrexate) [1].

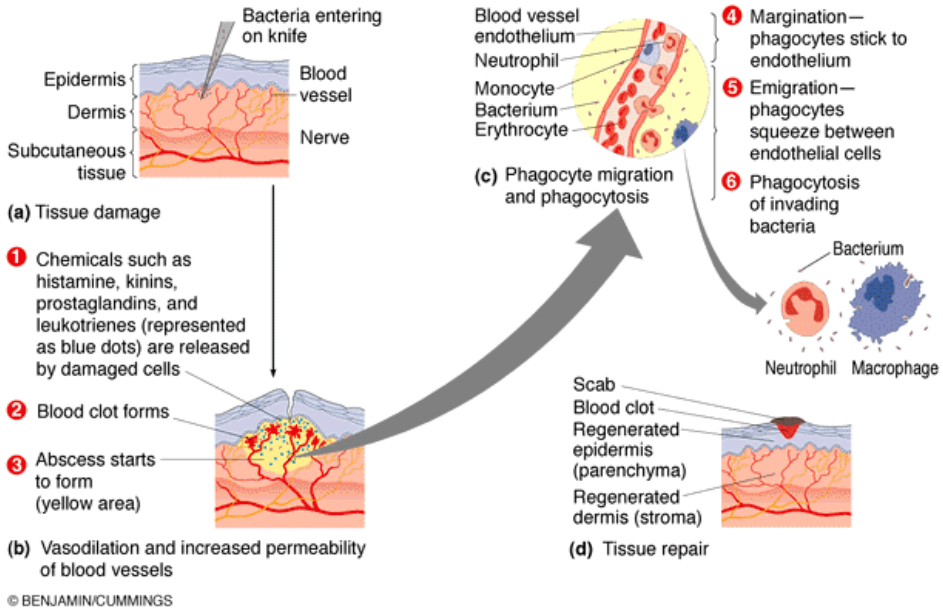

Figure 1. Process of Inflammation.

1.1. Major signaling pathways involved in inflammatory process

There are several fully established inflammatory signaling pathways, which are highly complex in terms of their components and layers of post-translational modifications but rely on only a few major principles of signal transduction. Numerous signaling mechanisms and cells types are involved in the inflammatory response and various anti-inflammatory potential drug targets [6].

1.1.1. NF-κB and inflammation

The most important mechanism by which LPS is sensed through LPS-binding protein (LBP)-LPS complex and then signaling through the Toll-like receptor 4 (TLR4)-MD-2 complex [7, 8]. LPS is also activated by cell surface molecules include the macrophage scavenger receptor (MSR) [6]. Intracellular signaling depends on binding of the intracellular TLR domain, TIR (Toll/IL-1 receptor homology domain), to IRAK (IL-1 receptor-associated kinase), a process that is facilitated by two adapter proteins, MyD88 (myeloid differentiation protein 88) and TIRAP (TIR domain containing adapter protein; also called MyD88-adapter-like protein or Mal), and inhibited by a third protein Tollip (Toll-interacting protein) **Fig. 2, Fig. 3** and **Fig. 4**.

MyD88-independent is another pathway by which TIRAP signals through an RNA-dependent protein kinase (PKR) and interferon regulatory factor (IRF)-3. Recently it has been proposed that cells may also be able to respond to LPS by intracellular receptors called NOD proteins (for nucleotide-binding oligomerization domain) [9]. The NOD proteins have some similarities to the resistance genes in plants that are involved in pathogen recognition with TLRs [10]. Expression of NOD1 and NOD2

confer responsiveness to Gram-negative LPS but not to lipoteichoic acid, which is found in Gram-positive bacteria [11].

Previous reports demonstrated that LPS-induced NF-κB pathways can be divided into two signaling pathways such as canonical and non-canocial/alternate pathway [12]. The common regulatory step in both of these cascades is activation of an IκB kinase (IKK) complex consisting of catalytic kinase subunits (IKKα and/or IKKβ) and the regulatory non-enzymatic scaffold protein NEMO (NF-κB essential modulator also known as IKKγ). Activation of NF-κB dimers is due to IKK-mediated phosphorylation-induced proteasomal degradation of the IκB inhibitor enabling the active NF-κB transcription factor subunits to translocate to the nucleus and induce target gene expression. In the canonical signaling pathway, binding of ligand to a cell surface receptor such as a member of the the Toll-like receptor superfamily leads to the recruitment of adaptors (such as TRAF) to the cytoplasmic domain of the receptor. These adaptors in turn recruit the IKK complex which leads to phosphorylation and degradation of the IκB inhibitor. The canonical pathway activates NF-κB dimers comprising of RelA, c-Rel, RelB and p50. While in alternate or non-canocial pathway utilizes an IKK complex that comprises two IKKα subunits, but not NEMO. In the non-canonical pathway, ligand induced activation results in the activation of NF-κB-inducing kinase (NIK), which phosphorylates and activates the IKKα complex, which in turn phosphorylates p100 leading to the processing and liberation of the p52/RelB active heterodimer [13].

1.1.2. Akt/PI3K and inflammatory signaling

Akt/protein kinase B (PKB) is a serine-threonine kinase that is well known for its ability to inhibit cell death and apoptosis signaling pathways [14, 15]. Generally, the activation of Akt is caused by various growth factors

and cytokines through phosphoinositide 3-kinase (PI3K) pathway. Upon stimulation, PI3K phosphorylates specific phosphoinositide lipids, which accumulate in the plasma membrane, creating docking sites for Akt. At the plasma membrane Akt undergoes phosphorylation, leading to its activation (**Fig. 3, 4, 5**).

Initially, NF-κB and Akt were thought to be the components of divergent signaling pathways. However, later on several reports have confirmed the convergence of the NF-κB and Akt signaling pathways [14]. Indeed, IκB kinase is a substrate of Akt, involved in NF-κB activation. Thus, the activation of Akt stimulates NF-κB activity.

1.1.3. Mitogen activated protein kinase (MAPK) and inflammatory signaling

The mitogen-activated protein kinases (MAPKs) are a group of signaling pathways that play a vital role in the regulation of cell differentiation and growth, as well as in the control of cellular responses to cytokines and stresses [16]. MAPK are a group of signaling molecules that appear to play important roles in inflammatory processes. At least three MAPK cascades are well-described: extracellular signal-regulated kinase (ERK), p38, and Jun N-terminal kinase (JNK)/stress-activated protein kinas (**Fig. 3, 4, 5**) [16]. The phosphorylation of MAPKs is known to be a critical component in the production of NO and pro-inflammatory cytokines in activated macrophages [16].

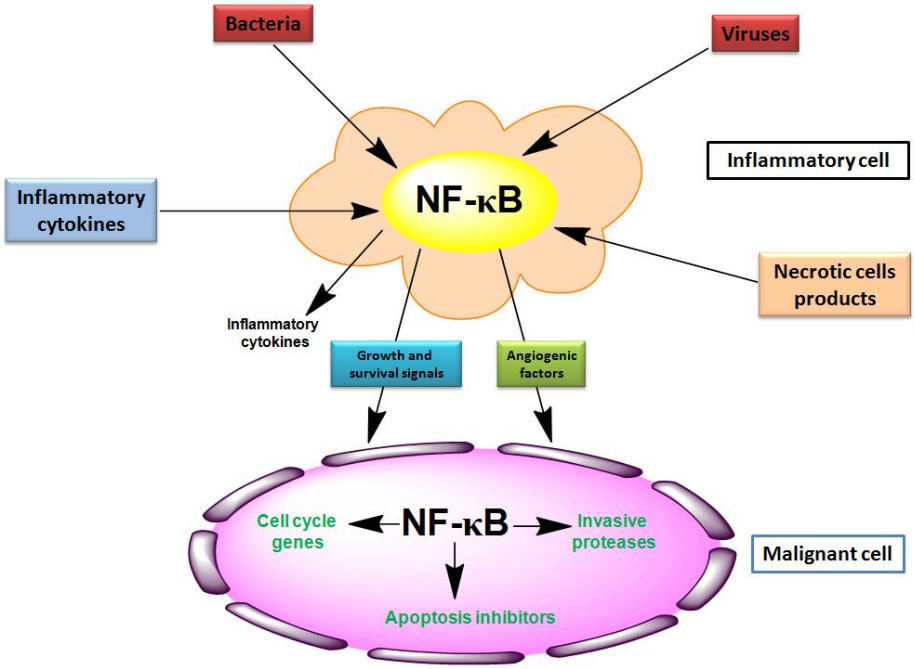

Figure 2. NF-κB activation and the interaction between inflammatory and malignant cells, can promote malignant conversion and progression.

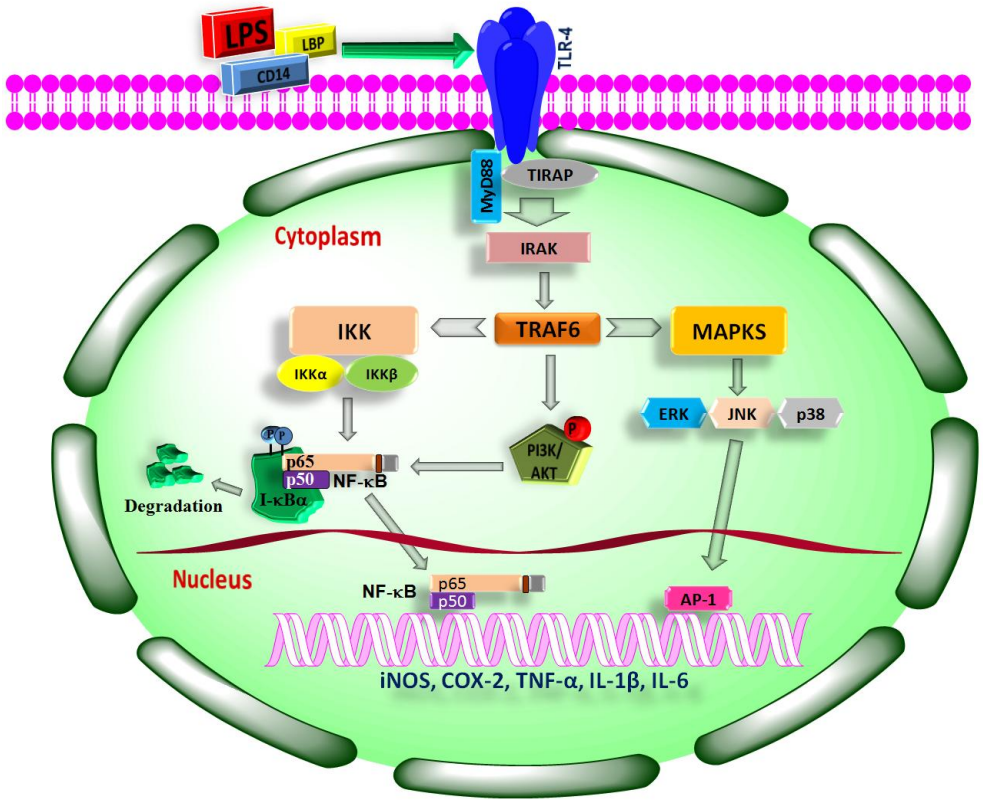

Figure 3. LPS-induced inflammatory signaling. The principal mechanism by which LPS is sensed via LPS-binding protein (LBP)–LPS complex and then signalling through the Toll-like receptor 4 (TLR4)–MD-2 complex. Intracellular signalling depends on binding of the intracellular TLR domain, TIR (Toll/IL-1 receptor homology domain), to IRAK (IL-1 receptor-associated kinase), a process that is facilitated by two adapter proteins, MyD88 (myeloid differentiation protein 88) and TIRAP (TIR domain containing adapter protein; also called MyD88- adapter-like protein or Mal), and inhibited by a third protein Tollip (Toll-interacting protein). The NF-κB, Akt/PI3K and MAPKs signaling pathways activated.

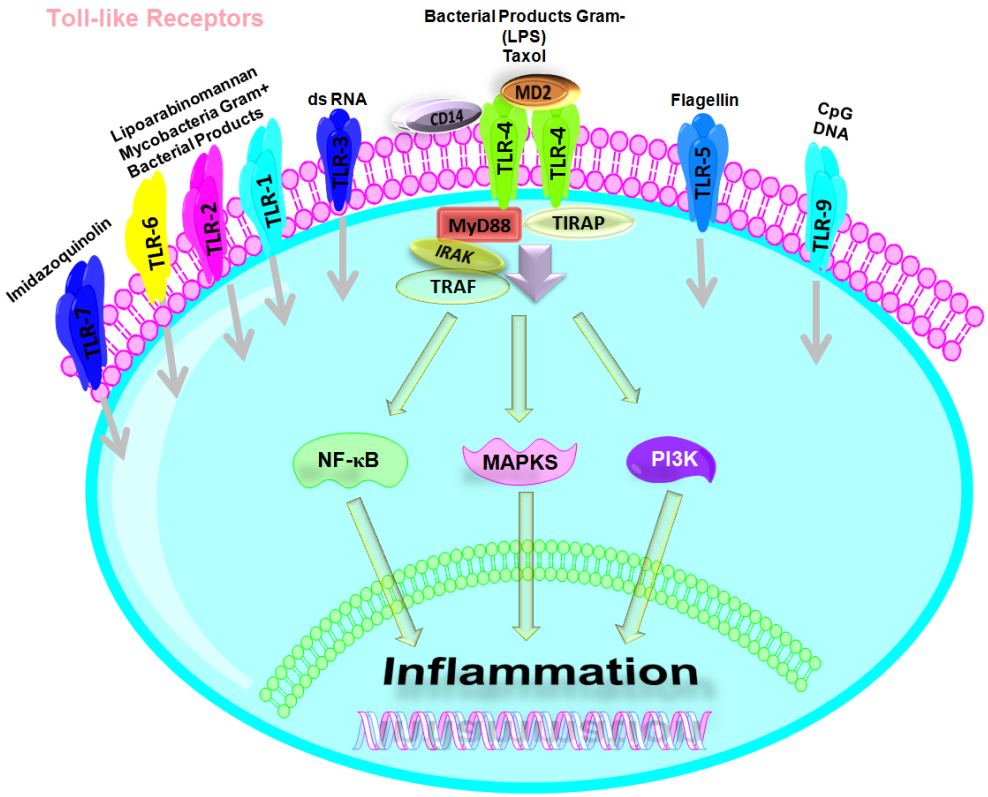

Figure 4. LPS activates macrophages via TLR4. TLR4 is one of a conserved family of receptors that recognize bacterial and viral ligands. Signaling via TLR4 results in the recruitment of adaptor proteins (MyD88 and TIRAP) and kinases (IRAK). Formation of this complex activates a number of signaling pathways that participate in the inflammatory response. Abbreviations: Toll-like receptor (TLR); myeloid differentiation factor 88 (MyD88); Toll-interleukin 1 receptor (TIR) domain-containing adapter protein (TIRAP); interleukin-1 receptor-associated kinase (IRAK); and tumor necrosis factor receptor-associated factor (TRAF).

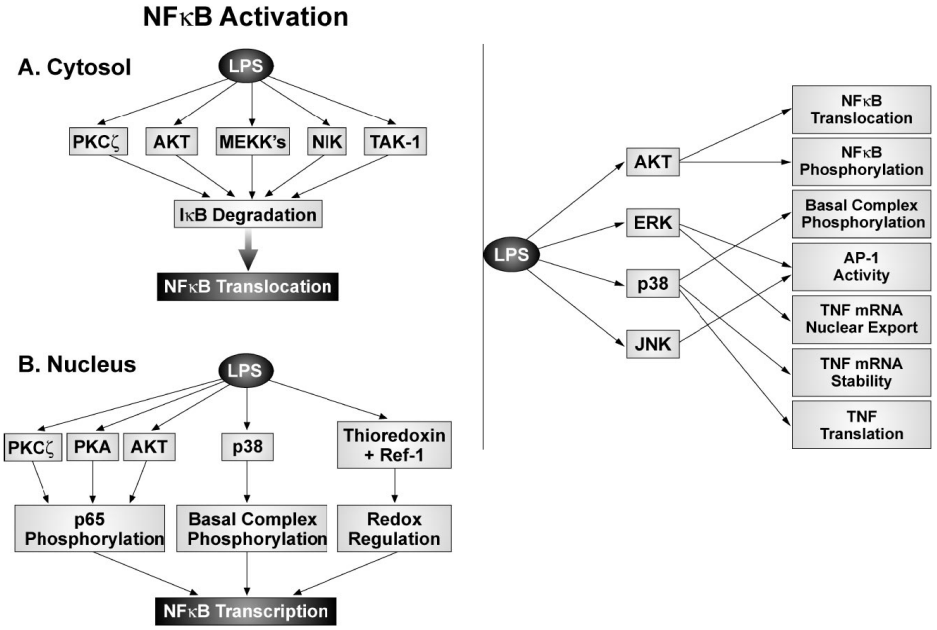

Figure 5. LPS activates multiple pathways [17]. Multiple pathways are involved in translocation from the cytosol (**A**) and transcriptional activity in the nucleus (**B**). LPS also induces activation of a number of signaling pathways. Whereas, LPS-induced Akt activates NF-κB translocation and transcriptional activity. LPS-induced ERK activates AP-1 and regulates TNF-α mRNA nuclear export. LPS-induced p38 regulates NF-κB via phosphorylation of TATA-binding protein in the basal transcription complex. LPS-induced p38 also regulates TNF-α mRNA stability and translation. LPS-induced JNK activates AP-1. Abbreviations: Nuclear factorκ κB (NF-κB), protein kinase C ξ (PKCξ), protein kinase B (Akt), MAP kinase kinase kinase (MEKK), NF-κB-inducing kinase (NIK), transforming growth factor beta–activating kinase 1 (TAK1), inhibitor of κB kinase (IKK), inhibitor of NF-κB (IκB), protein kinase A (PKA), redox factor 1 (REF-1).

2. Pain and nociception

Pain is defined as an "unpleasant sensory and emotional experience associated with actual or potential tissue damage, or described in terms of such damage" [18]. This definition implies that pain is a subjective experience, involving more than just physical injury. In order to assess pain and analgesia pre-clinically, researchers rely on two general categories of non-verbal behavioral manifestations of pain: (1) pain-stimulated behaviors and (2) pain-depressed behaviors [19, 20]. Pain-stimulated behaviors are behaviors that increase in rate, frequency, or intensity in response to the delivery of a painful stimulus (e.g. withdrawal reflexes). In contrast, pain-depressed behaviors are behaviors that decrease in rate, frequency, or intensity in response to a noxious stimulus (e.g. pain-depressed feeding or locomotion). Using these endpoints, pain as well as analgesia can be inferred from behavior in animals. Pain-related changes in behavior result from a series of signaling events occurring within the peripheral and central nervous systems [21]. Various agents involved in activation of nociceptors are described in **Fig 6**.

Agents that Activate or Sensitize Nociceptors:

Cell injury → arachidonic acid → prostaglandins → ↑ vasc. permeability
(cyclo-oxygenase) → sensitizes nociceptor

Cell injury → arachidonic acid → leukotrienes → ↑ vasc. permeability
(lipoxygenase) → sensitizes nociceptor

Cell injury → ↑ tissue acidity → ↑ kallikrein → ↑ bradykinin → ↑ vasc. permeability
→ activates nociceptors
→ ↑ synthesis & release of prostaglandins

Substance P (released by free nerve endings) → sensitize nociceptors
→ ↑ vasc. perm., plasma extravasation
(neurogenic inflammation)
→ releases histamine (from mast cells)

Calcitonin gene related peptide (free nerve endings) → dilation of peripheral capillaries

Serotonin (released from platelets & damaged endothelial cells) → activates nociceptors

Cell injury → potassium → activates nociceptors

Figure 6. Various agents which activate nociceptors.

Pain can be categorized as acute nociceptive pain, inflammatory pain, and neuropathic pain **Fig. 7** and **Fig. 8** [22].

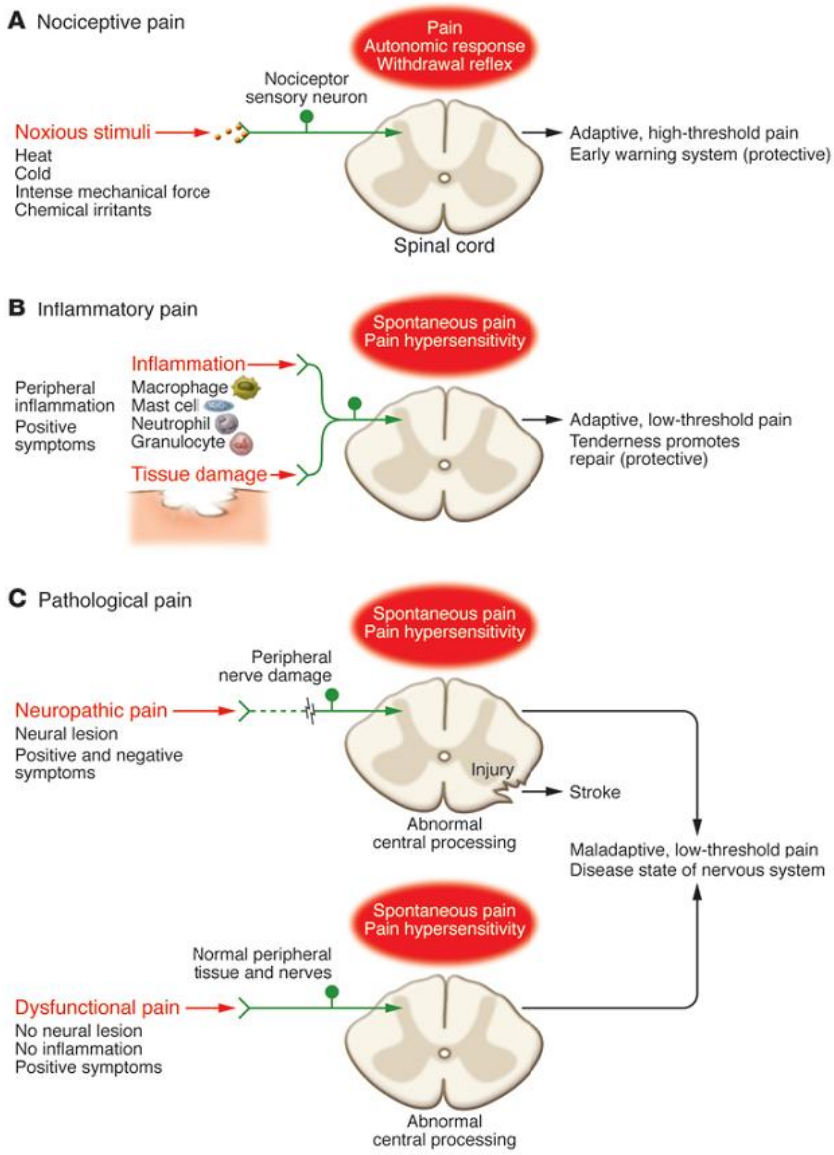

Figure 7. Pain classification [22].

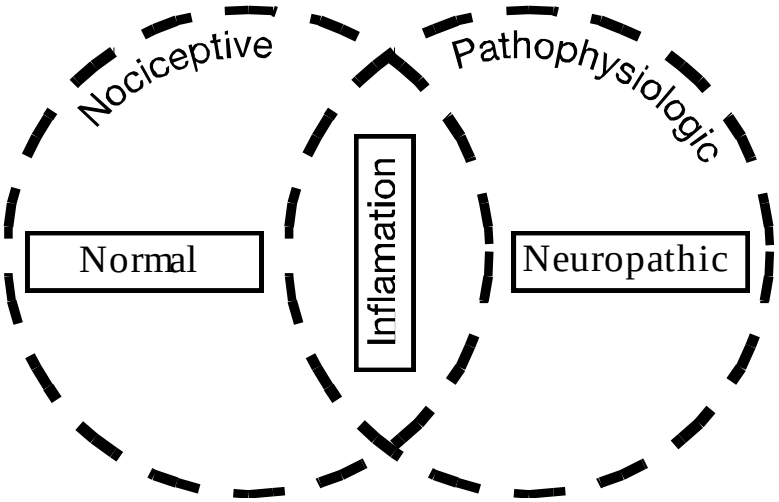

Figure 8. Three different types of pain.

Nociceptive pain: This type of pain serves a vital and adaptive purpose. It serves to detect, localize and limit tissue damage (**Fig. 9**). Acute pain evokes motor withdrawal reactions, which are protective responses that discontinue exposure to the noxious stimulus and terminate the pain. Pain is typically confiscate to the affected area, short in duration and resolved when the core problem is treated. Acute pain can result from injury or sudden illness and can affect skin, subcutaneous tissues, bone, muscle, blood vessels, connective tissue, organs or the linings of the body cavities. Pain associated with surgery, athletic injury and occasional headache are all examples of acute pain. The sensation of acute pain begins with the detection of a noxious stimulus by specialized peripheral nociceptors. Most primary afferent nociceptors respond to a variety of noxious stimuli-extreme hot or cold temperatures, intense pressure (pinching, pinpricks, cuts), increased tissue acidity, or chemical agents released from cells that are damaged or responding to an infectious agent [23].

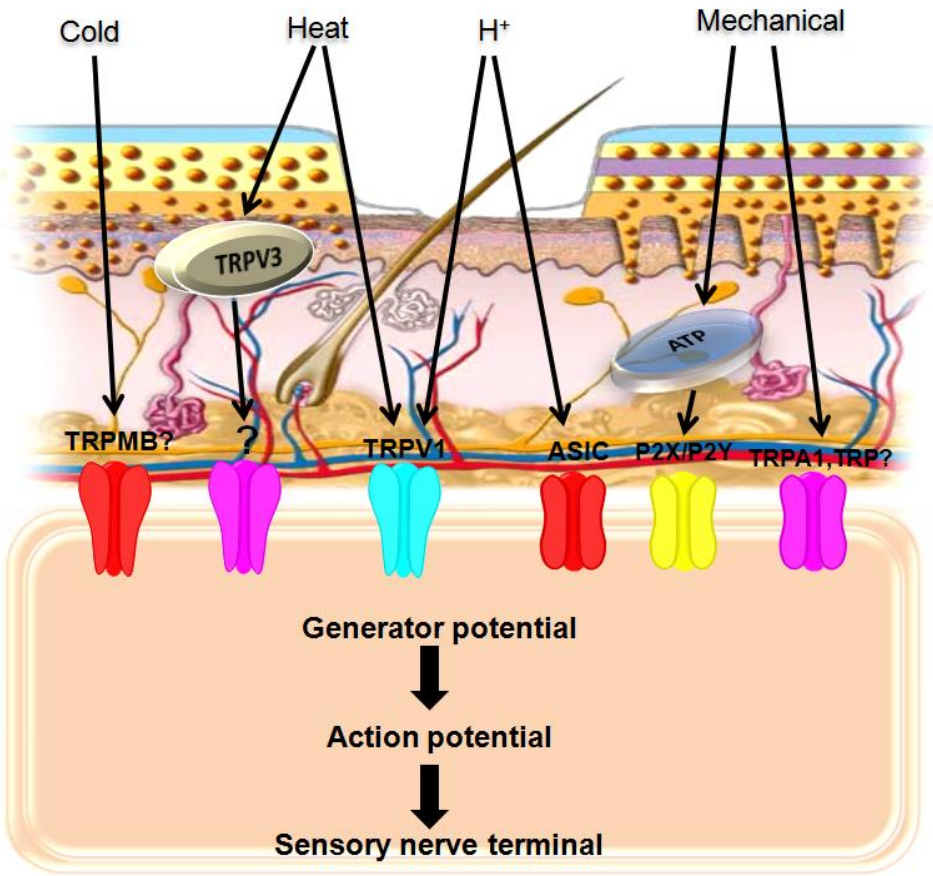

Figure 9. Nociceptive pain pain [23]. Nociceptors respond to acute tissue-damaging stimuli (such as heating the skin), either directly, through transduction of the stimulus energy by receptors (such as the transient receptor potential (TRP) channel TRPV1) on nerve terminals, or indirectly, through activation of TRP channels on keratinocytes (for example, TRPV3) and/or the release of intermediate molecules (such as ATP), which, in turn, act on sensory neuron receptors. Immune cells seem to have little, if any, part in this process. ASIC (amiloride-sensitive cation channel 2); P2X (ionotropic purinoceptor); P2Y (G-protein-coupled pyrimidinergic receptor); TRPA1, TRPM8, TRPV3, TRP channels.

Inflammatory pain: A type of pain that involves the mechanism of sensitization of nociceptive pathways (**Fig. 10**). Under inflammatory pain conditions, inflammatory cytokines (e.g. TNF-α, IL-6 and IL1β), small molecules (e.g. ATP, bradykinin, prostaglandins) and growth factors (e.g. NGF and BDNF) infiltrate the area of injury, bind to receptors expressed on sensory nerves and sensitize nociceptors. Sensitization leads to increased responsiveness of nociceptors to their normal input, and/or recruitment of responses to normally subthreshold inputs [21, 23]. Inflammatory mediators have diverse mechanisms and sites of action, including the activation and sensitization of nociceptive terminals; the regulation of primary nociceptive phenotype; and, in spinal cord, the pre-synaptic control of nociceptor transmitter release and the post-synaptic control of neuronal excitability [23, 24]. Clinically, sensitization can be inferred indirectly from phenomena such as hyperalgesia or allodynia. Hyperalgesia is defined as "increased pain from a stimulus that normally provokes pain", and allodynia is defined as "pain due to a stimulus that does not normally provoke pain" [18]. Pain associated with rheumatoid arthritis, inflammatory bowel disease (IBS), and pelvic inflammatory disease (PID), are all examples of inflammatory pain state.

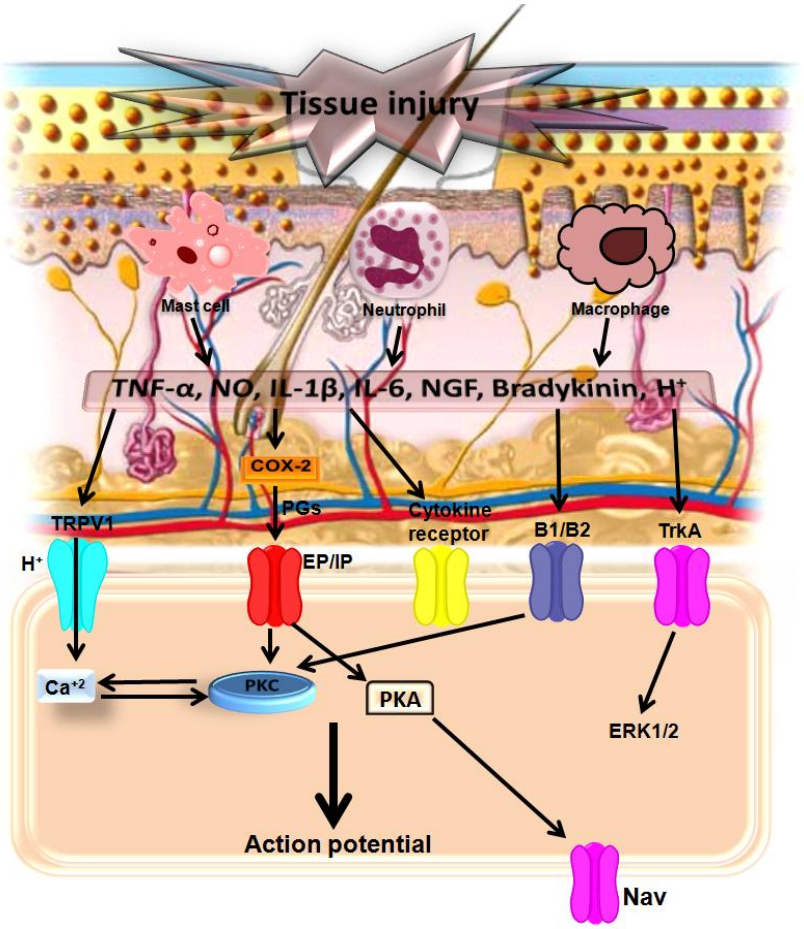

Figure 10. Inflammatory pain [23]. After tissue damage, mast cells and macrophages are activated and some blood-borne immune cells, including neutrophils, may be recruited. Various immune mediators are released (such as tumour necrosis factor-α (TNF-α), interleukin-1β (IL-1β), interleukin-6 (IL-6), nitric oxide (NO), bradykinin, nerve growth factor (NGF) and protons), which exert their algesic effects by acting directly on nociceptors or indirectly through the release of other mediators, most notably prostanoids. There is increasing knowledge of the intracellular cascades that are activated in nociceptors by these mediators, which ultimately either activate or sensitize these neurons. COX2, cyclooxygenase 2; B1/B2, bradykinin receptor; EP/IP, prostanoid receptor; ERK1/2, extracellular signal-regulated kinase 1/2; Nav, voltage-activated sodium channel; PGs, prostaglandins; PKA/PKC, protein kinase A/C; TrkA, tyrosine receptor kinase A; TRPV1, transient receptor potential channel.

Neuropathic pain: Neuropathic pain resembles inflammatory pain in some cases because spontaneous pain and hyperalgesia are present at the site of injury (**Fig. 11**). Nevertheless, the underlying pathology is specifically in nerve tissue. Neuropathic pain is initiated or caused by a pathological lesion or dysfunction in peripheral or central neurons [23]. After peripheral nerve injury, irregular regeneration may occur, resulting in unusual and spontaneous sensitivity to chemical, thermal and mechanical stimuli (peripheral sensitization). As a result of ongoing spontaneous activity in the periphery, central neurons in the spinal cord (spinothalamic tract neurons) adjust and rewire, causing a heightened responsiveness to afferent impulses, including normally innocuous tactile stimuli (central sensitization). Central sensitization commonly leads to allodynia. A reduction in afferent fiber input decreases the activity of interneurons inhibiting nociceptive neurons and causes hypoactivity of descending inhibitory pain modulating systems. This type of pain is maladalptive because it can occur not only at sites far removed from the original injured area but also at degrees of severity that bear little relationship to the extent of injury. All neuropathic pain is chronic. A wide variety of pathological processes affecting peripheral nerves, sensory ganglia, spinal roots and CNS structures can induce neuropathic pain. These include trauma, vascular and metabolic disorders, bacterial and viral infection, inflammation, autoimmune attack, genetic abnormalities, neurotoxins, etc [25].

Symptoms of neuropathic pain can range from numbness, paresthesias and tingling to shooting, burning, sharp, electric shock-like pain sensations. This is in contrast to most nociceptive pain that is commonly described as aching. Pain associated with multiple sclerosis, spinal cord injury, diabetic neuropathy, HIV related neuropathies, and cancer-related pain, are all examples of neuropathic pain.

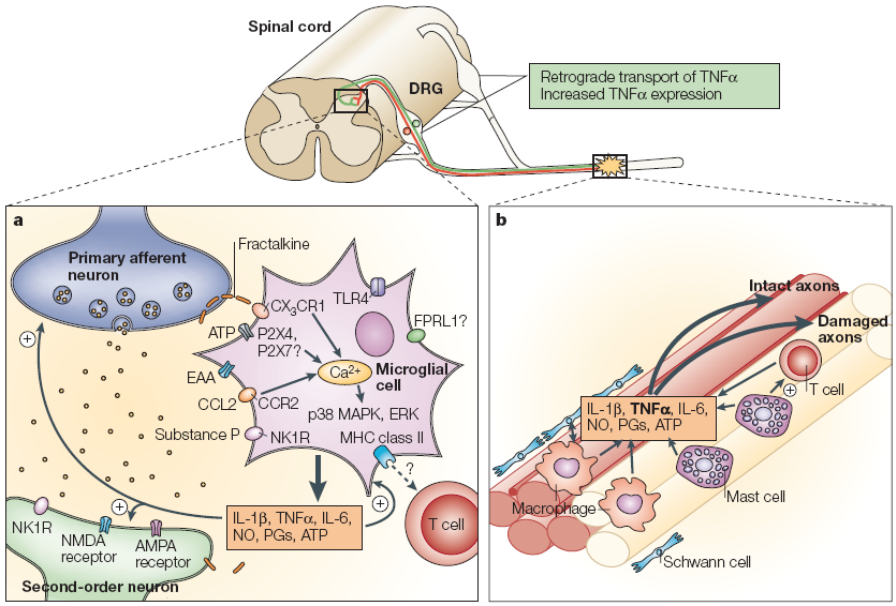

Figure 11. Neuropathic pain [23]. (a) Central events that occur after peripheral nerve injury. In neuropathic pain states, the microglial cells are activated, probably by the release of transmitters or modulators from primary afferents. The activated microglia release several pro-inflammatory cytokines, chemokines and other agents that modulate pain processing by affecting either presynaptic release of neurotransmitters and/or postsynaptic excitability. The release of inflammatory mediators, TNF-α, IL-1β, IL-6, NO, ATP and PGs initiates a self propagating mechanism of enhanced cytokine expression by microglial cells. This leads to an increase in intracellular calcium, and activation of the p38 and ERK pathway. (**b)** Changes that occur in sensory neurons after peripheral nerve injury. Damaged and spared fibres are shown juxtaposed after partial injury to a peripheral nerve. The site of injury is typified by the recruitment and proliferation of non-neuronal elements (such as Schwann cells, mast cells, macrophages and T cells), which release TNF-α, IL-1β, IL-6, chemokine (C-C motif) ligand 2 (CCL2), PGs and nerve growth factor (NGF) that initiate and maintain sensory abnormalities after injury. These factors might either induce activity in the axons they act on or be transported retrogradely to cell bodies in the dorsal root ganglion (DRG), where they alter the gene expression of neurons. Macrophages and mast cells may recruit T cells, which reinforce and maintain inflammatory reactions.

B. STATE of the PROBLEM

For the past decade, the numbers of molecular targets for approved anti-inflammatory and analgesic agents have been debated. The employment of variety of anti-inflammatory and analgesic agents may be helpful in the therapeutic treatment of those pathologies associated with inflammation [26]. Hundred of anti-inflammatory and analgesic drugs have been available in recent world. These include opiates that have been recognized for millennia, NSAIDs a folk remedy for pain and inflammation [27]. Cocaine was introduced hundred years ago without any knowledge of sodium channel. Recently, anti-depressant and anti-convulcent (carbamazapene and gabapentene) were found to produce severe analgesia empirically and the molecular targets are still unknown [28]. Another effort was made to developed COX-2 inhibitor, but due to specificity and produced serious side effects like less gastric and bleeding due to not inhibiting COX-1 [29]. Furthermore, the development of therapeutics to treat long lasting illness has been particularly challenging. Clinical studies revealed that numerous drugs have identified to treat chronic inflammation and pain [30]. Interestingly, none of these agents was successfully and effectively developed to treat chronic inflammation and pain [31]. Nevertheless, up to now, all drugs available for treating chronic pain have failed with respect to their effectiveness and safety, culminating in treatment disruption. The development and utilization of more effective anti-inflammatory and analgesic agents and specifically from natural origins are still desired and more challenging.

Natural products have been the single most productive source of leads for the new drug development. Numerous new products are in clinical development, particularly as anti-inflammatory and anti-cancer agents.

Various screening approaches are also being developed to improve the ease with which natural products can be used in drug discovery. In our continuous search for novel anti-inflammatory agents from traditional medicinal plants, *Saposhnikovia divaricata*, *Sesli resinosum*, *Leonurus japonicus* and *Artemisia capillaris* have been focused of our investigations.

The dry root of *Saposhnikovia divaricata* (Turcz.) Schischk. (Umbelliferae) is a perennial herb and is also known as Bang Pung in traditional herbal medicine. *S. divaricata* possesses analgesic, antipyretic, and antibacterial properties [32, 33]. Due to diverse pharmacological applications and traditional usage of Bang Pung convinced us to study about this herb in detail. In the present study, ample evidence exist to support the recommendations that isolated component (anomalin) mediated multiple molecular signaling pathways and considered to be therapeutic values in the treatment and prevention of inflammation and inflammatory associated disorders.

Several *Seseli* species are reported in previous literature for various healing effects, inflammation, swelling, rheumatism, pain and common cold [34]. Two structurally divergent coumarin compounds (calipteryxin and (3´*S*,4´*S*)-3´,4´-disenecioyloxy-3´,4´-dihydroseselin) were isolated from *Sesli resinosum*. However, limited studies have beed reported regarding the influence of divergent coumarin compounds on anti-inflammatory activity. Therefore, the present studies focused the anti-inflammatory activity of two structurally divergent coumarins in LPS-stimulated murin macrophages.

L. japonicus is widely used as a traditional medicine for various pharmacological purposes, such as anti-arrhythmic, antimicrobial, anticoagulant, antioxidant and anti-cancer activities [35, 36]. Several metabolites have been isolated from *L. japonicus* that substantiate the recorded activities. Among five labdane compounds, one of the labdane

diterpene derivative was conducted to evaluate the anti-inflammatory effect of 15,16-epoxy-3α-hydroxylabda-8,13(16),14-trien-7-one in LPS-stimulated macrophages via multicellular signaling pathways. The results demonstrated that labdane compound exhibited a potent inhibitory effect on LPS-stimulated RAW 264.7 macrophages by blocking NF-κB, MAPKs and Akt signaling.

Artemisia capillaris Thunberg (Compositae) have been used as traditional medicine as a diuretic, liver protective agent, and for amelioration of inflammatory and analgesic disorders [37]. The present study was carried out to establish the scientific rationale for treating inflammation and to find active principles from *A. capillaris*. The aim of the present study is to investigate the possible anti-inflammatory mechanism of the major component (capillarisin) isolated from *A. capillaris* via inhibition of MyD88/TIRAP inflammatory signaling.

The previous findings led us to hypothesize that anomalin and capillarisin could produce anti-nociceptive effects via various inflammatory pain signaling pathways, suggesting that anomalin and capillarisin are good potential candidates for the relief of both acute and chronic inflammatory pain. Our results illustrated that anomalin and capillarisin exhibited significant anti-hyperalgesic and anti-allodynic effects in CFA- and carrageenen-induced models *in vivo*. Similarly, the CFA- and carragenan-induced paw edema was remarkably reduced by anomalin and capillarisin in acute and chronic animal models. Furthermore, both the compounds showed promising neuroprotective and anti-neuroinflammatory activities against SNP-induced induced N2a cells. In addition, an attempt was also made to establish the possible mechanisms involved in its action. The *in vitro* neuroprotective and anti-neuroinflammatory properties of anomalin and capillarisin were explored further by designing STZ-induced diabetic type I

neuropathic pain model in mice. The STZ-induced diabetic type I neuropathic pain was evaluated during five days consecutively. Both the compounds exhibited significant reduction of mechanical allodynia versus vehicle control. Taken together, these results demonstrated remarkable effects agains inflammatory signaling, suggesting that both the phenolic compounds (anomalin and capillarisin) might be therapeutic candidates for inflammation, pain and associated disorders.

PART II

Anti-inflammatory activity of anomalin, calipteryxin, (3´*S*,4´*S*)-3´,4´-disenecioyloxy-3´,4´-dihydroseselin, 15, 16-epoxy-3α-hydroxylabda-8, 13(16), 14-trien-7-one and capillarisin

A. Anti-inflammatory mechanism of anomalin in RAW 264.7 macrophage

1. Introduction

Inflammation is an evolutionarily conserved host reaction that is initiated in response to trauma, tissue damage and infection and, leads to changes in tissue homeostasis and blood flow, immune cell activation and migration and the secretion of cytokines and other mediators in a spatio-temporally coordinated manner [3]. Inflammation involves diverse molecular pathways and is entangled with a wide array of physiological processes [38]. Research on the mechanisms of the inflammatory response has identified various mediators, cytokines and protein kinases that act as vital signaling components, which represent potential therapeutic targets [3]. Acute inflammation is generally down-regulated after the removal of pathogens and cellular debris. However, a chronic inflammatory state leads to local and systemic deleterious effects on host cells and tissues. Atherosclerosis, Alzheimer's disease, rheumatoid arthritis, bowel disease, ischemic heart, brain diseases and cancer are associated with chronic inflammation [39].

The transcription factor NF-κB has been of interest for inflammatory-mediated responses, primarily because several mediators and cytokines cause the activation of this transcription factor [38, 40]. Upon infection, pathogenic microorganisms activate NF-κB via the triggering of Toll-like receptors (TLRs), which are expressed on the cells of the innate immune system, including macrophages, dendritic cells (DCs) and mucosal epithelial cells [41, 42]. TLRs recognize invariant microbial molecules, including

components of the bacterial cell wall, such as lipopolysaccharide (LPS) and microbial nucleic acids [43]. The major subunits of activated NF-κB are p50 and p65 [40]. These transcription factors are kept inactive in the cytoplasm of resting cells by IκB (inhibitors of NF-κB) proteins. The activation of NF-κB is regulated by IκB kinase (IKK) [40, 44]. Various stimuli, such as viruses, bacteria, pro-oxidants, pro-inflammatory cytokines and IκB proteins, are first phosphorylated, ubiquitinated and then rapidly degraded by the proteasome, allowing NF-κB nuclear translocation and the transcriptional initiation of NF-κB-dependent genes. NF-κB is activated when IκB is phosphorylated by IKK [40]. The functions of NF-κB span diverse cellular processes, including adhesion, immune regulation, proliferation, apoptosis, differentiation and angiogenesis [45].

The functioning of the immune system is finely balanced by the activities of pro-inflammatory and anti-inflammatory enzymes and cytokines [1]. However, inflammatory iNOS, COX-2, TNF-α, and IL-6 production need to be regulated by NF-κB because, these mediators contribute not only to the destruction of invading pathogens but also, if excessive, to harmful inflammatory responses such as those observed in chronic inflammatory diseases (e.g., rheumatoid arthritis and septic shock) [46].

A variety of safe and effective anti-inflammatory agents are currently available, and many more drugs are under development. In particular, a new era of anti-inflammatory agents, the natural compounds, have received much attention because of their potential anti-inflammatory effects [1].

The dry root of *Saposhnikovia divaricata* (Turcz.) Schischk. (Umbelliferae) is a perennial herb that belongs to the carrot family and is also known as Fangfeng (Bang Pung) in traditional medicine. *S. divaricata* induces diaphoresis to dispel the pathogenic wind and is used to treat the

headache associated with the common cold, to alleviate rheumatic conditions, to mitigate spasms and to treat tetanus. It also possesses analgesic, antipyretic and antibiotic properties [32].

Earlier phytochemical investigations showed that '*S. divaricata*' contains various types of compounds, including chromones, coumarins, alkaalkynes, and polysaccharides [47]. Naturally occurring coumarins show significant pharmacological properties [48]. The pyranocoumarins in plants have antagonistic effects on calcium [48]. In addition, pyranocoumarins protect the liver from injury in mice [49]. However, limited studies regarding the influence of pyranocoumarin-type compounds on inflammatory activity have been performed.

The current investigation was undertaken to evaluate the anti-inflammatory effect and the anti-NF-κB activities of anomalin, a pyranocoumarin isolated from the ethyl acetate fraction of *S. divaricata*. The present study documented the promising activity of anomalin against the NF-κB signaling pathway in LPS-stimulated RAW 264.7 macrophages.

2. Materials and methods

2.1. Animals

Male BALB/c mice (Samtako, Osan, Korea), 3-4 weeks of age, weighing 25-30 g, were used in this study. Mice were acclimated for one week and fed a diet of animal chow and water *ad lib*. The animals were housed at 23±0.5^{o}C and 10% humidity in a 12 h light-dark cycle. All animal studies were performed in a pathogen-free barrier zone of the Seoul National University Animal Laboratory, according to the procedures outlined in the

Guide for the Care and Use of Laboratory Animals (Seoul National University, Korea).

2.2. Plant materials

The dried roots of *Saposhnikovia divaricata* (Turcz.) Schischk. (Umbelliferae), collected in China were obtained from the Omniherb Company (Daegu, South Korea) and identified by Professor Lee, Je-Hyun (College of Oriental Medicine, Dongguk University, South Korea). A voucher specimen has been deposited at the College of Pharmacy, Seoul National University, South Korea. The dried roots of *S. divaricata* (10 kg) were extracted with MeOH three times, using ultrasonic extraction three times and concentrated under a vacuum into a residue. The MeOH extract (1.9 kg) was suspended in H_2O and subsequently partitioned with ethyl acetate (EtOAc). Anomalin (34 mg) was purified from the EtOAc-soluble fraction (565 g) through repeated silica gel column chromatographic separation, which has described in detail elsewhere [33]. Its structure was confirmed by the interpretation of 1D and 2D-NMR spectroscopic data and comparison with previously published values [33]. The purity was assessed using HPLC analysis (**Fig. 12**) as previously described [33].

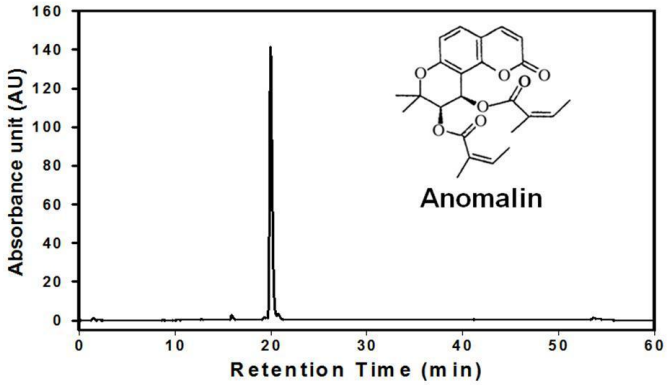

Figure 12. Structure of anomalin and HPLC chromatogram of isolated anomalin.

2.3. Cell culture

RAW 264.7 murine macrophages were obtained from the American Type Culture Collection (Manassas, VA). These cells were maintained at sub-confluence in a 95% air and 5% CO_2 humidified atmosphere at 37°C. The medium used for the routine subculture was Dulbecco's modified Eagle's medium (DMEM) supplemented with 10% fetal bovine serum (FBS), penicillin (100 units/ml) and streptomycin (100 μg/ml). The RAW 264.7 cells harboring a pNF-κB secretory alkaline phosphatase (SEAP)-NPT reporter construct [50] were cultured under the same conditions, except that the media was supplemented with 500 μg/ml geneticin.

2.4. The MTT assay for cell viability

The measurement of cell viability of anomalin was performed using the MTT (4, 5-dimethylthiazol-2-yl)-2, 5-diphenyl tetrazolium bromide) assay. Briefly, RAW 264.7 cells were plated at a density of 1×10^4 per well in a 96-well plate and incubated at 37°C for 24 h. The cells were treated with various concentrations of anomalin (1, 10, 50 and 100 µM) or vehicle alone. Anomalin was first dissolved in dimethyl sulfoxide (DMSO) to make 100 mM stock concentration and further diluted with DMSO for working concentration. Final DMSO concentrations on the cells were <0.25% and were shown not to interfere with the assay. After 20 h of incubation at 37^oC, 10 µl of the MTT (2 mg/ml in saline) solution was added to each well and incubated under the same conditions for another 2 h. Mitochondrial succinate dehydrogenase in live cells converts MTT into visible formazan crystals during incubation. The formazan crystals were then solubilized in DMSO, and the absorbance was measured at 595 nm using an enzyme-linked immunosorbent assay (Emax, Molecular Devices, Sunnyvale, CA). Relative cell viability was calculated by comparing the absorbance of the treated group to the untreated control group. All experiments were performed in triplicate.

2.5. NF-κB secretory alkaline phosphatase (SEAP) reporter gene assay

To determine the inhibitory activity of anomalin in LPS stimulated RAW 264.7 macrophages, NF-κB-dependent reporter gene transcription was analyzed using the secretory alkaline phosphatase (SEAP) assay as previously described, with some modifications [51]. In brief, 1×10^5 RAW 264.7 macrophages transfected with pNF-κB-SEAP-NPT encoding four copies of -κB sequences and the SEAP gene as a reporter were pre-incubated with different concentrations of anomalin for 2 h and challenged with LPS (1

μg/ml) for additional 18 h. Aliquots of the cell-free culture medium were heated at 65°C for 5 min and given an assay buffer (2 M diethanolamine, 1 mM $MgCl_2$, 500 μM 4-methylumbelliferyl phosphate (MUP)) in the dark at 37°C for 1 h. The fluorescence from the products of the SEAP/MUP was measured using a 96-well microplate fluorometer (Molecular Devices, Gemini XS, Sunnyvale, CA) at an excitation of 360 nm and an emission at 449 nm. *N-p*-tosyl-L-phenylalanyl chloromethyl ketone (TPCK), 10 μM was used as a positive control in this experiment.

2.6. Determination of nitric oxide production in RAW 264.7 cells

The inhibitory effect of anomalin on NO production in murine macrophage-like RAW 264.7 cells was evaluated in the medium using the Griess reaction method as described previously [50]. In brief, 1×10^5 RAW 264.7 cells were plated in 24-well plates, incubated for 24 h, pre-treated with different concentrations of anomalin or vehicle for another 2 h and, challenged with LPS (1 μg/ml) for an additional 18 h. Equal volumes of cultured medium and Griess reagent (1% sulfanilamide in 5% phosphoric acid and 0.1% naphtylethylenediamine dihydrochloride in distilled water) were mixed, and the absorbance at 540 nm was determined with a microplate reader (Molecular Devices, Gemini XS, Sunnyvale, CA). The absorption coefficient was calibrated using a sodium nitrite solution standard. For this experiment, 2-amino-5, 6-dihydro-6- methyl-4*H*-1, 3-thiazine (AMT) was used as a positive control.

2.7. Isolation of peritoneal macrophages and measurement of NO production

For the primary cultures, peritoneal exudates cells were collected from the peritoneal cavities of male BALB/c mice by washing with ice-cold 3%

FCS-PBS. The cells were suspended in supplemented DMEM and pre-cultured in 24-well microplates at 37^{o}C in 5% CO_2 for 2 h. The Non-adherent cells were removed and the adherent cells were cultured in the fresh medium. The cells were treated with different concentrations of anomalin for another 2 h then stimulated with LPS (10 μg/ml) for an additional 24 h. The NO production in each well was assessed as previously described.

2.8. Flourescence activating cell sorting (FACS)

The peritoneal macrophages were collected from the peritoneal cavity of the BALB/c mice elicited with cold 3% FCS-PBS. The peritoneal cells cultured at 37^{o}C in 5% CO_2 for 2 h. The non-adherent cells were removed and the adhered cells were washed and collected for FACS analysis.

2.9. Western immunoblot analysis

RAW 264.7 macrophages were pre-treated with the indicated concentrations of anomalin or vehicle for 2 h and stimulated with LPS (1 μg/ml) for 5, 10, 15 and 20 min (for the measurement of p-IKKα/β, phospho-IκBα, IκBα, p-p38, p-JNK, and p-ERK), 18 h (for the measurement of COX-2, and iNOS) and 3, 6, 12, and 24 h (for the measurement of phosphor-eIF2α). All of the primary and secondary antibodies were purchased from Santa Cruz Biotechnology (Santa Cruz, CA), while the phosphor-eIF2α monoclonal antibody was purchased from Cell Signalling Technologies (Danvers, MA). Ten micrograms of total proteins for iNOS, IκBα, and phosphor-IκBα, phosphor-eIF2α, p-IKKα/β, p-p38, p-JNK, and p-ERK while, 5 μg for COX-2, were separated on an SDS-PAGE, 8% (iNOS, COX-2 and COX-1) and 10% (phosphor-IκBα, IκBα and β-actin), respectively. After electrophoresis, the proteins were electro-transferred to nitrocellulose membranes (Whatman GmbH, Dassel), blocked with 5% non-fat milk in

TBS-T buffer and, blotted with each primary antibody (1:1000) and its corresponding secondary antibody (1:5000) according to the manufacturer's instructions. The antibodies were detected with the WEST-SAVE Up™ luminol-based ECL reagent (LabFrontier, Seoul). The target bands were quantified using UN-SCAN-IT™ software version 6.1 (Silk Scientific Co, Orem, Utah).

2.10. RNA extraction and reverse transcriptase (RT)-PCR

RT-PCR was performed with total RNA extracted using TRI REAGENT™, according to the manufacturer's recommendations (Sigma-Aldrich, St Louis, MO). The purity of the RNA preparation was assessed by measuring the absorbance ratio at 260/280 nm. The primer used for the amplifications of iNOS, COX-2 and GAPDH transcripts and the condition for the amplifications were the same as previously described [51], with the modification of the use of 30-40 cycles for amplification. The sense and antisense primers for iNOS were 5′CCCTTCCGAAGTTTCTGGCAGC-3′ and 5′-GGCTGTCAGAGCCTCGTGGCTT-3′, respectively. The sense and antisense primers for COX-2 were 5′-GGAGAGACTATCAAGATAGTGATC- 3′ and 5′-ATGGTCAGTAGACTTTTACA-GCTC-3′, respectively. The sense and antisense primers for rat GAPDH mRNA expression (used as a control for total RNA content for each sample) were 5′-TGAAGGTCGGTGTGAACGGATTTGGC-3′ and 5′-CATGTAGGCCATGAGGTCCACCAC-3′, respectively. RT-PCR was performed using the one-step-RT-PCR PreMix kit (Intron Biotechnology) according to the manufacturer's instructions. The amplified cDNA products were separated by 2% agarose gel electrophoresis and stained with ethidium bromide. The gels were viewed using the Doc-It LS Image Analysis software

(UVP Inc, Upland, CA) and quantified using the UN-SCAN-IT™ software version 6.1 (Silk Scientific Co, Orem, Utah). The PCR products were normalized to the amount of GAPDH for each band.

2.11. Quantitative real time polymerase chain reaction (qRT-PCR)

Total RNA was extracted from cells by the Tri-Reagent method (MRC, Cincinnati, OH), according to the manufacturer's instructions. Total RNA (1 µg) was reverse-transcribed into cDNA using the SuperScriptIII First-Strand Synthesis Supermix for qRT-PCR kit (Invitrogen, Carlsbad, CA), under the following conditions: 65°C for 5 min, 42°C for 50 min, and 70°C for 10 min. The expression of the genes was determined by qRT-PCR (LightCycler® 2.0 Real-Time PCR System, Roche Diagnostics, Mannheim) using the TaqMan Expression Assays (Roche Diagnostics, Mannheim). Two microliter of cDNA was used for qRT-PCR, and the reaction was performed at 95°C for 10 min, followed by 45 cycles of 94°C for 10 s and 55°C for 30 sec. The expression level of the genes was normalized to GAPDH. The data was analyzed using the LightCycle software version 4.0 (Roche Diagnostics, Mannheim).

2.12. Measurement of TNF-α production in the medium

The TNF-α production in the culture medium was determined using commercially available TNF-α ELISA kit (eBioscience, Inc, CA).

2.13. Measurement of PGE_2 production

PGE_2 was determined by using methodology described previously [51].

2.14. Electrophoretic mobility shift assay (EMSA)

EMSA was performed to investigate the inhibitory effect of anomalin on NF-κB- and AP-1-DNA binding as previously described [51]. Briefly, nuclear extracts prepared from LPS-treated cells were incubated with ^{32}P-end-labeled 22-mer double-stranded NF-κB and AP-1 consensus oligonucleotides (Promega, Madison, WI) with the sequences: 5′-AGT TGA GGG GAC TTT CCC AGG C-3′, and 5′-CGC TTG ATG AGT CAG CCG GAA-3′ for 30 min at room temperature. To verify the specificity for NF-κB, a fifty-fold excess of unlabeled NF-κB oligonucleotide was added to the reaction mixture as a competitor. For the super-shift assay, 5 μg of the p50, p65, and c-rel antibodies were added, followed by 30-min incubation at room temperature. The samples were electrophoresed through a 6% native polyacrylamide gel. Finally, the gels were dried and exposed to x-ray film. The signals obtained from the dried gel were quantitated with an FLA-3000 apparatus (Fuji, Tokyo, Japan) using the BAS reader version 3.14 and Aida Version 3.22 software (Fuji-Raytest, Straubenhardt). The binding conditions have been previously optimized by Shin et al. [51].

2.15. Statistical analysis

Unless otherwise stated, the results were expressed as means ± standard deviations (S.D) from three different experiments. One-way analysis of variance (ANOVA) followed by Dunnett's *t*-test was applied to assess the statistical significance of the differences between the study groups (SPSS version 10.0, Chicago, IL). A value of $P<0.05$ was chosen as the criterion for statistical significance.

3. Results

3.1. Effect of anomalin on cell viability

To determine the effect of anomalin on cell viability, anomalin was tested in the MTT cell viability assay using RAW 264.7 murine macrophages. The cytotoxic effect was tested to establish the appropriate concentration ranges of anomalin for the analysis of ongoing experiments (**Fig. 13A**). The non-toxic concentrations (1, 10 and 50 μM) were used for the experiments in the entire experimental model.

3.2. Inhibitory effect of anomalin on NF-κB SEAP in LPS-stimulated RAW 264.7 macrophages

To evaluate the inhibitory activity of anomalin on NF-κB transcriptional activity, pNF-κB-SEAP-NPT construct-transfected RAW 264.7 macrophages were employed. After a challenge to LPS alone, SEAP expression increased 3.4-fold over basal expression, confirming the successful NF-κB dependent transcription in the cell system (**Fig. 13B**). Anomalin dramatically inhibited LPS-induced SEAP expression in a dose-dependent manner (**Fig. 13B)**. TPCK was used as a control and inhibited LPS-induced SEAP expression more than 95% at 10 μM (**Fig. 13B**).

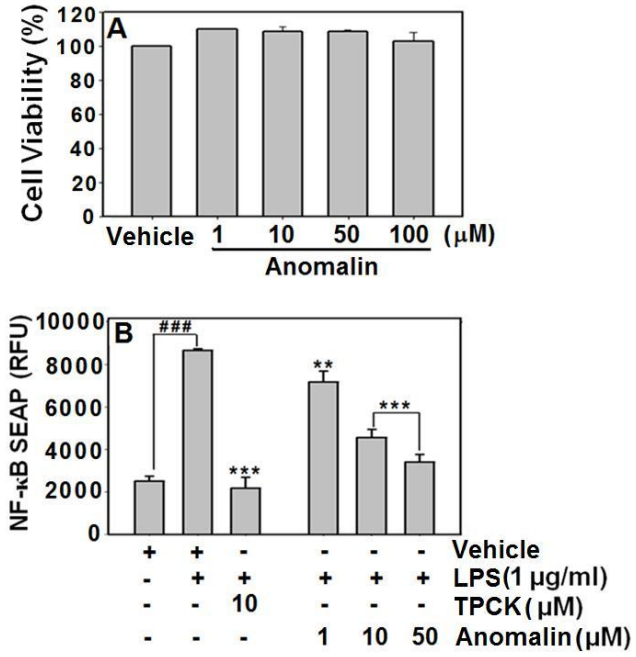

Figure 13. (A) Effect of anomalin of cell viability using RAW 264.7 macrophage cells. RAW 264.7 cells were cultured with the indicated concentrations of anomalin and incubated at 37°C in a 96-well plate for 24 h. Cell viability was evaluated as described in the "Materials and methods," and is expressed as a percentage of the vehicle control. Values are expressed as the mean ± S.D. of three individual experiments. (**B)** Dose-dependent suppression of LPS-induced and NF-κB-dependent alkaline phosphatase (SEAP) expression by anomalin in transfected RAW 264.7 macrophages. Data were derived from three independent experiments and are expressed as the mean ± S.D. (**) *P<0.01* and *(***) P<0.001* indicate a significant difference from the LPS-challenged group. $^{###}P<0.001$ indicates a significant difference from the unstimulated control group. Control (Vehicle), LPS; (LPS + vehicle)-treated cells alone; TPCK 10 μM, *N-p*-tosyl-L-phenylalanyl chloromethyl ketone was used as a positive control.

3.3. Inhibitory effect of anomalin on nitrite production in LPS stimulated RAW 264.7 cells

We examined whether the inhibitory effects of anomalin on NF-κB-transcriptional activity translated into a reduction of the expression and activity of the pro-inflammatory enzyme iNOS. LPS-stimulated RAW 264.7 cells were used as a model system, and the quantified nitrite concentration was used as a measure of NO production catalyzed by the iNOS enzyme. After 18 h, LPS (1 μg/ml) produced considerable nitrite in the culture media. Anomalin drastically inhibited nitrite production in a dose-dependent manner with a maximum inhibitory effect at 50 μM (95%) (**Fig. 14A**).

Similar results were seen in the primary cultured peritoneal macrophages (**Fig. 14B**). The results clearly indicate that anomalin dose-dependently inhibited NO production in peritoneal macrophages (**Fig. 14B**). The positive iNOS inhibitor, AMT, significantly inhibited LPS-induced NO production (**Figs. 14A, 14B**). Moreover, the FACS analysis revealed that the peritoneal macrophages isolated from the mice elicited with 3% FCS-PBS were labeled 88.5% by the anti-CD14 FITC antibody, whereas, the RAW 264.7 cells were labeled 100% as shown in (**Figs. 14C, 14D**).

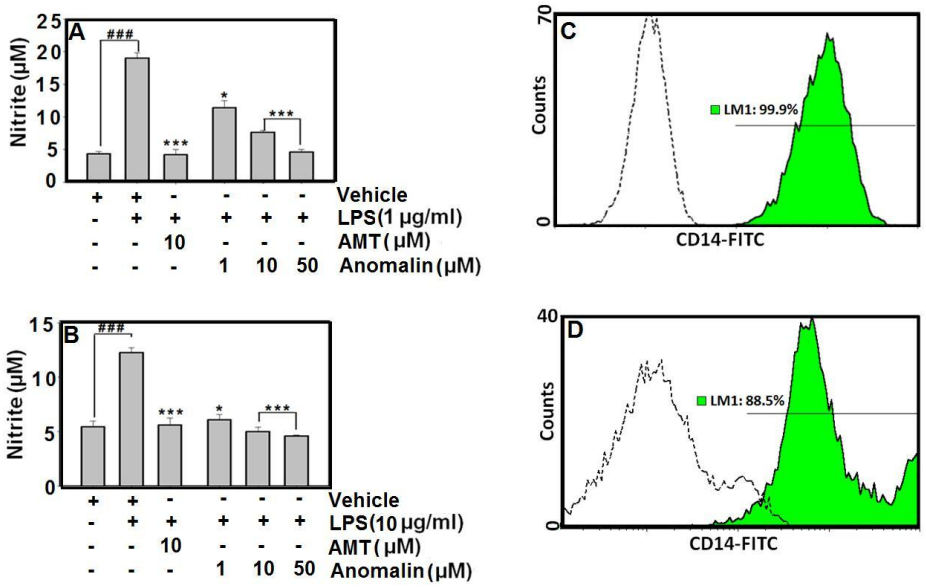

Figure 14. (**A**) Anomalin inhibited the NO production in a dose-dependent manner using LPS-stimulated RAW 264.7 macrophages. (**B**) Inhibitory effect of anomalin using LPS-stimulated primary cultured peritoneal macrophages. The Griess reagent assay was performed to measure nitrite production as described in the "Materials and methods". (**C**) Fluorescence activating cell sorting (FACS) analysis of RAW 264. 7 cells labeled with anti-CD FITC (**D**) Mice peritoneal macrophages labeled with anti-CD FITC. The data were obtained from three independent experiments and are expressed as the mean ± S.D. (*) $P<0.05$ and (***) $P<0.001$ indicate a significant difference from the LPS-challenged group. $^{###}P<0.001$ indicates a significant difference from the unstimulated control group. Control (Vehicle), LPS; (LPS + vehicle)-treated cells alone; AMT 10 μM, 2-amino-5,6-dihydro-6-methyl-4*H*-1, 3-thiazine was used as positive control.

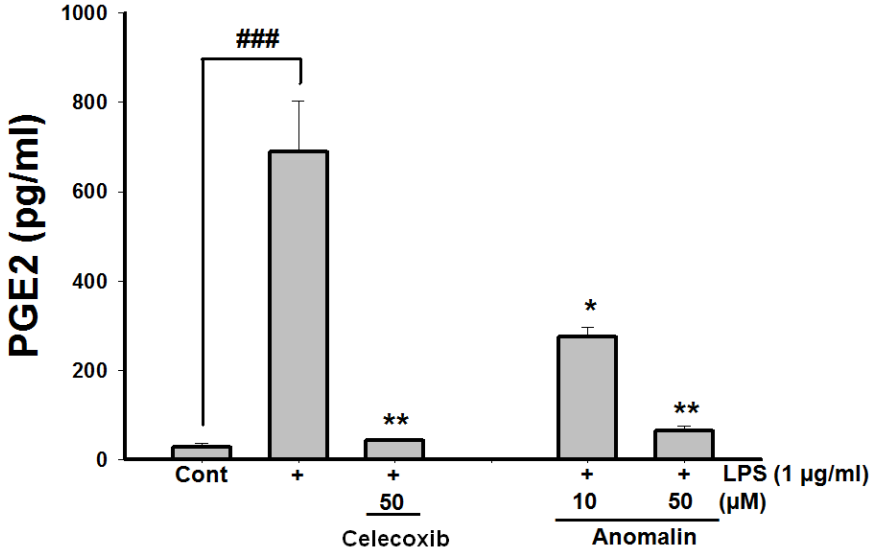

Figure 15. Effect of anomalin on PGE_2 production. The data were obtained from three independent experiments and are expressed as the mean ± S.D. (*) $P<0.05$ and (**) $P<0.01$ indicate a significant difference from the LPS-challenged group. ($^{###}$) $P<0.001$ indicates a significant difference from the unstimulated control group. Control (vehicle), LPS; (LPS + vehicle)-treated cells alone; celecoxib 50 µM was used as positive control.

3.4. Effect of anomalin on PGE_2 production

Fig. 15. Illustrated that PGE_2 production was significantly increased in LPS stimulation. This increased production was remarkably inhibited by anomalin at 10 and 50 μM. The results of anomalin inhibition were almost same as positive control (celecoxib).

3.5. Inhibitory effect of anomalin on iNOS and COX-2 mRNA and protein expression levels in LPS-stimulated RAW 264.7 cells

The promising suppressive effect of anomalin, a reduction in *de novo* protein synthesis involved the suppression of iNOS activity. Therefore, the effect of anomalin on the expression level of iNOS protein was also evaluated. A Western immunoblot analysis was performed. Importantly, anomalin completely inhibited iNOS protein expression at 18 h (**Fig. 16A**).

Because iNOS expression is regulated at the level of transcription, one step-RT-PCR was performed to study the effect of anomalin on iNOS mRNA expression. The response of iNOS was observed 5 h after LPS-stimulation. iNOS mRNA expression consistently decreased with increasing concentrations of anomalin (**Fig. 16C**). These results illustrated that the suppression of iNOS mRNA and protein expression was responsible for the inhibitory effect of anomalin on LPS-stimulated NO production.

COX-2 is an inflammatory factor associated with LPS stimulation. To investigate the anti-inflammatory activity of anomalin, the effect of anomalin on LPS-induced COX-2 protein up-regulation in RAW 264.7 cells was studied by Western blot analysis, and the results are summarized in (**Fig. 16B**). A considerable suppression of the COX-2 gene was observed in cells treated with anomalin at different concentrations (**Fig. 16B**).

Anomalin displayed a remarkable inhibitory effect on COX-2 protein expression; therefore, LPS-induced mRNA expression was further investigated using One-Step-RT-PCR (**Fig. 16D**). Anomalin significantly inhibited LPS-induced COX-2 mRNA expression. In this regard, the suppressive effect of anomalin on COX-2 production may be primarily through transcriptional mechanisms.

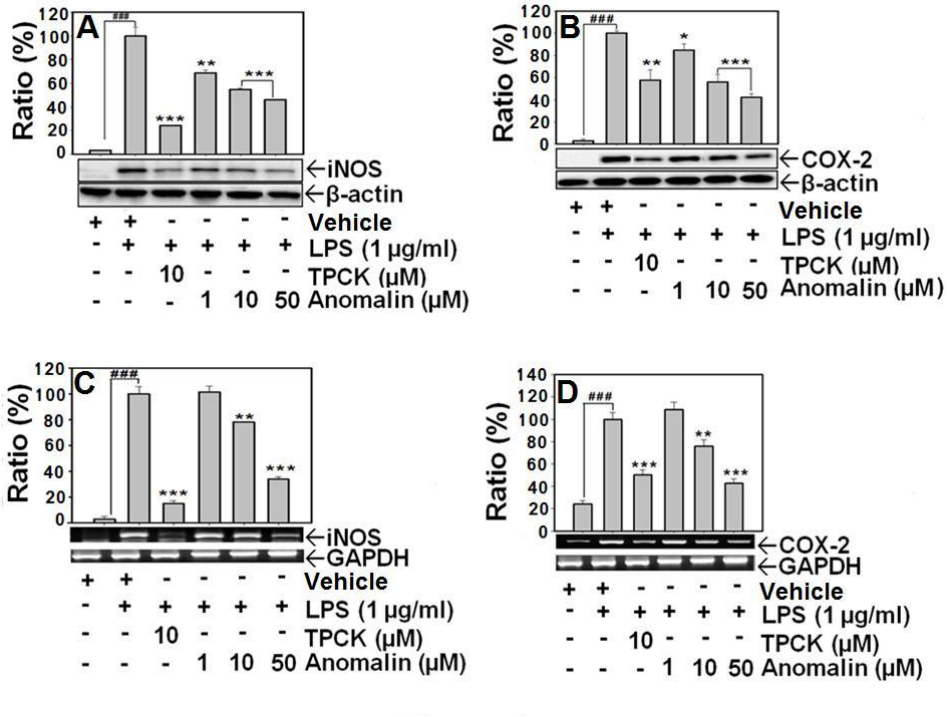

Figure 16. Down-regulation of iNOS and COX-2 proteins and mRNA expressions by anomalin in LPS-stimulated RAW 264.7 macrophages using Western blotting as described in "Material and methods". **(A)** iNOS protein expression **(B)** COX-2 protein expression. While the mRNA expression, using the One-Step-RT-PCR PreMix kit (Intron Biotechnology, Korea) as described in the "Materials and methods"**. (C)** The effect of anomalin on iNOS mRNA expression, and **(D)** COX-2 mRNA expression. Data are expressed as the mean ± S.D. from three separate experiments. For quantification, the mRNA expression data were normalized to the GAPDH signal. Control (vehicle), LPS; (LPS + vehicle)-treated cells alone, and TPCK served as a positive control. *(**) P<0.05*, *(**) P<0.01* and *(***) P<0.001* indicate significant differences from the LPS-treated group. ($^{###}$) *P<0.001* indicate a significant difference from the unstimulated control group.

3.6. Effect of anomalin on mRNA expressions of the pro-inflammatory cytokines (TNF-a and IL-6)

As illustrated above, anomalin potently inhibited the LPS-induced production of pro-inflammatory iNOS and COX-2 mRNA and protein expression. To examine the effect of anomalin on the LPS-stimulated pro-inflammatory cytokines, TNF-α and IL-6, mRNA expression was further investigated using qRT-PCR. In response to LPS, TNF-α and IL-6 expression was significantly up-regulated (**Fig. 17A, 17B**). Treatment with anomalin considerably inhibited the LPS induction of TNF-α and IL-6 (**Figs. 17A, 17B**), respectively.

TNF-α production has been considered a pivotal cytokines in the pathogenesis of inflammatory diseases [52]. Therefore, TNF-α was selected for the further study. The TNF-α production was determined in the medium after 6 and 12 h of LPS-stimulation in RAW 264.7 cells using TNF-α ELISA kit. The results demonstrated that anomalin inhibited the TNF-α production in the culture medium in concentration dependent manner as show in (**Fig. 18**). The positive control, TPCK suppressed the TNF-α production at 20 μM (**Fig. 18**).

These results indicated that anomalin might have elicited its overall anti-inflammatory effects through the same transcription factor or pathway, including NF-κB, which regulates the transcription level of these pro-inflammatory enzymes and cytokines.

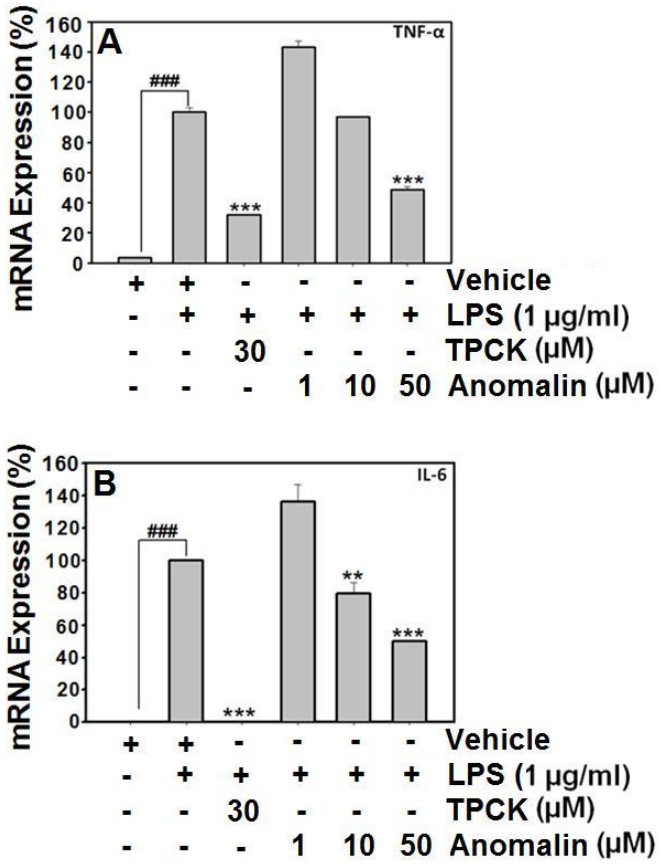

Figure 17. Suppression effect of anomalin on the mRNA expressions of the pro-inflammatory cytokines TNF-α **(A)** and IL-6 **(B)**. The RAW 264.7 cells were stimulated with 1 μg/ml of LPS only or LPS plus different concentrations of anomalin (1, 10 and 50 μM) for 5 h. Total RNA was isolated and the expressions of TNF-α and IL-6 were determined by qRT-PCR, as described in the "Material and methods". GAPDH was used as a control. Control (vehicle), LPS; (LPS + vehicle)-treated cells alone and TPCK (30 μM) served as a positive control. (*) $P<0.05$, (**) $P<0.01$ and (***) $P<0.001$ indicate significant differences from the LPS-treated group. ($^{###}$) $P<0.001$ indicate a significant difference from the unstimulated control group.

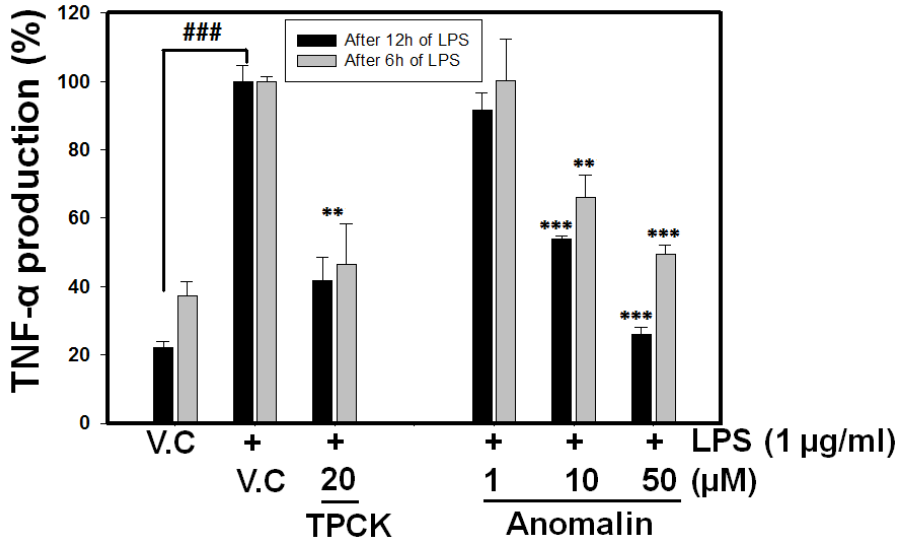

Figure 18. Inhibitory effect of anomalin on TNF-α production in the culture medium was determined using commercially available TNF-α ELISA kit. The data were obtained from three independent experiments and are expressed as the mean ± S.D. *(*) P<0.05* and *(***) P<0.001* indicates a significant difference from the LPS-challenged group. ($^{###}$) *P<0.001* indicate a significant difference from the unstimulated control group. Control (vehicle), LPS (LPS + vehicle)-treated cells alone; TPCK 20 μM, was used as positive control.

3.7. Effect of anomalin on phosphorylation, degredation of IκBα protein and measurement of protein synthesis capacity using Western blot analysis in LPS-stimulated RAW 264.7 macrophages

To further investigate the molecular mechanism involved in the anomalin-mediated inhibitions of iNOS, COX-2, TNF-α and IL-6, we focused on the NF-κB signaling pathway, which is known to be responsible for the transactivation of these genes. One of the major mechanisms involving the transcriptional activation of NF-κB is the phosphorylation of (IKK)α/β and the concomitant degradation of the IκBα protein, which allows the release of free NF-κB and its translocation to nucleus. The immunoblot analysis was performed with cytoplasmic extracts of LPS-stimulated RAW 264.7 macrophages to understand whether anomalin could affect IκBα degradation and phosphorylation. After exposure to LPS alone, IκBα was degraded within 15 min (**Fig. 19A**). IκBα can be phosphorylated at Ser-32 and -36 residues by the IKK complex, which marks for ubiquitin-dependent IκBα degradation [53]. IκBα phosphorylation was also analyzed using Western immunoblotting. After exposure to LPS alone for 10 min, IκBα phosphorylation was markedly caused. After 10 min of LPS stimulation, IκBα phosphorylation was completely inhibited by anomalin (**Fig. 19**B).

The protein synthesis capacity was analyzed with phosphorylation eukaryotic initiation factor 2α (phosphor-eIF2α) protein initiation factor using Western blotting (**Fig. 19C**). The phosphorylation of eIF2α was measured after 3, 6, 12 and 24 h of LPS stimulation using RAW 264.7 cells. The results revealed that anomalin showed no significant inhibitory effect on the stimulation of eIF2α phosphorylation. Thus, the protein synthesis was not interfering by the anomalin as shown in (**Fig. 19C**).

3.8. Effect of anomalin on NF-κB DNA binding activity measured by EMSA

To investigate the effect of anomalin on the activation of NF-κB, the LPS-stimulated RAW 264.7 cells were incubated with various concentrations of anomalin for 1 h and EMSA was performed**.** The NF-κB DNA binding activity was elucidated through an analysis of EMSA with NF-κB ^{32}P-labeled oligonucleotides. The RAW 264.7 cells showed a marked increase in NF-κB DNA binding activity after a 1 h exposure to LPS alone (**Fig. 20A**). Anomalin exhibited a promising inhibitory activity on LPS-induced NF-κB DNA binding, and the results are summarized in (**Fig. 20A**).

To determine the specificity and the identity of NF-κB in RAW 264.7 cells, EMSA was performed with excess amounts of unlabeled NF-κB oligonucleotides for the competition assay and with antibodies against the typical NF-κB subunit p50, p65 and c-rel for the supershift assay. As demonstrated in **Fig. 20B**, the incubation of the LPS-stimulated nuclear extract with excess unlabeled NF-κB oligonucleotide before EMSA abolished the NF-κB DNA binding (**Fig. 20B**). The result indicates that the retarded band observed in the EMSA is indeed NF-κB. Moreover, the incubation of LPS-stimulated nuclear extracts with antibodies against p50, p65 and c-rel were dramatically supershifted (**Fig. 20B**). It has been shown that p50 protein have DNA-binding activity and p65 and c-rel proteins have transactivation domains in their C termini and thus are able to activate transcription of target genes [54]. This finding suggests that anomalin may inhibit the formation of either p50/c-rel or p50/p65 heteromdimers based on the supershift studies (**Fig. 20B**). Moreover, anomalin also start inhibiting p-IKKα/β and p-Akt activsation after 10 and 15 min after LPS stimulation

respectively. Complete inhibitions were observed after 15 min of LPS (**Fig. 21**).

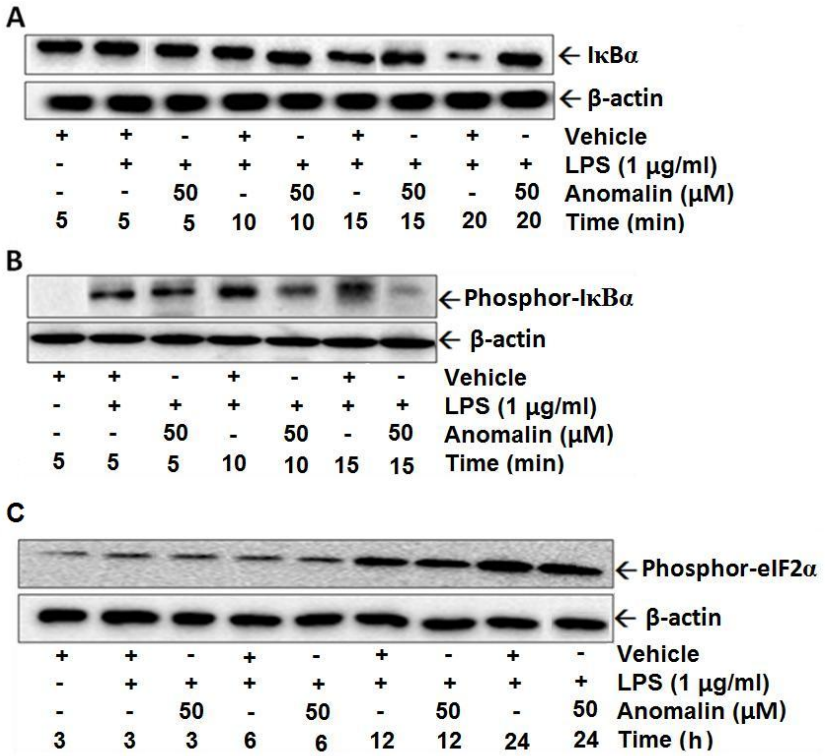

Figure 19. (A) The expressions of IκBα **(B)** phosphorylated IκBα and **(C)** Phosphor-eIF2α protein in the cytosolic extracts were determined by Western blot analysis, as described in the "Materials and methods". The RAW 264.7 cells were pretreated with 50 μM of anomalin for 2 h and treated with LPS (1 μg/ml) for the specified time periods. A representative result from three separate experiments is shown.

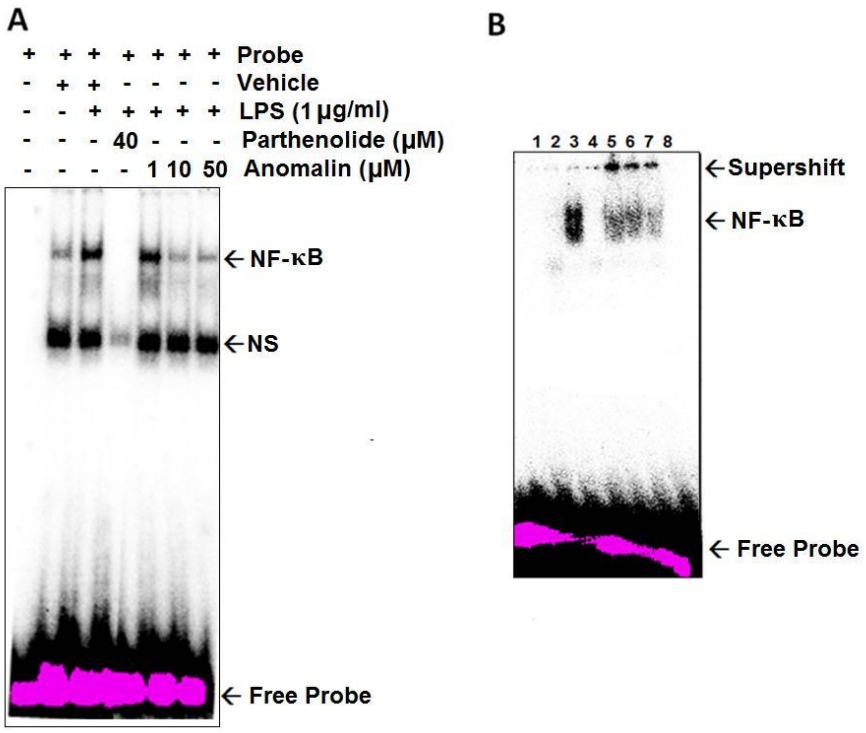

Figure 20. (A) Effects of anomalin on NF-κB DNA binding activity. Electrophoretic mobility shift assay (EMSA) was performed as described in the "Material and methods". RAW 264.7 macrophages were pretreated with the indicated concentrations of anomalin for 2 h and stimulated with LPS (1 µg/ml) for 1 h. Five micrograms of nuclear extract was incubated with ^{32}P-labeled oligonucleotide specific to NF-κB and electrophoresed on a 6% PAGE. An EMSA result is represented and NF-κB complexes, nonspecific signals (NS) and excessive probe are indicated by arrows. Parthenolide 40 and 20 µM was used as a positive control. **(B)** Competition and supershift assays for NF-κB DNA binding using lane (**1**) probe alone; lane (**2**) the control or vehicle; lane (**3**) the LPS-stimulated nuclear extract; lane (**4**) anomalin 50 µM; lane (**5**) the p50 antibody; lane (**6**) p65 antibody; lane (**7**) c-rel antibody; and lane (**8**) the unlabeled NF-κB oligonucleotide.

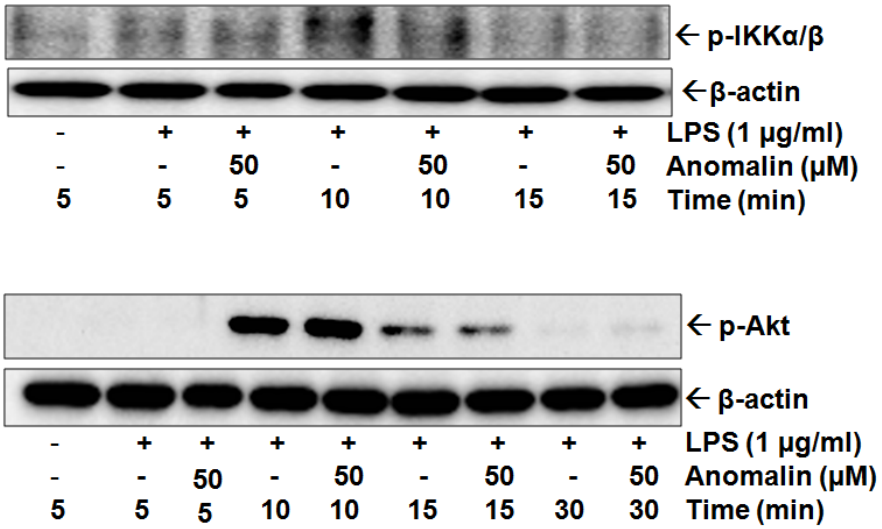

Figure. 21. The expressions of p-IKKα/β and phosphor-Akt in the cytosolic extracts were determined by Western blot analysis, as described in the "Materials and methods". The RAW 264.7 cells were pretreated with 50 μM of anomalin for 2 h and treated with LPS (1 μg/ml) for the specified time periods. A representative result from three separate experiments is shown.

3.9. Effect of anomalin on MAPKs pathway and AP-1 DNA binding activity

As we demonstrated before that anomalin exhibited remarkable inhibitory effect against NF-κB pathway. In order to explore more in deep the molecular mechanism of anomalin, MAPKs pathway was investigated. **Fig. 22** shows that anomalin start reducing the p-p38, p-JNK and p-ERK protein expressions after 15 min of LPS stimulation. Complete inhibition of all MAPKs proteins were seen after 30 min of LPS.

To evaluate the MAPKs transcription factor, AP-1, we next examine the effect of anomalin on AP-1 DNA binding activity by EMSA. **Fig. 23** illustrated that AP-1 DNA binding was significantly enhanced after LPS stimulation. Whereas, this increase binding affinity was completely abolish by anomalin at 50 µM concentration.

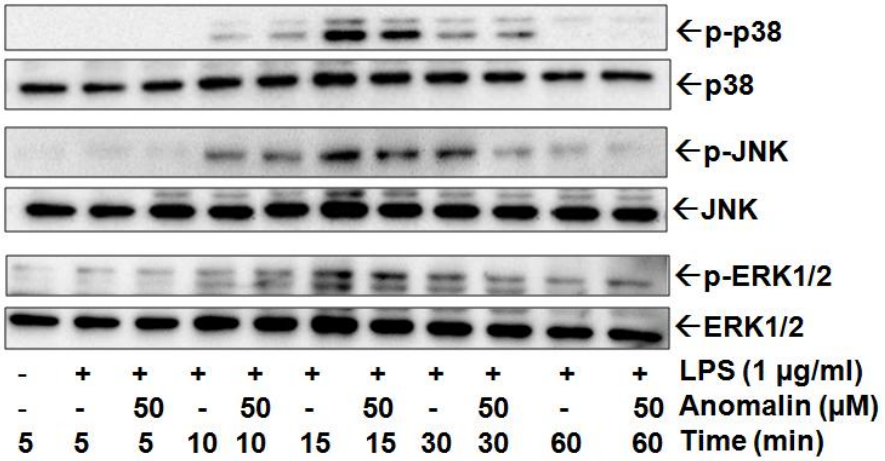

Figure. 22. The expressions of p-p38, phosphor-JNK and p-ERK in the cytosolic extracts were determined by Western blot analysis, as described in the "Materials and methods". The RAW 264.7 cells were pretreated with 50 μM of anomalin for 2 h and treated with LPS (1 μg/ml) for the specified time periods. A representative result from three separate experiments is shown.

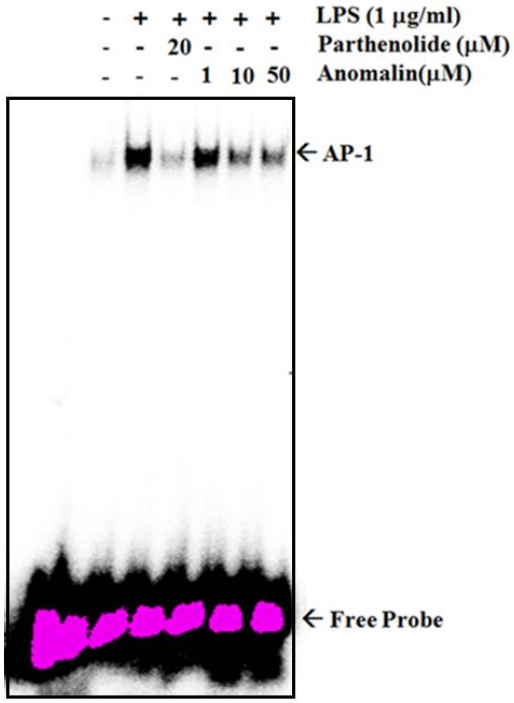

Figure 23. Effects of anomalin on AP-1-DNA binding activity. Electrophoretic mobility shift assay (EMSA) was performed as described in the "Material and methods". RAW 264.7 macrophages were pretreated with the indicated concentrations of anomalin for 2 h and stimulated with LPS (1 μg/ml) for 1 h. Five micrograms of nuclear extract was incubated with ^{32}P-labeled oligonucleotide specific to AP-1 and electrophoresed on a 6% PAGE. An EMSA result is represented and AP-1 complexes, nonspecific signals (NS) and excessive probe are indicated by arrows. Parthenolide 40 and 20 μM was used as a positive control.

4. Discussion

The transcription factor NF-κB plays a significant role in several signal transduction pathways involved in chronic inflammatory diseases and various cancers [55]. The activation of NF-κB can protect cancer cells from apoptotic stimuli, apparently through the induction of survival genes. Therefore, agents that are inhibiting NF-κB transcriptional regulation and modulate the inflammatory response could have therapeutic use and a chemoprotective value. Recently, there has been a growing interest among researchers in the targeting of the NF-κB signaling pathway for the fight against carcinogenesis [56, 57]. The current study was conducted to investigate the potential anti-inflammatory and anti-NF-κB responses of anomalin using RAW 264.7 macrophages. Because of the limited number of studies concerning anomalin on NF-κB transactivation, the effect of anomalin isolated from *S. divaricata* on the transcription activity of NF-κB was investigated. Because *S. divaricata* has been reported to have anti-pyretic and anti-proliferative activity the effect of anomalin isolated from *S. divaricata* was assessed. To have a therapeutic purpose and a chemotherapeutic value, the suppression of NF-κB activity of anomalin needed to be translated into an anti-inflammatory action.

The regulation of enzymes (NO and PGE_2) and cytokines (TNF-α, and IL-6) can be mediated by NF-κB [58]. NF-κB is highly activated at sites of inflammation in a diverse set of diseases and can induce the transcription of pro-inflammatory mediators and cytokines. As a consequence of its critical role in several pathological conditions, NF-κB is major drug target in a variety of diseases [59-61]. Naturally occurring compounds have played a significant role in the drug discovery of anti-inflammatory agents, especially for diseases that have existed since antiquity.

We found that the suppressive effect of anomalin on LPS-induced production of NO was mediated at the transcriptional level. Because of the strong anti-inflammatory properties of anomalin, we also assessed its ability to inhibit NO production using LPS-stimulated peritoneal macrophages isolated from mice. Our results clearly demonstrated that anomalin inhibited NO production in a concentration-dependent manner using peritoneal macrophages. Additionally, anomalin dose-dependently down-regulated LPS-induced iNOS and COX-2 mRNA and protein production. Furthermore, the mRNA expression of the pro-inflammatory cytokines, TNF-α and IL-6, stimulated by LPS treatment was attenuated by anomalin.

eIF2 is involved in the initiation of protein translation and plays a significant role in limiting rate of protein synthesis [62]. Initiation of protein translation requires a ternary complex consisting of a GTP molecule bound to eIF2 and Met-tRNA. The Met-tRNA enables binding of 40S ribosomal subunit, and positioning of the AUG initiation codon to an mRNA [62]. During translation initiation GTP is hydrolyzed to GDP plus inorganic phosphate. For the next cycle of translation initiation, the GDP on eIF2 must be released and replaced by GTP; this is accomplished by eIF2B. However, if the eIF2 is phosphorylated on the α subunit by the eIF2 kinases, then the eIF2αPO4 binds to eIF2B irreversibly which prevent the GDP on eIF2 from being replaced by GTP. The number of eIF2B molecules is limited in the cell, and when free eIF2B is depleted, the initiation of protein synthesis is inhibited which leads to apoptosis. The results illustrated that anomalin showed no inhibitory effect on the initiation of protein synthesis (**Fig. 19C**).

LPS-induced gene expression is mediated by a series of signaling pathways, including NF-κB [63]. Many compounds isolated from natural plants exhibit anti-inflammatory activity associated with their potency. The ability of NF-κB to regulate pro-inflammatory gene expression is controlled

by chemical modifications and by interactions with other proteins, notably members of the IκB family [64]. The phosphorylation of IκB leads to its degradation and the subsequent translocation of NF-κB to the nucleus, where it activates the transcription of target genes [54, 65]. We examined these signaling pathways after an LPS challenge in RAW264.7 macrophages. To study a mechanism for anomalin inhibition, we evaluated the cytoplasmic degradation and phosphorylation of IκBα as shown in **Figs. 19A** and **19B**. Consistently, we found that anomalin inhibited LPS-mediated NF-κB activation via the prevention of IκB phosphorylation and degradation and the subsequent suppression of NF-κB DNA binding activity (**Fig. 20A**). It is clearly evident that anomalin inhibited the transactivation of NF-κB via the stabilization of IκBα.

The expression of inflammatory enzymes and cytokines is regulated via the MAPK pathway, but others have reported that anti-inflammatory agents may alter gene expression through a MAPK-dependent or a MAPK-independent pathway [66]. Because the anomalin protected the degradation and phosphorylation of IκBα, the upstream factors. In addition to NF-κB, another early transcription, ATF_2 (member of AP-1), regulates the expression of a number of pro-inflammatory genes either alone or by coupling with NF-κB. The present study demosnstrated that anomalin significantly inhibited the activation of MAPKs pathway by blocking p-p38, p-JNK, and p-ERK respectively. Taken together, further investigations are still required to clarify the detailed mechanisms of anomalin's anti-inflammatory properties.

B. Mechanism underlying anti-inflammatory properties of two coumarin derivatives by inhibiting pro-inflammatory enzymes and cytokines

1. Introduction

It is well known that large amounts of the pro-inflammatory mediators, such as nitric oxide (NO) and prostaglandin E_2 (PGE_2), as well as the pro-inflammatory cytokines, such as tumor necrotic factor-α (TNF-α), interleukin-1β (IL-1β) and interleukin-6 (IL-6) are released at sites of inflammation during chronic inflammation [55]. Key pro-inflammatory stimuli including bacterial lipopolysaccharide (LPS), cytokines, UV irradiation [37] modulate their effects by inducing the activation of transcription factor NF-κB and AP-1. NF-κB activates a number of rapid response genes involved in the inflammatory response including iNOS, COX-2, TNF-α, IL-1β, and IL-6 [55]. Production of pro-inflammatory mediators and cytokines by these NF-κB response genes may reflect the degree of inflammation and has been suggested to be a measure to assess the effect of anti-inflammatory agents on the inflammatory process. Thus, inhibition of NO and PGE_2 production has been proposed to be a useful approach for the treatment of various inflammatory diseases as well as potential anti-inflammatory agents strategy [67].

In the present study, two structurally divergent coumarin derivatives, calipteryxin (**1**) and (3´*S*,4´*S*)-3´,4´-disenecioyloxy-3´,4´-dihydroseselin) (**2**)

isolated from *Sesli recinosum*, were studied in terms of LPS-induced inflammatory signaling. The genus *Seseli* L., belongs to the Apiaceae family which is composed of aromatic herbs and that are used as foods, spices, condiments and ornamentals [68]. This herb having various pharmacological applications such as anthelmintic, carminative, stomachic and stimulant properties [68]. It has been reported that *Seseli* plant showed significant and dose-dependent anti-inflammatory activity in carrageenan-induced acute inflammations in rats and analgesic effect [68]. However, only a few pharmacological and biological activity studies have been reported about single component from *Seseli*. Therefore, the present study was carried out on LPS-induced inflammatory signaling in murin macrophages. Moreover, comparative investigation was performed between two coumarin type compounds.

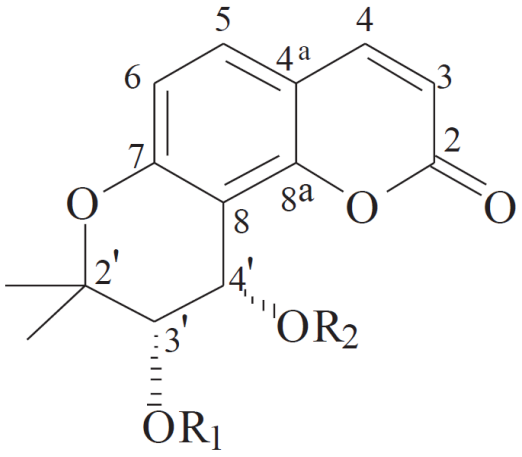

	R_1	R_2	
1	$COCH=C(CH_3)_2$	$COC(CH_3)=CHCH_3$	(3´R,4´R)-3´-Senecioiloxy-4´-angeloiloxy-3´,4´-dihydroseselin (Calipteryxin)
2	$COCH=C(CH_3)_2$	$COCH=C(CH_3)_2$	(3´*S*,4´*S*)-3´,4´-Disenecioyloxy-3´,4´-dihydroseselin

2. Materials and methods

2.1. Isolation and purification of calipteryxin and (3´S,4´S)-3´,4´-disenecioyloxy-3´,4´-dihydroseselin

Calipteryxin and (*3´S,4´S)-3´*,4´-disenecioyloxy-3´,4´-dihydroseselin, were separated and purified from *Seseli resinosum* by counter-current chromatography coupled with an evaporative light scattering detector (CCC-The two-phase solvent gradients used for separation were composed of n-hexane/ethyl acetate/methanol/water at a volume ratio of 3:2:3:2 and 2:1:2:1 based on optimum K_D values of the target compounds. The peak fractions were collected on the basis of CCC-ELSD chromatogram. The collected peak fractions were dried under reduced pressure and analyzed by HPLC-ELSD. The results indicated that the purity of each compound was greater than 99%. Finally, the structures of isolated coumarins, including calipteryxin and (3´*S,4´S)-3´*,4´-disenecioyloxy-3´,4´-dihydroseselin, were confirmed on the basis of ESI-MS/MS, ^{1}H-NMR and ^{13}C-NMR data.

2.2. Cells and culture medium

RAW 264.7 murine macrophages were obtained from the American Type Culture Collection (Manassas, VA). These cells were maintained and subcultured according to the methodology described previously [33]. All the samples were dissolved in dimethyl sulfoxide (DMSO) to make a 100 mM stock concentration and were then further diluted with DMSO for working concentrations. Final DMSO concentrations were <0.2% and not to interfere with the assays.

2.3. Cell Viability and nitric oxide determination

To determine the cell viability of calipteryxin and (3´*S*,4´*S*)-3´,4´-disenecioyloxy-3´,4´-dihydroseselin), a MTT assay was carried out according to Khan et al. [33]. Briefly, RAW 264.7 cells were plated at a density of 1×10^5 per well in a 24-well plate and incubated at 37°C for 24 h. The cells were treated with various concentrations (2.5~30 μM) of calipteryxin and (3´*S*,4´*S*)-3´,4´-disenecioyloxy-3´,4´-dihydroseselin) or vehicle alone for 2 h before LPS (1 μg/ml) stimulation and then incubated at 37°C for an additional 18 h. After incubation for 18 h, 100 μl aliquots of the cell-free culture medium were taken for NO measurement according to the Griess reaction method and cell viability was measured as described previously[33]. 2-amino-5,6-dihydro-6-methyl-4*H*-1,3-thiazine (AMT) was used as a positive control.

2.4. Western immunoblot analysis

RAW 264.7 macrophages were pre-treated with the indicated concentrations of calipteryxin and ((3´*S*,4´*S*)-3´,4´-disenecioyloxy-3´,4´-dihydroseselin)or vehicle for 2 h and then stimulated with LPS (1 μg/ml) for 20 h (COX-2 and iNOS). Ten micrograms of total protein for iNOS, and 5 μg for COX-2 were separated by SDS-PAGE, 8% (iNOS, COX-2 and β-actin). After electrophoresis, the proteins were electro-transferred to nitrocellulose membranes (Whatman GmbH, Dassel, Germany), blocked with 5% nonfat milk in TBS-T buffer, and blotted with each primary antibody (1:1000) and its corresponding secondary antibody (1:5000), according to the manufacturer's instructions. The antibodies were detected with the WEST-SAVE Up™ luminol-based ECL reagent (LabFrontier, Seoul, Korea). The target bands were quantified using UN-SCAN-IT™ software Version 6.1 (Silk Scientific Co., Orem, UT).

2.5. RNA extraction and quantitative real-time (RT)-PCR

RT-PCR was performed with total RNA extracted using easyBlue™, according to the manufacturer's recommendations (Sigma-Aldrich, St Louis, MO). The purity and concentrations of RNA were determined using the ND-1000 spectrophotometer (Nanodrop Technologies, Wilmington, DE). All of the RNA samples were stored at -80^{o}C until used for analysis. Total RNA (1 µg) was converted to cDNA by RT-PCR (Genius FGEN05TD, Teche, England) using iScript^{TM} cDNA Synthesis Kit (BIO-RAD, Hercules, CA) under the following conditions. 25^{o}C for 5 min, 42^{o}C for 30 min and 85^{o}C for 5 min. Quantitative real-time polymerase chain reaction (qRT-PCR) analysis was performed using an Applied Biosystems 7300 Real-Time PCR system and software (Applied Biosystem, Carlsbad, CA). qRT-PCR was conducted in 0.2 ml PCR tubes with forward and reverse primers and the SYBR green working solution (iTaq^{TM} Universal SYBR Green Supermix, BIO-RAD, Hercules, CA), using customer PCR master mix with following conditions: 95^{o}C for 30 min, followed by 40 cycles of 95^{o}C for 15 sec, x ^{o}C for 20 sec and 72^{o}C for 35 sec. The melting point, optimal conditions and the specificity of the reaction were first determined. The sequences of the PCR primers were described preciously [69, 70]. The sense and antisense primers for iNOS were 5′CCCTTCCGAAGTTTCTGGCAGC-3′ and 5′-GGCTGTCAGAGCCTCGTGGCTT-3′, respectively. The sense and antisense primers for COX-2 were 5′-GGAGAGACTATCAAGATAGTGATC- 3′ and 5′-ATGGTCAGTAGACTTTTACA-GCTC-3′, respectively. The sense and antisense for ; for TNF-α, sense primer, 5′-AGC ACA GAA AGC ATG ATC CG-3′ and antisense primer, 5′-CTG ATG AGA GGG AGG CCA TT-3′; for IL-6, sense primer, 5′-GAG GAT ACC ACT CCC AAC AGA CC-3′, and antisense primer, 5′-AAG TGC ATC ATC GTT GTT CAT ACA-3′; for IL-

1β, sense primer, 5′-ACCT GCT GGT GTG TGA CGT T-3′, and antisense primer, 5′-TCG TTG CTT GGT TCT CCT TG-3′, respectively. The sense and antisense primers for rat actin mRNA expression (used as a control for total RNA content for each sample) were 5′-TGAAGGTCGGTGTGAACGGATTTGGC-3′ and 5′-CATGTAGGCCATGAGGTCCACCAC-3′, respectively.

2.6. NF-κB secretory alkaline phosphatase (SEAP) reporter gene assay in transfected-RAW 264.7 cells

The NF-κB SEAP inhibitory activity of calipteryxin and (3´*S*,4´*S*)-3´,4´-disenecioyloxy-3´,4´-dihydroseselin) was determined in LPS stimulated RAW 264.7 macrophages. The NF-κB-dependent reporter gene transcription was analyzed by the SEAP assay, as described previously with some modifications [33, 36].

2.7. Electrophoretic mobility shift assay (EMSA)

EMSA was performed to investigate the inhibitory effect on NF-κB and AP-1 DNA binding, as described previously [33, 36].

2.8. Statistical analysis

Unless otherwise stated, results are expressed as means ± standard deviations (S.D) from three different experiments. One-way analysis of variance (ANOVA) followed by Dunnett's *t*-test was applied to assess the statistical significance of the differences between the study groups (SPSS version 10.0, Chicago, IL). A value of $P < 0.05$ was chosen as the criterion for statistical significance.

3. Results

3.1. Effect of calipteryxin and (3´S,4´S)-3´,4´-disenecioyloxy-3´,4´-dihydroseselin on cell viability in RAW 264.7 cells

The cell viability of calipteryxin and (3´*S*,4´*S*)-3´,4´-disenecioyloxy-3´,4´-dihydroseselin were evaluated in **Fig. 24**. No cytotoxic effect was observed until 30 µM concentration. Therefore, non-toxic concentrations were used for the following experiments.

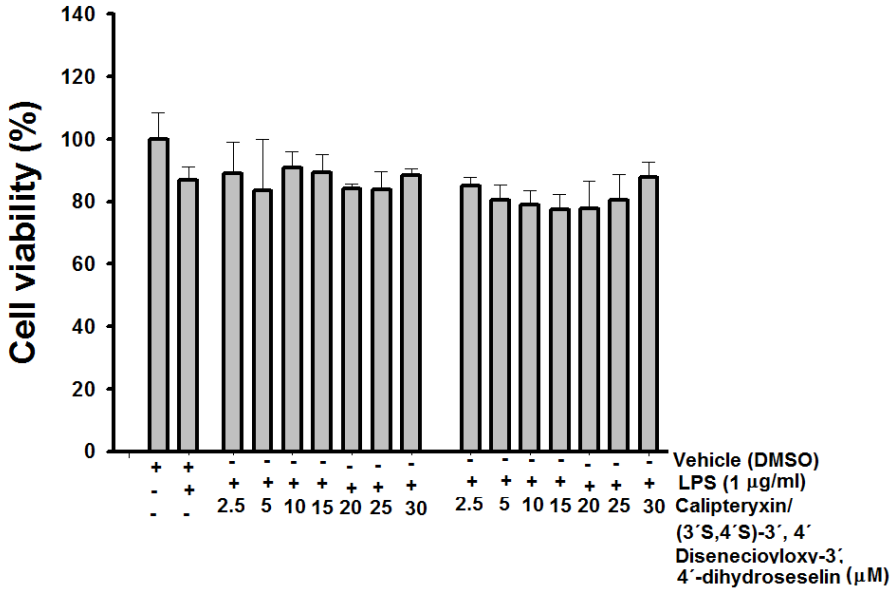

Figure 24. Effect of calipteryxin and (3´*S*,4´*S*)-3´,4´-disenecioyloxy-3´,4´-dihydroseselin) on cell viability in RAW 264.7 cells as described in "Materials and methods".

3.2. Inhibitory effect of calipteryxin and (3´S,4´S)-3´,4´-disenecioyloxy-3´,4´-dihydroseselin on NO production in LPS-stimulated RAW 264.7 macrophages

To determine NO production, we measured nitrite released into the culture medium. RAW 264.7 cells were treated with various concentrations of calipteryxin and (3´*S*,4´*S*)-3´,4´-disenecioyloxy-3´,4´-dihydroseselin) (2.5~30 μM). Incubation with LPS alone markedly increased NO production from the cells, compared with that generated under control conditions (**Fig. 25**). However, pre-treatment with calipteryxin and (3´*S*,4´*S*)-3´,4´-disenecioyloxy-3´,4´-dihydroseselin) prevented this increased level of NO production in LPS-stimulated RAW 264.7 cells in a concentration dependent manner (**Fig. 25**).

3.3. Effect of calipteryxin and (3´S,4´S)-3´,4´-disenecioyloxy-3´,4´-dihydroseselin on LPS-induced proteins and mRNA expressions of iNOS and COX-2

As calipteryxin and (3´*S*,4´*S*)-3´,4´-disenecioyloxy-3´,4´-dihydroseselin) were found to inhibit NO production, we examined the relationship between protein and mRNA expressions of iNOS and COX-2 (**Fig. 26**). The inhibitory effects of calipteryxin and (3´*S*,4´*S*)-3´,4´-disenecioyloxy-3´,4´-dihydroseselin on the protein and mRNA expressions of iNOS and COX-2 were determined by Western blotting and qRT-PCR respectively. Expression levels of iNOS and COX-2 protein and mRNA were markedly up-regulated after LPS treatment, and calipteryxin and (3´*S*,4´*S*)-3´,4´-disenecioyloxy-3´,4´-dihydroseselin) significantly attenuated iNOS and COX-2 mRNA expressions in LPS-stimulated macrophages in a concentration-dependent manner (**Fig. 27**).

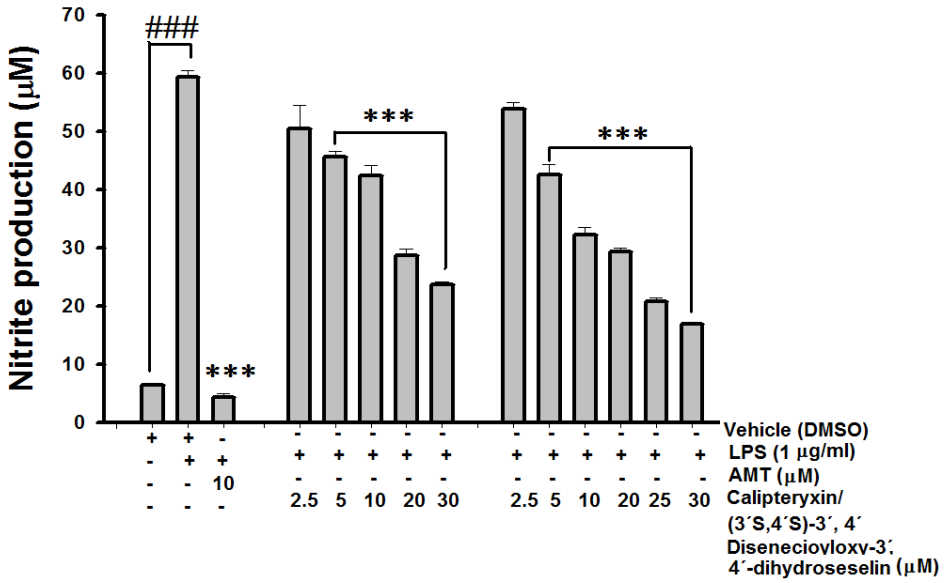

Figure 25. Dose-dependent suppression of LPS-induced NO production by calipteryxin and (3´*S*,4´*S*)-3´,4´-disenecioyloxy-3´,4´-dihydroseselin) in RAW 264.7 macrophages. Data were derived from three independent experiments and are expressed as the mean ± S.D. *(***) P<0.001* indicate a significant difference from the LPS-challenged group. ($^{###}$) *P<0.001* indicates a significant difference from the unstimulated control group. Control (vehicle), LPS; (LPS + vehicle)-treated cells alone.

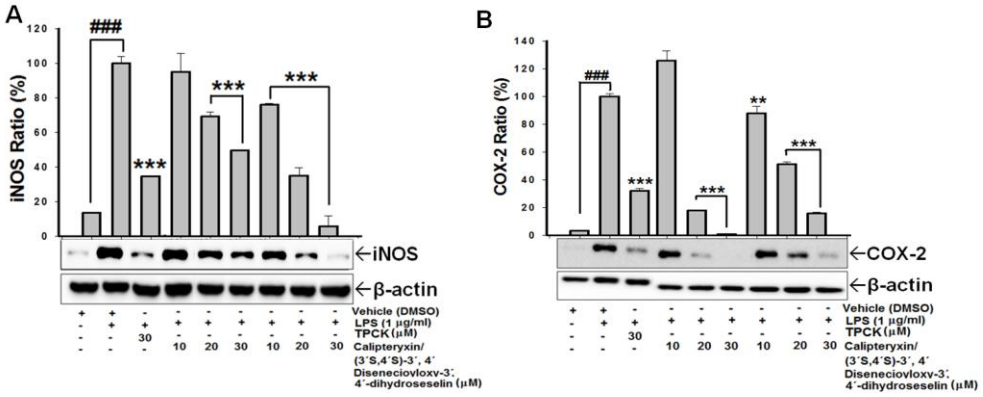

Figure 26. Effect of calipteryxin and (3´*S*,4´*S*)-3´,4´-disenecioyloxy-3´,4´-dihydroseselin) on LPS-induced iNOS protein (**A**) and COX-2 protein (**B**) expression levels in RAW 264.7 macrophages using Western Blotting as described in "Materials and methods". Data were derived from three independent experiments and are expressed as the mean ± S.D. (*) *P<0.05*, (**) *P<0.01* and *(***) P<0.001* indicate a significant difference from the LPS-challenged group. ($^{###}$) *P<0.001* indicates a significant difference from the unstimulated control group. Control (vehicle), LPS; (LPS + vehicle)-treated cells alone; TPCK 30 μM, *N-p*-tosyl-L-phenylalanyl chloromethyl ketone was used as a positive control.

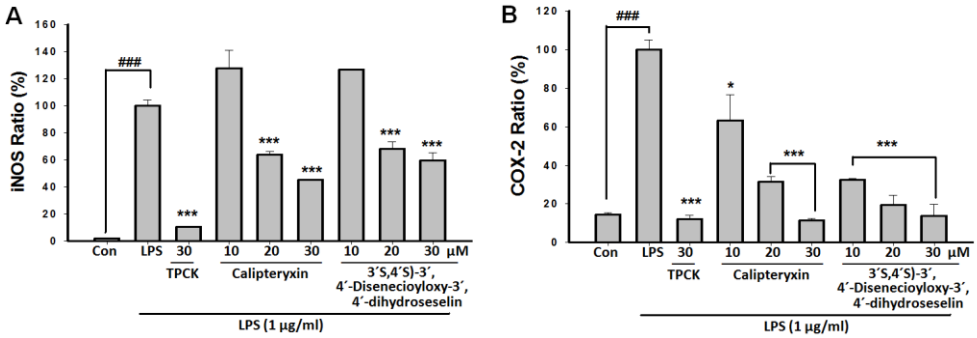

Figure 27. Effect of calipteryxin and (3´*S*,4´*S*)-3´,4´-disenecioyloxy-3´,4´-dihydroseselin) on LPS-induced iNOS mRNA (**A**) and COX-2 mRNA (**B**) expression levels in RAW 264.7 macrophages using qRT-PCR as described in "Materials and methods". Data were derived from three independent experiments and are expressed as the mean ± S.D. (*) *P<0.05*, (**) *P<0.01* and *(***) P<0.001* indicate a significant difference from the LPS-challenged group. ($^{###}$) *P<0.001* indicates a significant difference from the unstimulated control group. Control (vehicle), LPS; (LPS + vehicle)-treated cells alone; TPCK 30 µM, *N-p*-tosyl-L-phenylalanyl chloromethyl ketone was used as a positive control.

3.4. Inhibitory effect of calipteryxin and (3´S,4´S)-3´,4´-disenecioyloxy-3´,4´-dihydroseselin on NF-κB signaling

Since our results indicated that calipteryxin and (3´*S*,4´*S*)-3´,4´-disenecioyloxy-3´,4´-dihydroseselin) affects processes in iNOS and COX-2 induction, we focused our interest on the two pivotal transcription factors critical in iNOS and COX-2 induction, i.e. NF-κB and AP-1 [13, 33]. Initially, calipteryxin and (3´*S*,4´*S*)-3´,4´-disenecioyloxy-3´,4´-dihydroseselin) inhibitory effect on NF-κB in the medium was evaluated. **Fig. 28** showed that both the compounds showed remarkable inhibitory effect on NF-κB in culture media. In order to investigate further, transcription factors DNA-binding affinity was performed using EMSA (**Fig. 29**). Calipteryxin and (3´*S*,4´*S*)-3´,4´-disenecioyloxy-3´,4´-dihydroseselin) in fact significantly attenuated LPS-induced DNA binding activity of both NF-κB and AP-1 (**Fig. 29**). Specificity of bands was confirmed by adding a 50-fold excess of unlabelled NF-κB, and AP-1 oligonucleotides to the binding reaction (**Fig. 29)**.

3.5. Effect of calipteryxin and (3´S,4´S)-3´,4´-disenecioyloxy-3´,4´-dihydroseselin on pro-inflammatory cytokines in LPS-stimulated macrophages

Due to the observation that calipteryxin and (3´*S*,4´*S*)-3´,4´-disenecioyloxy-3´,4´-dihydroseselin) inhibit the activation of the two pro-inflammatory transcription factors NF-κB and AP-1, it was anticipated that calipteryxin and (3´*S*,4´*S*)-3´,4´-disenecioyloxy-3´,4´-dihydroseselin) could affect pro-inflammatory cytokines. Therefore, qRT-PCR analysis was performed. TNF-α and IL-6 are predominantly regulated on the transcriptional level whereby the transcription factors NF-κB and AP-1 play a crucial role [71]. Treatment of LPS-activated cells with calipteryxin and

(3´*S*,4´*S*)-3´,4´-disenecioyloxy-3´,4´-dihydroseselin) in fact lead to a significantly reduced secretion of TNF-α and IL-6 in RAW 264.7 cells (**Fig. 30**).

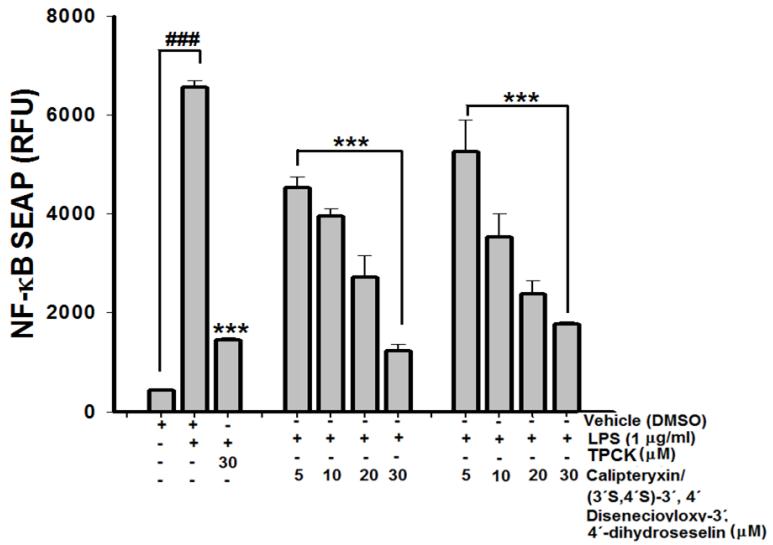

Figure 28. Effect of calipteryxin and (3´*S*,4´*S*)-3´,4´-disenecioyloxy-3´,4´-dihydroseselin) on LPS-induced and NF-κB-dependent alkaline phosphatase (SEAP) expression in transfected-RAW 264.7 macrophages as described in "Materials and methods". Data were derived from three independent experiments and are expressed as the mean ± S.D. *(***) P<0.001* indicate a significant difference from the LPS-challenged group. ($^{###}$) *P<0.001* indicates a significant difference from the unstimulated control group. Control (vehicle), LPS; (LPS + vehicle)-treated cells alone; TPCK 30 µM, *N*-*p*-tosyl-L-phenylalanyl chloromethyl ketone was used as a positive control.

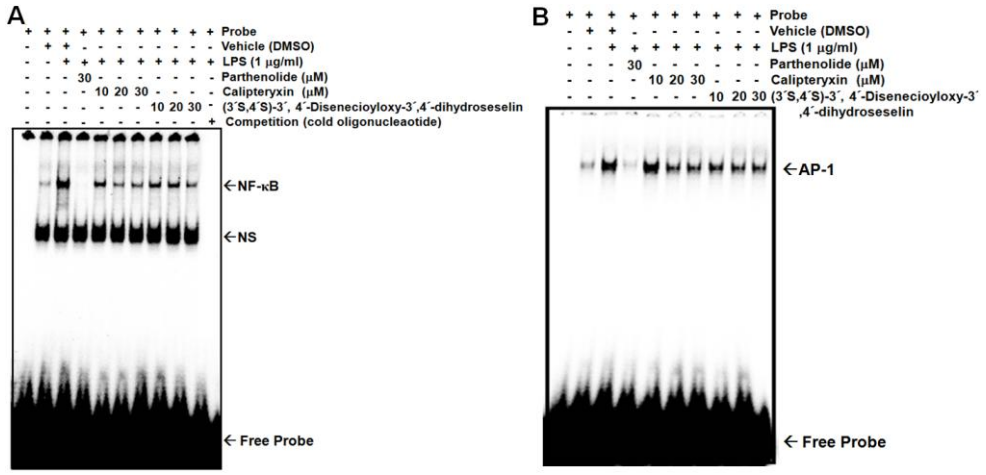

Figure 29. Effects of calipteryxin and (3´*S*,4´*S*)-3´,4´-disenecioyloxy-3´,4´-dihydroseselin) on NF-κB (**A**) and AP-1 (**B**)-DNA binding activity. Electrophoretic mobility shift assay (EMSA) was performed as described in the "Material and methods".

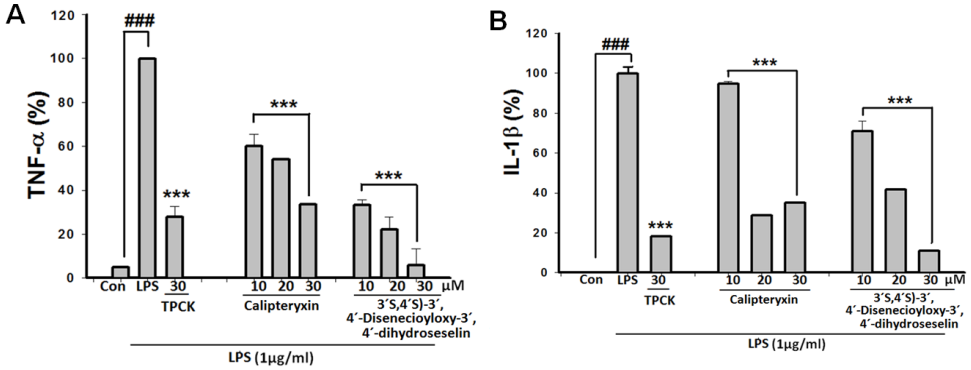

Figure 30. Suppression effect of calipteryxin and (3´*S*,4´*S*)-3´,4´-disenecioyloxy-3´,4´-dihydroseselin) on the mRNA expressions of the pro-inflammatory cytokines TNF-α **(A)** and IL-6 **(B)**. Total RNA was isolated and the expressions of TNF-α and IL-6 were determined by qRT-PCR, as described in the "Material and methods". Con (vehicle), LPS; (LPS + vehicle)-treated cells alone and TPCK (30 μM) served as a positive control. (***) *P<0.00*1 indicate significant differences from the LPS-treated group. ($^{###}$) *P<0.001* indicate a significant difference from the unstimulated control group.

4. Discussion

Macrophages play a pivotal role in the inflammatory signaling and serve as an essential interface between innate and adaptive immunity. Stimulation of macrophages by LPS act on TLR4 and triggers the recruitment of the cytoplasmic adaptor protein MyD88 and the activation of TIRAP, which subsequently stimulate down-stream signaling pathways such as the NF-κB and MAPKs pathways. These pathways induce the expressions of various inflammatory mediators, including NO, PGs and inflammatory cytokines that are well-known to be involved in the pathogenesis of inflammatory response [72]. Based on these hypotheses, modulation of LPS-induced NF-κB and MAPKs signaling or regulation of cytokines productions may constitute a therapeutic strategy in many inflammatory diseases.

Recently, the search for natural products with anti-inflammatory activity has increased extremely. Coumarins have been identified as having a various pharmacological and biological activities [68]. In the present study, two different types of coumarins were investigated in terms of LPS-stimulated macrophages through inhibition of transcription factor NF-κB and AP-1 signaling pathway. We examined the effect of calipteryxin and (3´*S*,4´*S*)-3´,4´-disenecioyloxy-3´,4´-dihydroseselin) on the production of NO and on the regulatory genes for iNOS, COX-2 in LPS-stimulated RAW264.7 macrophage cells. In addition, LPS-induced down-regulation of the pro-inflammatory mediators was based on the suppression of the NF-κB and AP-1 signaling. The inhibitory effect of calipteryxin and (3´*S*,4´*S*)-3´,4´-disenecioyloxy-3´,4´-dihydroseselin) on the expression of pro-inflammatory mediators forms a basis for therapeutic approach against inflammatory diseases.

NO is an important cellular second messenger and free radical produced from *L*-arginine by nitric oxide synthases (NOS). NO can elicit intracellular signals to affect the functions of immune and resident cells of different tissues and organs [33, 37]. The high level of NO can cause inflammatory damage to target tissue during an infection [73]. Therefore, the regulation of NO release via inhibiting iNOS is helpful to alleviate the inflammatory destruction. In the present study, we also found that calipteryxin and (3´*S*,4´*S*)-3´,4´-disenecioyloxy-3´,4´-dihydroseselin) significantly decreased iNOS expression level in RAW264.7 cells induced by LPS. Therefore, the result of NO reduction by calipteryxin and (3´*S*,4´*S*)-3´,4´-disenecioyloxy-3´,4´-dihydroseselin) was due to the inhibition of iNOS expression. COX-2 is an inducible isoform of cyclooxygenase, and mainly exerts its important role in the inflammation [74]. Calipteryxin and (3´*S*,4´*S*)-3´,4´-disenecioyloxy-3´,4´-dihydroseselin) also suppressed LPS-stimulated COX-2 expression level in RAW264.7 cells.

We have demonstrated previously that LPS stimulation induces its inflammatory effects through the activation of NF-κB and AP-1 signaling pathways, which play a crucial role in the control of cellular responses to cytokines and stresses [33, 36]. NF-κB participates in regulating the expression of pro-inflammatory cytokines and other mediators that are involved in the inflammatory response [75]. Therefore, inhibition of the production of this signaling may explain the potent activity of calipteryxin and (3´*S*,4´*S*)-3´,4´-disenecioyloxy-3´,4´-dihydroseselin) as a suppressor of inflammatory cytokines. In inactivated condition, NF-κB is located in the cytoplasm as an inactive NF-κB/IκBα complex and controlled by the inhibitory protein IκBα. Degradation of IκBα by its phosphorylation releases NF-κB to translocate into the nucleus and initiate transcription of the target genes [37]. Therefore, the activation of NF-κB could be evaluated in RAW

264.7 cells by measuring the NF-κB-DNA binding affinity. In this study, LPS caused a marked increased of NF-κB DNA binding, but two coumarin derivatives significantly inhibited NF-κB DNA binding activity. In addition, transcription factor, AP-1 also inhibited by both the compounds. This means that calipteryxin and (3´*S*,4´*S*)-3´,4´-disenecioyloxy-3´,4´-dihydroseselin) could suppress the activation of NF-κB and AP-1 (MAPKs), indicating that NF-κB pathway is also involved in the anti-inflammatory effects of calipteryxin and (3´*S*,4´*S*)-3´,4´-disenecioyloxy-3´,4´-dihydroseselin).

C. Anti-inflammatory mechanism of 15,16-epoxy-3α-hydroxylabda-8,13(16),14-trien-7-one in LPS-stimulated RAW 264.7 cells

1. Introduction

Inflammatory responses require the coordinated activation of various signaling pathways that regulate the expression of pro-inflammatory mediators [76]. Inflammation also has a significant role in priming the immune response to generate immunological memory [33]. The deregulation of this complex pathophysiological process may lead to chronic inflammation or inappropriate priming of adaptive immunity and autoimmune diseases [76].

The NF-κB pathway has been implicated strongly in the pathogenesis of chronic inflammatory diseases [33, 76]. NF-κB appears to play a pleiotropic role in the immune and inflammatory responses. However, the recent description of a second, evolutionarily conserved, NF-κB pathway has revealed new insights into the regulation of NF-κB activation and the role of this pathway in innate and adaptive immunity [16, 77, 78] [. NF-κB and activator protein 1 (AP-1) are key transcription factors that coordinate expression of several inflammatory genes [79]. Even though NF-κB and AP-1 are regulated by different mechanisms, they appear to be activated concurrently by the same multitude of stimuli [80]. Numerous reports have demonstrated that these transcription factors appear to be regulated by the same intracellular signal transduction cascades. Various inflammatory and cancer mediators require the concomitant activation of AP-1 and NF-κB

[14]. Moreover, the activation of other signaling pathways, such as PI3K/Akt and MAPK, are also involved in the activation of NF-κB [16, 81].

Akt, also known as protein kinase B (PKB), is a serine/threonine protein kinase that plays a key role in multiple cellular processes [14]. Numerous reports have confirmed the convergence of the NF-κB and Akt signaling pathways [14, 81]. Indeed, IκB kinase is a substrate of Akt, involved in NF-κB activation, thus, activation of Akt stimulates NF-κB. The modulation of Akt activity can affect the pro-inflammatory mediators through NF-κB activation [81].

The mitogen-activated protein kinases (MAPKs) are a group of signaling pathways that play a vital role in the regulation of cell differentiation and growth, as well as in the control of cellular responses to cytokines and stresses [16, 82].The MAPKs are the extracellular signal-regulated kinase (ERK), the p38 mitogen-activated protein kinase (p38 MAPK) and the c-Jun NH_2-terminal kinase (JNK). The phosphorylation of MAPKs is known to be a critical component in the production of NO and pro-inflammatory cytokines in activated macrophages [16, 82].

Leonurus japonicus Miq. (Lamiaceae) is used widely as a traditional remedy for various therapeutic purposes, such as its purported antiarrhythmic, antimicrobial, anticoagulant, antioxidant, and anticancer effects [35, 83, 84]. Several metabolites have been isolated from *L. japonicus* that substantiate these recorded properties. Some labdane diterpenoids isolated from plants in the genus *Leonurus* are used for the treatment of cardiovascular disease, and for their sedative and uterotonic effects. Labdanes demonstrate a significant potential as new pharmacological agents [85]. Recently, some labdane diterpenes have been shown to exert anti-inflammatory [86], neuroprotective [87], antispasmodic [88], and cytotoxic and trypanocidal [89] activities.

As part of a research project into the biological activities of terpenoids, the naturally occurring labdane compound, 15,16-epoxy-3α-hydroxylabda-8,13(16),14-trien-7-one (**1**) has been investigated as a potential anti-inflammatory agent. To evaluate the mechanism of action of **1**, targets relevant to the regulation of the inflammatory response were studied. The present investigation was focused on the detailed anti-inflammatory mechanism of **1**, isolated from *L. japonicus*, in terms of its activity on LPS-stimulated macrophages that influence three different cellular signaling pathways.

2. Material and methods

2.1. Plant Material

The dried aerial parts of *Leonurus japonicus* were purchased from a herbal store at Gyeong-dong Market, Seoul, Korea, in 2008. The plant material was identified by Professor Je-Hyun Lee, Dongguk University, Korea. A voucher specimen (09E1001) was deposited in the Herbarium of the School of Oriental Medicine, Dongguk University, Korea.

2.2. Extraction and Isolation

The dried roots of *Leonurus japonicus* (15.0 kg) were extracted three times with 100% MeOH for 2 h each time, and a residue (1.18 kg) was obtained after removing the solvent under reduced pressure. This MeOH extract was suspended with distilled water and partitioned with *n*-hexane, EtOAc, and *n*-BuOH successively. The *n*-hexane fraction (241 g) was chromatographed on a silica gel column eluted with hexane-EtOAc (100:1→10:1) to give eight fractions (H1-H8). Fraction H2 was applied to a

HP-20 resin column and eluted with 90% to 100% MeOH to afford three fractions (H2-1–H2-3). Using reversed-phase MPLC (MeOH–H_2O, 10:90→90:10, C18 360 g column (Redisep®), 20 mL/min), fraction H2-1 (8.3 g) was separated to give seven fractions (H2-1-1–H2-1-7). Of these, fraction H2-1-6 (1.2 g) was separated by reversed-phase HPLC (MeOH–H_2O, 70:30, J'sphere ODS, 250 x 10mm I.D. (YMC HPLC®), 2 mL/min), to afford five fractions (H2-1-6-1–H2-1-6-5). Compound **1** (30 mg) was separated from fraction H2-1-6-3 (253 mg) by recrystalization. HPLC analysis was conducted and its purity was determined as 95%. The identity of **1** was confirmed by comparison of ^{1}H-NMR data with literature values for this compound [36].

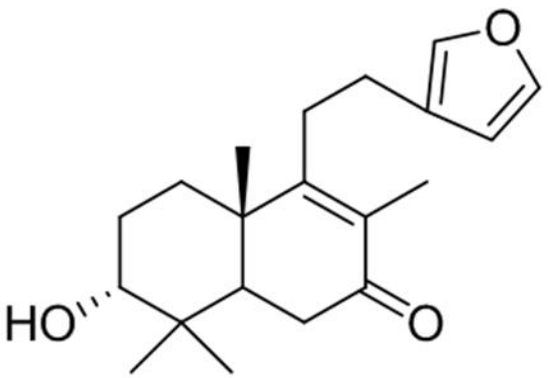

1

Figure 31. 15,16-epoxy-3α-hydroxylabda-8,13(16),14-trien-7-one (**1**).

2.3. Cell viability and nitric oxide determination

To determine the cell viability of **1**, a MTT assay was carried out. Briefly, RAW 264.7 cells were plated at a density of 1×10^5 per well in a 24-well plate and incubated at 37 °C for 24 h. The cells were treated with various concentrations (5, 15, 25, 50, 75, and 100 μM) of **1** or vehicle alone for 2 h before LPS (1 μg/ml) stimulation and then incubated at 37 °C for an additional 18 h. After incubation for 18 h, 100 μl aliquots of the cell-free culture medium were taken for NO measurement according to the Griess reaction method and cell viability was measured as described previously. For this experiment, 2-amino-5,6-dihydro-6-methyl-4*H*-1,3-thiazine (AMT) was used as a positive control.

2.4. NF-κB Secretory alkaline phosphatase (SEAP) reporter gene assay

The NF-κB SEAP inhibitory activity of **1** was determined in LPS stimulated RAW 264.7 macrophages. The NF-κB-dependent reporter gene transcription was analyzed by the SEAP assay, as previously described with some modifications [33]. In brief, 1×10^5 RAW 264.7 macrophages transfected with pNF-κB-SEAP-NPT, encoding four copies of the -κB sequence and the SEAP gene as a reporter, were pre-incubated with different concentrations of **1** for 2 h and were then challenged with LPS (1 μg/ml) for an additional 18 h. *N*-*p*-tosyl-L-phenylalanyl chloromethyl ketone (10 μM) (TPCK) was used as the positive control for this experiment.

2.5. Western immunoblot analysis

RAW 264.7 macrophages were pre-treated with the indicated concentrations of **1** or vehicle for 2 h and then stimulated with LPS (1 μg/ml) for 5, 10, 15, 20, 30 and 60 min (phosphor-IκBα and, IκBα, p-p38, p-JNK, p-ERK, p-Akt) and 18 h (COX-2, and iNOS). All of the primary and secondary

antibodies were purchased from Santa Cruz Biotechnology (Santa Cruz, CA). Ten micrograms of total protein for iNOS, IκBα, phosphor-IκBα, p-p38, p38, p-JNK, JNK, p-ERK, ERK, p-Akt, Akt, p65, p50 and 5 μg for COX-2 were separated by SDS-PAGE, 8% (iNOS, and COX-2) and 10% (phosphor-IκBα, IκBα p-p38, p38, p-JNK, JNK, p-ERK, ERK, p-Akt, Akt, p65, p50 and β-actin). After electrophoresis, the proteins were electro-transferred to nitrocellulose membranes (Whatman GmbH, Dassel, Germany), blocked with 5% nonfat milk in TBS-T buffer, and blotted with each primary antibody (1:1000) and its corresponding secondary antibody (1:5000), according to the manufacturer's instructions. The antibodies were detected with the WEST-SAVE Up™ luminol-based ECL reagent (LabFrontier, Seoul, Korea). The target bands were quantified using UN-SCAN-IT™ software Version 6.1 (Silk Scientific Co., Orem, UT).

2.6. Electrophoretic mobility shift assay (EMSA)

EMSA was performed to investigate the inhibitory effect on NF-κB and AP-1 DNA binding, as previously described [33]. Briefly, nuclear extracts prepared from LPS (1 μg/ml)-treated cells were incubated with ^{32}P-end-labeled 22-mer double-stranded NF-κB and AP-1 consensus oligonucleotide (Promega, sequence: 5′-AGT TGA GGG GAC TTT CCC AGG C-3′, and 5′-(CGC TTG ATG AGT CAG CCG GAA)-3′) for 30 min at room temperature. To verify the specificity for NF-κB, a 50-fold excess of unlabeled NF-κB oligonucleotide was added to the reaction mixture as a competitor and the DNA protein complexes were then separated from the free oligonucleotides on 6% native polyacrylamide gels. The signals obtained from the dried gel were quantified with an FLA-3000 apparatus (Fuji), using the BAS reader version 3.14 and Aida Version 3.22 software

(Amersham Biosciences, Piscataway, NJ). The binding conditions were optimized as reported earlier [51].

2.7. Measurement of TNF-α production

TNF-α production in the culture medium was determined using a commercially available TNF-α ELISA kit (eBioscience, Inc., San Diego, CA)**.**

2.8. Statistical analysis

Unless otherwise stated, results are expressed as means ± standard deviations (S.D) from three different experiments. One-way analysis of variance (ANOVA) followed by Dunnett's *t*-test was applied to assess the statistical significance of the differences between the study groups (SPSS version 10.0, Chicago, IL). A value of $P < 0.05$ was chosen as the criterion for statistical significance.

3. Results

*3.1. Effect of **1** on cell viability and NO assay*

The cytotoxic effects of **1** on LPS-stimulated RAW 264.7 macrophages were determined initially. The results demonstrated that **1** did not affect cell viability at concentrations up to 50 μM. Therefore, non-toxic concentrations were used in subsequent experiments on **1 (Fig. 32)**.

NO is involved in various biological processes, including inflammation and immunoregulation [90, 91]. Therefore, the inhibition of nitric oxide (NO) production by inducible nitric oxide synthase (iNOS) may have potential therapeutic value when related to inflammation-associated diseases. Compound **1** displayed an inhibitory effect on NO production, with an IC_{50} value of 27.0 μM **(Fig. 32)**.

*3.2. Effect of **1** on iNOS and COX-2 protein expression levels in RAW 264.7 cells*

To investigate whether the inhibitory effect of **1** on NO production was via the inhibition of the corresponding gene expression, the protein iNOS was evaluated by Western blot analysis (**Fig. 33**). Additionally, cyclooxygenase-2 (COX-2) protein expression was also evaluated (**Fig. 33**). In unstimulated RAW 264.7 cells, the iNOS and COX-2 protein expression levels were almost undetectable. However, after LPS treatment, the protein expression levels of iNOS and COX-2 were augmented markedly and pretreatment of the cells with different concentrations of **1** attenuated LPS-induced iNOS and COX-2 protein and gene expression in a concentration-

dependent manner. These data suggest that **1** can down-regulate LPS-induced iNOS and COX-2 expression at the transcriptional level.

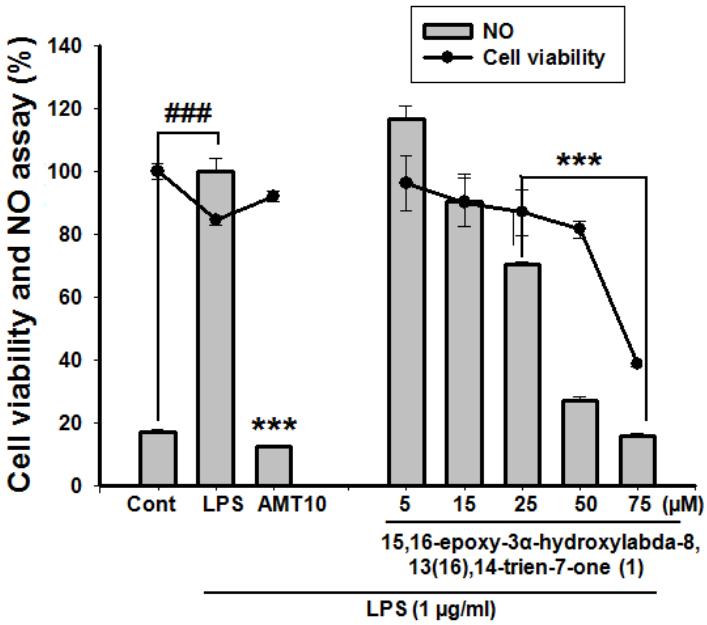

Figure 32. Effect of **1** on cell viability and NO in RAW 264.7 macrophages. Data were derived from three independent experiments and are expressed as the means ± S.D. (***) P <0.001 indicates a significant difference from the LPS (1 μg/ml)-challenged for 18 h incubation group. ($^{###}$) P <0.001 indicates a significant difference from the unstimulated control group.

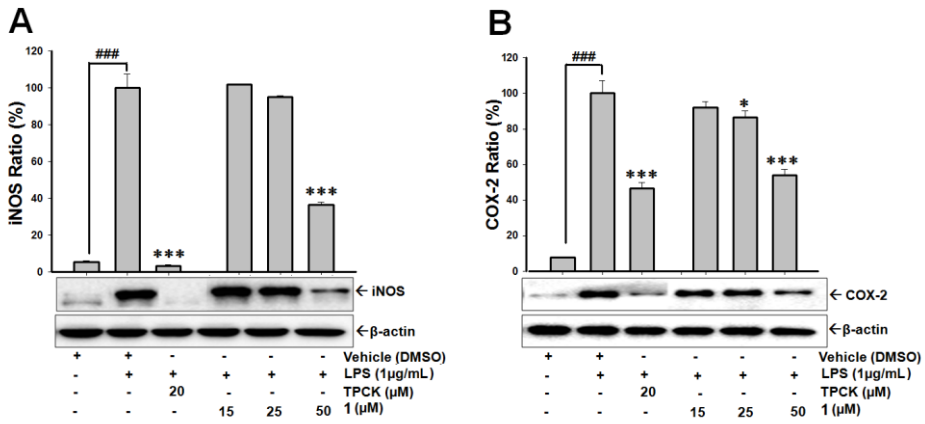

Figure 33. Down-regulation of iNOS (**A**) and COX-2 (**B**) protein expression levels by **1** in LPS (1 μg/ml)-stimulated RAW 264.7 macrophages for 18 h using Western blotting as described in the "Materials and methods". Data are expressed as the means ± S.D. from three separate experiments. (*) P <0.05, and (***) P <0.001 indicate significant differences from the LPS (1 μg/mL)-treated group. ($^{###}$) P <0.001 indicates a significant difference from the unstimulated control group. *N*-*p*-Tosyl-L-phenylalanyl chloromethyl ketone (TPCK 20 μM) was used as a positive control.

*3.3. Effect of **1** on NF-κB signaling pathway*

NF-κB transcription factor has been shown to play a significant role in LPS-induced expression of pro-inflammatory mediators, including iNOS and COX-2 [92]. To investigate the molecular mechanism of inhibition of iNOS and COX-2 transcription mediated by **1**, NF-κB transcriptional activity was investigated using a reporter gene assay system. RAW 264.7 cells were stably transfected with a pNF-κB-secretory alkaline phosphatase (SEAP)-NPT plasmid containing four copies of the κB sequence fused to SEAP as the reporter [91]. LPS treatment of the transfected cells for 18 h increased the SEAP expression approximately 6.6-fold over the basal level (**Fig. 34**). The pretreatment of cells with **1** inhibited LPS-induced SEAP expression significantly in a concentration-dependent manner, corresponding to 20.9±6.1% at 5 μM, 56.6±4.6% at 15 μM, 69.1±0.7% at 25 μM, and 90.3±2.5% at 50 μM. As a positive control, TPCK also showed a significant inhibitory effect on NF-κB transcription activity (**Fig. 34**).

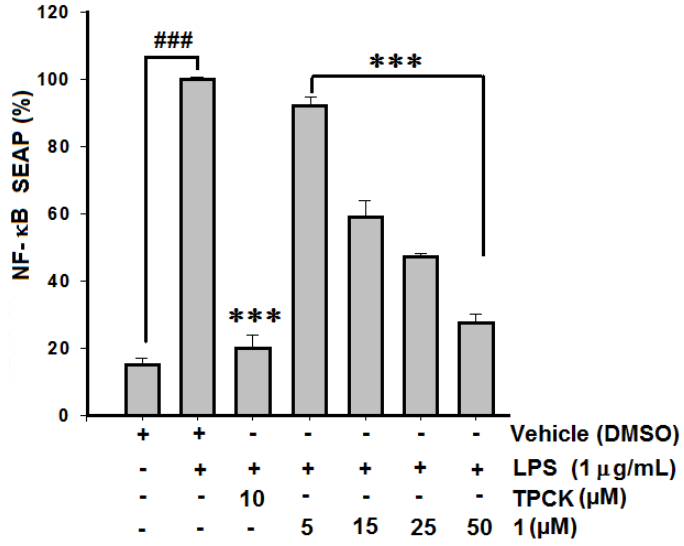

Figure 34. Effect of **1** on NF-κB-dependent alkaline phosphatase (SEAP) expression in transfected RAW 264.7 macrophages. Data were derived from three independent experiments and are expressed as the means ± S.D. (***) $P<0.001$ indicates a significant difference from the LPS (1 μg/ml)-challenged for 18 h incubation group. ($^{###}$) $P<0.001$ indicates a significant difference from the unstimulated control group. *N*-*p*-Tosyl-L-phenylalanyl chloromethyl ketone (TPCK 10 μM) was used as a positive control.

Since phosphorylation of inhibitory κB (IκB) and its subsequent degradation is a critical step in NF-κB activation by various stimuli [33], the effect of **1** on LPS-induced degradation and phosphorylation of IκBα protein was investigated by immunoblot analysis. A time-course experiment showed that the phosphorylated forms of IκBα were barely detectable at 5 min in LPS-stimulated RAW 264.7 cells. However, on exposure to LPS (1 μg/ml) alone for 15 min, IκBα phosphorylation was manifested. LPS-mediated IκBα phosphorylation was inhibited by **1** after 15, and 20 min at 50 μM (**Fig 35A**). Furthermore, the IκBα degradation was completely protected after 10 and 20 min of LPS (1 μg/ml) stimulation at 50 μM (**Fig. 35B**).

To elucidate the inhibitory mechanism on NF-κB and AP-1 activation, the DNA binding activity of NF-κB and AP-1 of **1** in LPS-stimulated RAW 264.7 macrophages was determined, which was analyzed by EMSA with NF-κB and AP-1 specific ^{32}P-labeled oligonucleotides. The RAW 264.7 cells increased the DNA binding activity of NF-κB and AP-1 complexes significantly upon exposure to LPS alone for 1 h (**Fig. 36**). On the other hand, **1** suppressed the LPS-induced DNA binding activity of NF-κB and AP-1 complexes in a dose-dependent manner (**Fig. 36**). For the competition assay, EMSA were performed with excess amounts of unlabeled NF-κB oligonucleotide. The results obtained showed that the LPS-stimulated nuclear extract with excess unlabeled NF-κB oligonucleotide before EMSA abolished NF-κB DNA binding (**Fig. 37**).

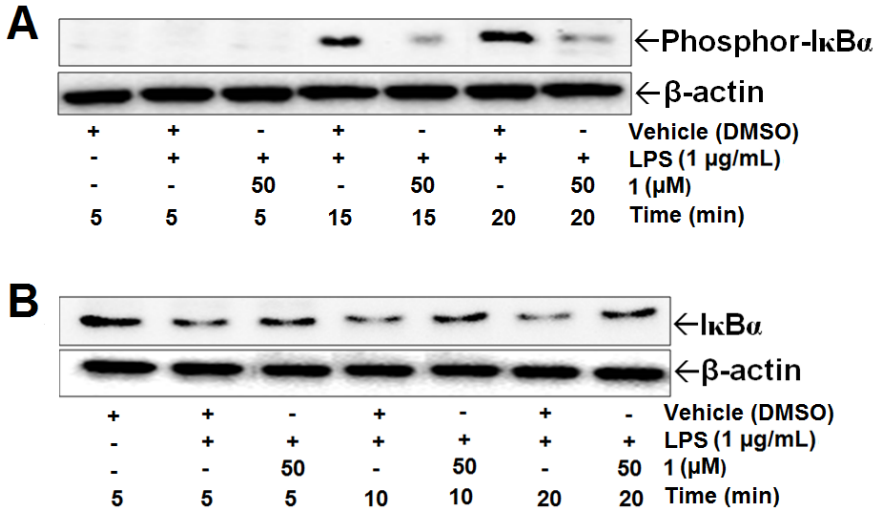

Figure 35. Effect of **1** on (**A**) The expressions of phosphorylated IκBα and (**B**) IκBα protein in cytosolic extracts were determined by Western blot analysis, as described in the "Materials and methods". The RAW 264.7 cells were pretreated with 50 μM of **1** for 2 h and treated with LPS (1 μg/ml) for the time periods specified.

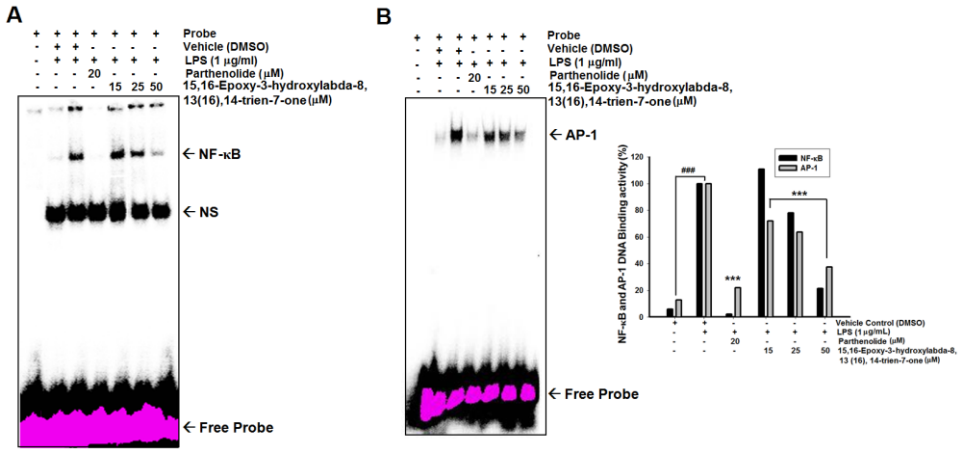

Figure 36. Effect of **1** on NF-κB and AP-1 DNA binding activity. An electrophoretic mobility shift assay (EMSA) was performed as described in the "Materials and methods". RAW 264.7 macrophages were pretreated with the indicated concentrations of **1** for 2 h and stimulated with LPS (1 μg/ml) for 1 h. Then, 5 μg (NF-κB) and 3 μg (AP-1) from nuclear extracts were incubated with a ^{32}P-labeled oligonucleotides specific to NF-κB and AP-1 and electrophoresed on a 6% PAGE. The EMSA result is represented, NF-κB complexes (**A**), AP-1 complexes (**B**), nonspecific signals (NS), and excessive probe are indicated by arrows.

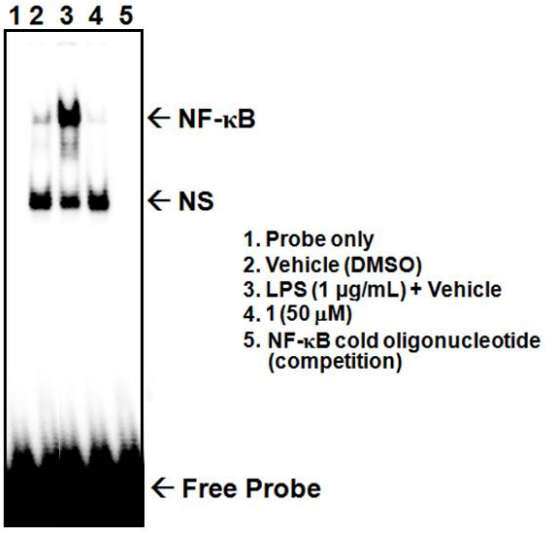

Figure 37. EMSA competition assay. An electrophoretic mobility shift assay (EMSA) was performed as described in the "Materials and methods". RAW 264.7 macrophages were pretreated with the indicated concentrations of **1** for 2 h and stimulated with LPS (1 μg/ml) for 1 h. For competition assay a 50-fold excess of unlabeled NF-κB oligonucleotide was added to the reaction mixture as a competitor. Then, 5 μg from nuclear extracts were incubated with ^{32}P-labeled oligonucleotide specific to NF-κB and electrophoresed on a 6% PAGE. An EMSA result is represented; NF-κB complexes, nonspecific signals (NS), and excessive probe are indicated by arrows. Lane (1) Probe alone, lane (2) the control or vehicle, lane (3) the LPS-stimulated nuclear extract, lane (4) **1** 50 μM, lane (5) the unlabeled NF-κB oligonucleotide.

In order to evaluate more specifically whether **1** can affect the nuclear translocation of NF-κB, Western immunoblot analysis for NF-κB p50 and p65 was conducted with nuclear extracts of LPS-stimulated RAW 264.7 macrophages. The amounts of NF-κB p50 and p65 in the nucleus were increased significantly upon exposure to LPS alone (**Fig. 38**). The LPS-induced nuclear translocation of NF-κB p50 and p65 was inhibited by **1** in a dose-dependent manner (**Fig. 38**).

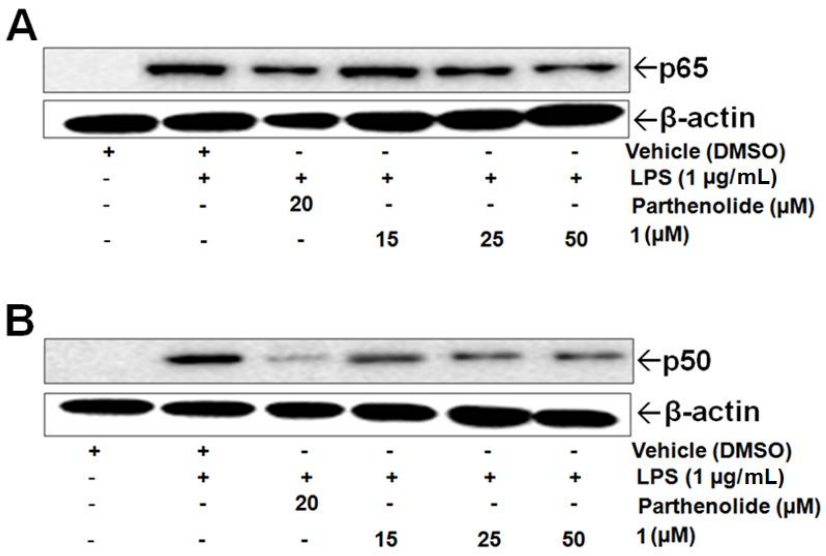

Figure 38. Effect of 1 on NF-κB subunits (**A**) p65 and (**B**) p50 nuclear protein levels using Western blot analysis as described in the "Materials and methods". Parthenolide (20 μM) was used as a positive control.

*3.4. Effect of **1** on LPS-induced TNF-α production*

After the observation that **1** reduces the activation of the two critical pro-inflammatory transcription factors NF-κB and AP-1, the potential effect was investigated of **1** on TNF-α, another important target mediator of inflammation. Treatment of LPS-stimulated macrophages with **1** led to a reduction of TNF-α secretion with in RAW 264.7 cells, with an IC_{50} value of 38.5±1.63 μM (**Table. 1**). Therefore, **1** attenuated the release of a crucial mediator of inflammatory disease [93].

Table 1. Effect of **1** on TNF-α production in culture medium in LPS-stimulated RAW 264. 7 cells

Compound	**TNF-α % inhibition**				
	5 μM	15 μM	25 μM	50 μM	IC_{50} (μM)
15,16-epoxy-3α-hydroxylabda-8, 13(16),14-trien-7-one	-	16.2	48.5	53.4	38.5

*3.5. Effect of **1** on Akt and MAPKs pathway*

To further explore the inhibitory mechanism of **1**, the Akt signaling pathway was also investigated. The phosphorylated form of Akt was evaluated using Western blotting. A time-course investigation conducted showed that **1** suppressed the phosphorylated form of Akt after 15 and 30 min of stimulation by LPS (**Fig. 39**). These results demonstrate that the inhibition of LPS-induced Akt activation led to the suppression of NF-κB activation, resulting in down-regulation of pro-inflammatory enzymes (iNOS, COX-2) and therefore NO, and TNF-α production. The activation of NF-κB requires phosphorylation of IκB, which then targets IκB for ubiquitination and degradation. Inhibition of Akt, which was demonstrated as suppressed Akt phosphorylation in the present study, caused reduced phosphorylation of IκB and attenuated IκB degradation. This might inhibit translocation of NF-κB to the nucleus, where it generally activates gene transcription [14]. Hence, since IκB kinase is a substrate of Akt [14], activation of Akt might consequently stimulate NF-κB activation. Thus, increased inflammatory mediators may result from convergence of the Akt and NF-κB signaling pathways in LPS-stimulated RAW 264.7 macrophages.

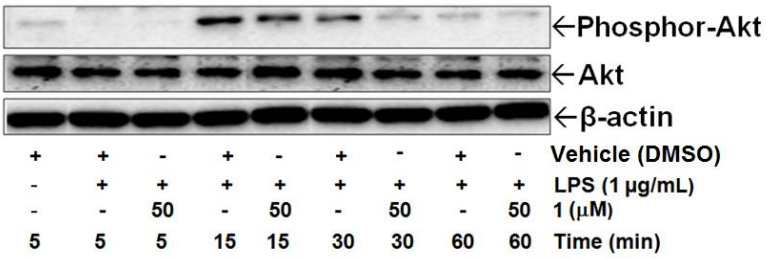

Figure 39. Effect of **1** on Akt. Phosphorylated Akt protein in the cytosolic extract was determined by Western blot analysis, as described in the "Materials and methods". The RAW 264.7 cells were pretreated with 50 μM of **1** for 2 h and treated with LPS (1 μg/ml) for the time periods specified.

When NF-κB and AP-1 are activated simultaneously, the increased level of the NF-κB downstream target gene *elk-1* can be further activated by ERK1/2, p38, and JNK for better induction of *fos* expression and AP-1 activation, which enhance the expression of AP-1 downstream target genes [81]. Several reports have demonstrated the importance of MAPKs in the transcriptional regulation of the LPS-induced inflammatory enzymes (iNOS) through the activation of transcription factors, especially NF-κB or AP-1 [93]. To evaluate whether the inhibition of NF-κB activation and NO production by **1** is mediated through the MAPK pathway, the effect of **1** on LPS-induced phosphorylation of p38 MAPK, JNK, and ERK was investigated using Western blot analysis (**Fig. 40**). A time-course experiment demonstrated that **1** (50 μM) suppressed LPS-induced phosphorylation of p38 MAPK and JNK at 30 min, whereas LPS-mediated ERK phosphorylation inhibition began after 10 min, and was suppressed after 30 min of LPS-stimulation (**Fig. 40**).

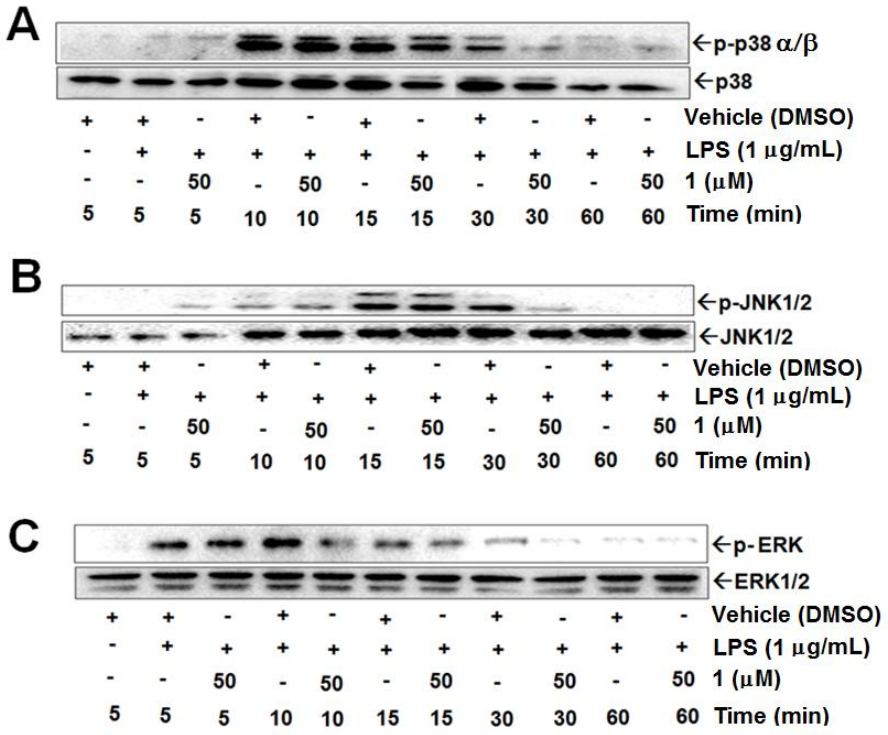

Figure 40. Effect of **1** on MAPKs, (**A**) p-p38α/β (**B**) p-JNK and (**C**) p-ERK protein in cytosolic extracts were determined by Western blot analysis, as described in the "Materials and methods". RAW 264.7 cells were pretreated with 50 μM of **1** for 2 h and treated with LPS (1 μg/ml) for the time periods specified.

4. Discussion

Inflammatory mediators (NO and PGE_2) play significant roles in the process of macrophage activation and are associated with both acute and chronic inflammation [33, 36]. Therefore, the suppression of NO and PGE_2 production by the inhibition of iNOS and COX-2 protein expressions can be a very important therapeutic approach in the development of anti-inflammatory agents. The present study demonstrated that 15,16-epoxy-3α-hydroxylabda-8,13(16),14-trien-7-one significantly inhibit NO production in LPS-stimulated RAW 264.7 cells (**Fig. 32**), likely because of the involvement of iNOS and COX-2 in inflammatory processes. The inhibitory effects of 15,16-epoxy-3α-hydroxylabda-8,13(16),14-trien-7-one were caused by decrease in iNOS and COX-2 protein expressions in a dose-dependent manner.

NF-κB and AP-1, mediate the expressions of iNOS and COX-2 in immune and inflammatory processes. Specifically, the regulation of iNOS and COX-2 via the NF-κB pathway is an important mechanism in inflammatory responses [37]. From the NF-κB-SEAP reporter gene assay system and EMSA experiment, we found that **1** exhibited an inhibitory effect on NF-κB activation (**Fig.34**). It is well known that the degradation of IκBα following phosphorylation of IκBα and the rapid translocation of NF-κB subunits are essential processes for the activation of NF-κB in response to various stimuli. Therefore, we investigated the effect of **1** on the phosphorylation of IκBα and the translocation of p65 and p50 subunits into the nucleus. Similar to the effect of **1** on NF-κB, the phosphorylation and degradation of IκBα and the nuclear translocation of p65 and p50 proteins were all significantly inhibited in LPS-stimulated RAW 264.7 cells that had been pretreated with **1**.

MAPKs are a highly conserved family of protein serine/threonine kinases and have been shown to play important roles in iNOS and COX-2 up-regulation induced by various stimuli. Several studies have shown that the phosphorylation of MAPKs and the subsequent activation of AP-1 are also involved in LPS-induced iNOS and COX-2 expressions [37]. Our data indicated that **1** inhibited the phosphorylation of ERK, JNK and p38 MAPK (**Fig. 40**) as well as the transcriptional activity of AP-1 (**Fig. 36B**) in the LPS-stimulated RAW 264.7 cells.

PI3K and its downstream target kinase, Akt, appear to be important components of LPS-induced NF-κB activation following its translocation to the nucleus [36]. Additional experiments were carried out to assess the upstream signaling proteins controlling NF-κB, AP-1 and MAPK. The inhibition of the LPS-induced Akt activation, which was demonstrated as the decreased phosphorylation of Akt by **1**, caused decreased phosphorylation and degradation of IκBα in LPS-stimulated RAW264.7 cells.

D. Anti-inflammatory mechanism of capillarisin in LPS-stimulated RAW 264.7 cells

1. Introduction

Inflammatory responses can be triggered by physical or chemical trauma, invading organisms and antigen-antibody reactions and are often exacerbated by the resultant swelling, tissue edema, and pain due to increased pressure in tissues caused by the formation of edema, inflammatory mediators (enzymes and cytokines) or even cell damage [94]. Various infectious agents such as bacteria and viruses caused inflammation [95] via induction of several interconnecting mechanisms, generally through specific surface molecules called pathogen-associated molecular patterns, which bind to Toll-like receptors (TLRs) [96] and lead to the release of a wide variety of inflammatory mediators. TLR4, the most studied receptor, recognizes lipopolysaccharide (LPS), the major component of the outer membrane of Gram-negative bacteria [97]. The LPS-initiated signaling cascade leads to the stimulation of both a myeloid differentiation primary response gene (88) (MyD88)-dependent and a MyD88-independent pathway [98] involving the NF-κB, MAPKs and PI3K/Akt pathways. Intracellular signaling depends on binding of the intracellular TLR domain, TIR (Toll/IL-1 receptor homology domain), and IRAK (IL-1 receptor-associated kinase), a process that is facilitated by two adapter proteins, MyD88 (myeloid differentiation protein 88) and TIRAP (TIR domain containing adapter protein; also called MyD88-adapter-like protein or Mal), and inhibited by a third protein, Tollip (Toll-interacting protein). The activation of NF-κB is regulated by IκB kinase (IKK) [40]. Numerous pathogens, such as bacteria,

viruses, pro-inflammatory cytokines, and IκB proteins, are phosphorylated, ubiquitinated, and then rapidly degraded by the proteasome, allowing NF-κB nuclear translocation and the transcriptional initiation of NF-κB-dependent genes. NF-κB is activated when IκB is phosphorylated by IKK [40]. The functions of NF-κB gene targets span diverse cellular processes, including adhesion, immune regulation, apoptosis, proliferation, and angiogenesis [45].

LPS activates monocytes and macrophages by binding to TLR4, and stimulates the production of inflammatory cytokines (tumor necrosis factor-α (TNF-α) and enzymes (nitric oxide (NO) and PGE_2) [43]. TNF-α- and NO-mediated signaling play various physiological processes, including immune defense and smooth muscle relaxation [99]. However, over expression of TNF-α, NO and PGE_2 are responsible for the origin and progression of inflammatory diseases ([100].

The employment of a variety of anti-inflammatory agents may be helpful in the therapeutic treatment of pathologies associated with inflammation. The development and utilization of more effective anti-inflammatory agents of natural origin are therefore required. This present study reports that a plant-derived molecule, capillarisin, exhibited anti-inflammatory properties. Capillarisin, a naturally occurring chromone, was isolated from the plant species *Artemisia capillaris. A. capillaris* is a well known traditional herb used as diuretics, analgesics and anti-inflammatory [101], anti-obesity [102], and liver protective [103] effects. Due to significant anti-inflammatory properties of *A. capillaris*, we next focus on the maker compound of this herb in *in vitro* model. The results demonstrated that capillarisin effectively suppressed LPS-induced signaling through the NF-κB, Akt and MAPKs pathways by inhibiting MyD88 and TIRAP-mediated signaling mechanisms. The current study was undertaken to assess

the anti-inflammatory properties of capillarisin and attempted to establish the possible mechanisms involved in its action.

2. Materials and methods

2.1. Plant materials

The whole plants of *Artemisia capillari*s Thunberg (Compositae) was purchased at the local retailer and authenticated by Prof. J. H. Lee (Dongguk University, Korea). The voucher specimen (No. 20090920) was deposited to Prof. J. S. Choi's laboratory, Pukyong National University, Korea. The whole plants were dried and grinded to powder. Capillarisin was isolated according to the previous report [104]. The purity was determined by HPLC as described elsewhere [104].

2.2. Cells and culture medium

RAW 264.7 murine macrophages were obtained from American Type Culture Collection (Manassas, VA). These cells were maintained at sub-confluence in a 95% air and 5% CO_2 humidified atmosphere at 37°C. For routine subculturing, Dulbecco's modified Eagle's medium (DMEM) supplemented with 10% fetal bovine serum (FBS), penicillin (100 units/ml), and streptomycin (100 μg/ml) was used. The RAW 264.7 cells harboring the pNF-κB-secretory alkaline phosphatase (SEAP)-NPT reporter construct were cultured under the same conditions, except that the medium was supplemented with 500 μg/ml geneticin [105]. All the samples were dissolved in dimethyl sulfoxide (DMSO) to make a 100 mM stock concentration and were then further diluted with DMSO for working

concentrations. Final DMSO concentrations were <0.2% and not to interfere with the assays.

2.3. Cell viability and nitric oxide determination

To determine the cell viability of capillarisin, a MTT assay was carried out according to Khan et al. [33]. Briefly, RAW 264.7 cells were plated at a density of 1×10^5 per well in a 24-well plate and incubated at 37°C for 24 h. The cells were treated with various concentrations (5, 25, 50, 75, and 100 μM) of capillarisin or vehicle alone for 2 h before LPS (1 μg/ml) stimulation and then incubated at 37°C for an additional 20 h. After incubation for 20 h, 100 μl aliquots of the cell-free culture medium were taken for NO measurement according to the Griess reaction method and cell viability was measured as described previously [33]. 2-amino-5,6-dihydro-6-methyl-4*H*-1,3-thiazine (AMT) was used as a positive control. In order to assess the effect of capillarisin on various inhibitors, RAW264.7 cells were pretreated with the 20 μM of each inhibitor, TPCK, SB202190, SP600125, U0126, and LY294002 alone or with capillarisin (100 μM) for 2 h and then treated with LPS (1 μg/ml). After 20 h incubation, the nitrite production was measured.

2.4. Western immunoblot analysis

RAW 264.7 macrophages were pre-treated with the indicated concentrations of capillarisin or vehicle for 2 h and then stimulated with LPS (1 μg/ml) for 5, 10, 15, 20, 30 and 60 min (phosphor-IκBα and, IκBα, p-p38, p-JNK, p-ERK, p-Akt, MyD88, and TIRAP) and 20 h (COX-2, and iNOS). Ten micrograms of total protein for iNOS, IκBα, phosphor-IκBα, p-p38, p38, p-JNK, JNK, p-ERK, ERK, p-Akt, Akt, p65, p50 and 5 μg for COX-2 were separated by SDS-PAGE, 8% (iNOS, and COX-2) and 10% (phosphor-IκBα,

IκBα p-p38, p38, p-JNK, JNK, p-ERK, ERK, p-Akt, Akt, p65, p50, MyD88, TIRAP and β-actin). After electrophoresis, the proteins were electro-transferred to nitrocellulose membranes (Whatman GmbH, Dassel, Germany), blocked with 5% nonfat milk in TBS-T buffer, and blotted with each primary antibody (1:1000) and its corresponding secondary antibody (1:5000), according to the manufacturer's instructions. The antibodies were detected with the WEST-SAVE Up™ luminol-based ECL reagent (LabFrontier, Seoul, Korea). The target bands were quantified using UN-SCAN-IT™ software Version 6.1 (Silk Scientific Co., Orem, UT).

2.5. RNA extraction and reverse transcriptase (RT)-PCR

RT-PCR was performed using easy-BLUE^{TM} total RNA extraction kit (iNtRON Biotechnology, Inc.) according to the manufacturer's recommendations. The purity and concentrations of RNA were determined using the ND-1000 spectrophotometer (Nanodrop Technologies, Wilmington, DE). All of the RNA samples were stored at -80^{o}C until used for analysis. The primer used for the amplifications of iNOS, COX-2 and GAPDH transcripts and the condition for the amplifications were the same as described previously [33], with the modification of the use of 30-40 cycles for amplification. The sense and antisense primers for iNOS were 5′CCCTTCCGAAGTTTCTGGCAGC-3′ and 5′-GGCTGTCAGAGCCTCGTGGCTT-3′, respectively. The sense and antisense primers for COX-2 were 5′-GGAGAGACTATCAAGATAGTGATC- 3′ and 5′-ATGGTCAGTAGACTTTTACA-GCTC-3′, respectively. The sense and antisense primers for rat GAPDH mRNA expression (used as a control for total RNA content for each sample) were 5′-TGAAGGTCGGTGTGAACGGATTTGGC-3′ and 5′-

CATGTAGGCCATGAGGTCCACCAC-3′, respectively. RT-PCR was performed using the one-step-RT-PCR PreMix kit (Intron Biotechnology) according to the manufacturer's instructions. The amplified cDNA products were separated by 2% agarose gel electrophoresis and stained with ethidium bromide. The gels were viewed using the Doc-It LS Image Analysis software (UVP Inc, Upland, CA) and quantified using the UN-SCAN-IT™ software version 6.1 (Silk Scientific Co, Orem, Utah). The PCR products were normalized to the amount of GAPDH for each band.

2.6. Dtermination of pro-inflammatory cytokines by quantitative real-time (qRT)-PCR

RT-PCR was performed with total RNA extracted using easyBlue™, according to the manufacturer's recommendations (Sigma-Aldrich, St Louis, MO). The purity and concentrations of RNA were determined using the ND-1000 spectrophotometer (Nanodrop Technologies, Wilmington, DE). All of the RNA samples were stored at -80^{o}C until used for analysis. Total RNA (1 µg) was converted to cDNA by RT-PCR (Genius FGEN05TD, Teche, England) using iScript^{TM} cDNA Synthesis Kit (BIO-RAD, Hercules, CA) under the following conditions. 25^{o}C for 5 min, 42^{o}C for 30 min and 85^{o}C for 5 min. Quantitative real-time polymerase chain reaction (qRT-PCR) analysis was performed using an Applied Biosystems 7300 real-time PCR system and software (Applied Biosystem, Carlsbad, CA). qRT-PCR was conducted in 0.2 ml PCR tubes with forward and reverse primers and the SYBR green working solution (iTaq^{TM} Universal SYBR Green Supermix, BIO-RAD, Hercules, CA), using customer PCR master mix with following conditions: 95^{o}C for 30 min, followed by 40 cycles of 95^{o}C for 15 sec, x ^{o}C for 20 sec and 72^{o}C for 35 sec. The melting point, optimal conditions and the specificity of the reaction were first determined. The sequences of the PCR

primers were described preciously [69, 70]. The sense and antisense for ; for TNF-α, sense primer, 5′-AGC ACA GAA AGC ATG ATC CG-3′ and antisense primer, 5′-CTG ATG AGA GGG AGG CCA TT-3′; for IL-6, sense primer, 5′-GAG GAT ACC ACT CCC AAC AGA CC-3′, and antisense primer, 5′-AAG TGC ATC ATC GTT GTT CAT ACA-3′; for IL-1β, sense primer, 5′-ACCT GCT GGT GTG TGA CGT T-3′, and antisense primer, 5′-TCG TTG CTT GGT TCT CCT TG-3′, respectively. The sense and antisense primers for rat actin mRNA expression (used as a control for total RNA content for each sample) were 5′-TGAAGGTCGGTGTGAACGGATTTGGC-3′ and 5′-CATGTAGGCCATGAGGTCCACCAC-3′, respectively.

2.7. NF-κB secretory alkaline phosphatase (SEAP) reporter gene assay in transfected-RAW 264.7 cells

The NF-κB SEAP inhibitory activity of capillarisin was determined in LPS stimulated RAW 264.7 macrophages. The NF-κB-dependent reporter gene transcription was analyzed by the SEAP assay, as described previously with some modifications [33, 36]. In brief, 1×10^5 RAW 264.7 macrophages transfected with pNF-κB-SEAP-NPT, encoding four copies of the -κB sequence and the SEAP gene as a reporter, were pre-incubated with different concentrations of capillarisin for 2 h and were then challenged with LPS (1 μg/ml) for an additional 20 h. *N-p*-tosyl-L-phenylalanyl chloromethyl ketone (TPCK, 30 μM) was used as the positive control for this experiment.

2.8. Electrophoretic mobility shift assay (EMSA)

EMSA was performed to investigate the inhibitory effect on NF-κB and AP-1 DNA binding, as described previously [33, 36]. Briefly, nuclear extracts prepared from LPS (1 μg/ml)-treated cells were incubated with ^{32}P-

end-labeled 22-mer double-stranded NF-κB and AP-1 consensus oligonucleotides (Promega, sequence: 5′-AGT TGA GGG GAC TTT CCC AGG C-3′, and 5′-(CGC TTG ATG AGT CAG CCG GAA)-3′) for 30 min at room temperature. To verify the specificity for NF-κB, a 50-fold excess of unlabeled NF-κB oligonucleotide was added to the reaction mixture as a competitor. For the super-shift assay, 5 µg of the p65, and p50 antibodies were added, followed by 30-min incubation at room temperature. The DNA protein complexes were then separated from the free oligonucleotides on 6% native polyacrylamide gels. The signals obtained from the dried gel were quantified with an FLA-3000 apparatus (Fuji), using the BAS reader version 3.14 and Aida version 3.22 software (Amersham Biosciences, Piscataway, NJ). The binding conditions were optimized as reported earlier [33].

2.9. Measurement of TNF-α production

TNF-α production in the culture medium was determined using a commercially available TNF-α ELISA kit (eBioscience, Inc., San Diego, CA).

2.10. Determination of PGE_2 levels in RAW 264.7 cells

The methodology used was similar to that described previously [106]. For measurement of PGE_2 levels, a standard sandwich ELISA technique was used according to the recommendations of the manufacturer (Cayman Chemical, Ann Arbor, MI).

2.11. Statistical analysis

Unless otherwise stated, results are expressed as the means ± standard deviations (S.D.) from three different experiments. One-way analysis of variance (ANOVA) followed by Dunnett's *t*-test was applied to

assess the statistical significance of the differences between the study groups (SPSS version 10.0, Chicago, IL). A value of $P < 0.05$ was chosen as the criterion for statistical significance.

3. Results

3.1. Effect of capillarisin on cell viability, nitric oxide, and PGE_2 levels

Cell viability was evaluated by the MTT assay (**Fig. 41B**). Capillarisin was found to be nontoxic at concentrations up to 100 μM (**Fig. 41B**). Consequently, nontoxic concentrations were used in subsequent experiments.

The effect of capillarisin on nitric oxide (NO) production in LPS-stimulated RAW 264.7 macrophages was determined initially. To determine NO production, we measured the nitrite released into the culture medium. RAW 264.7 cells were treated with various concentrations of capillarisin (5, 25, 50, 75, and 100 μM) for 2 h before the addition of LPS (1 μg/ml). Incubation with LPS alone markedly increased NO production compared to that generated under control conditions (**Fig. 42A**). However, pretreatment with capillarisin prevented this increase in NO production in LPS-stimulated macrophages in a concentration-dependent manner (**Fig. 42A**). A significant suppression was observed with 25 μM capillarisin.

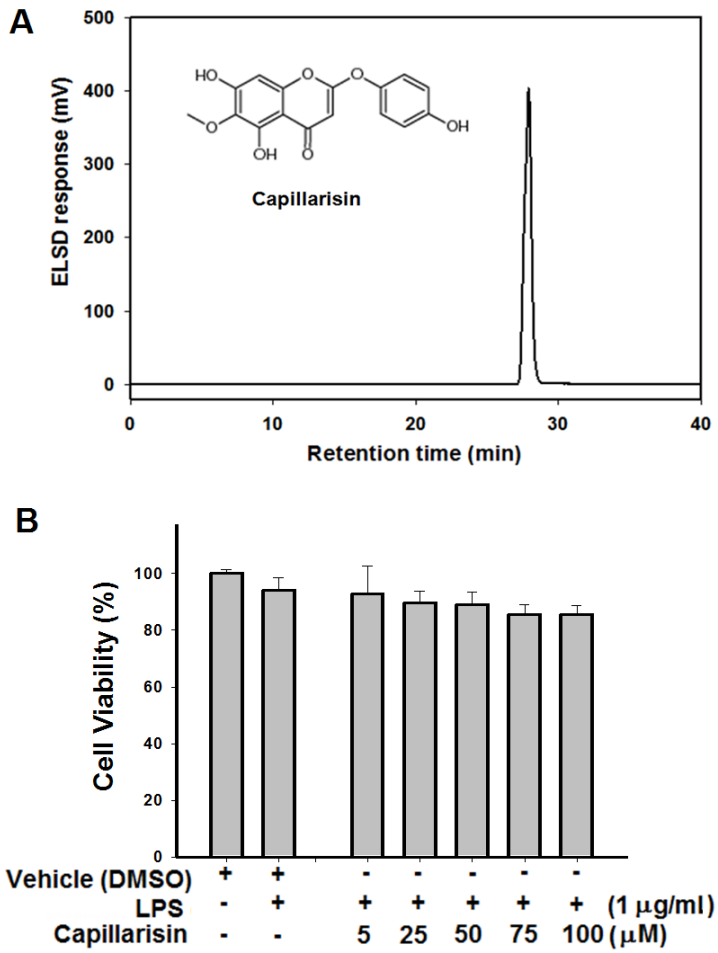

Figure 41. (A) Chemical structure and purity of capillarisin (B) Effect of capillarisin on cell viability in LPS-stimulation using RAW 264.7 macrophage cells. Cell viability was evaluated as described in the "Materials and methods".

Capillarisin also inhibited the LPS-induced increase in the production of the secreted form of PGE_2 in the media in a dose-dependent manner (**Fig. 42B**). PGE_2 production decreased significantly, from 688.84±113.60 pg/ml in controls to 354.8±46.32 pg/ml and 108.12±2.37 pg/ml in the media when treated with 50 and 100 μM capillarisin, respectively (**Fig. 42B**). This considerable decrease in the PGE_2 level is in good agreement with the COX-2 inhibitory effect seen in LPS-stimulated macrophages. Treatment with 50 μM celecoxib, a COX-2 inhibitor, was also shown to have potent inhibitory activity on the PGE_2 level.

3.2. Effect of capillarisin on the mRNA and protein expression levels of the inflammatory enzymes iNOS and COX-2

Because capillarisin was found to inhibit NO production, the relationship between capillarisin levels and the mRNA and protein levels of iNOS and COX-2 was examined by Western blot analysis and RT-PCR. The levels of iNOS and COX-2 protein were markedly up-regulated after 20 h of LPS (1 μg/ml) treatment, and capillarisin significantly attenuated iNOS and COX-2 protein expression in LPS-stimulated RAW 264.7 cells in a concentration-dependent manner (**Fig. 43**). The effects of capillarisin on iNOS and COX-2 mRNA expression were also evaluated (**Fig. 43**). RT-PCR analysis showed that the reduction in iNOS and COX-2 mRNA correlated with a reduction in the corresponding protein levels.

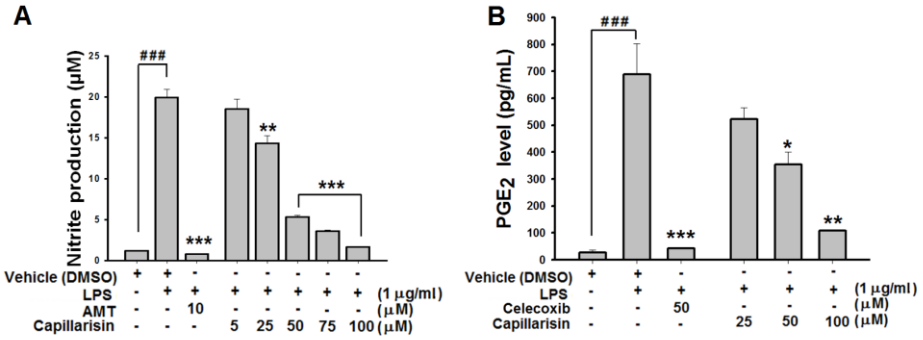

Figure 42. (**A**) Effect of capillarisin on nitrite production using RAW 264.7 macrophage cells. (**B**) Capillarisin inhibits PGE_2 production in LPS-challenged RAW264.7 macrophages as assessed by ELISA. Data were obtained from at least three independent experiments and are expressed as the mean±S.D. (**) $P<0.01$ and (***) $P<0.001$ indicate a significant difference from the LPS-challenged group. $^{###}P<0.001$ represents a significant difference from the vehicle control. Control (DMSO treated, 0.2%); LPS (LPS+ DMSO)-treated cells alone; Celecoxib (50 μM) was used as a positive control.

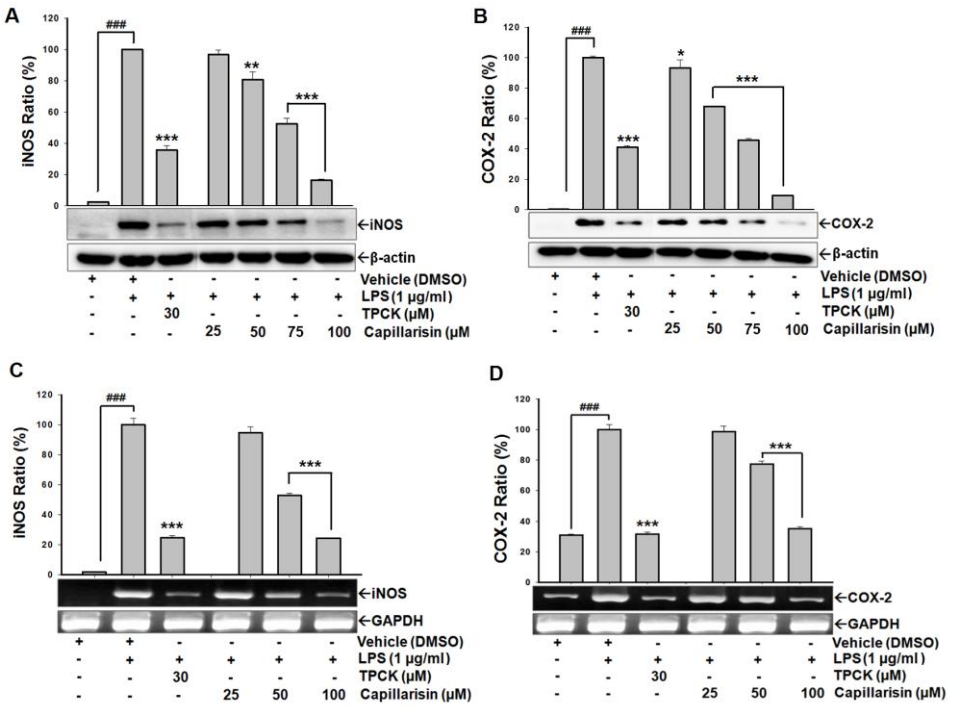

Figure 43. Down-regulation of iNOS and COX-2 proteins and mRNA expression by capillarisin in LPS-stimulated RAW 264.7 macrophages using Western blotting as described in "Material and methods". (**A**) iNOS protein expression (**B**) COX-2 protein expression (**C**) The effect of capillarisin on iNOS mRNA expression, and (**D**) COX-2 mRNA expression. Data are expressed as the mean±S.D. from three separate experiments. For quantification, the mRNA expression data were normalized to the GAPDH signal. Control (DMSO treated, 0.2%), LPS; (LPS + DMSO)-treated cells alone, and TPCK served as a positive control. (*) P <0.05, (**) P < 0.01 and (***) P < 0.001 indicate significant differences from the LPS-treated group. ($^{###}$) P < 0.001 indicate a significant difference from the unstimulated control group.

3.3. Inhibitory effect of capillarisin on NF-κB SEAP, nitrite production, phosphorylation of IKKα/β, and the phosphorylation and degradation of IκBα in macrophages

NF-κB activation is a critical event in the LPS-induced activation of several inflammatory genes, including iNOS and COX-2 [55]. We therefore investigated the effect of capillarisin (5, 25, 50, 75, and 100 μM) on the LPS-induced activation of NF-κB in macrophage cells. NF-κB activation was detected by measuring NF-κB-dependent transcription in macrophages that were stably transfected with a luciferase reporter construct. Cells incubated with LPS alone showed remarkable increases in NF-κB activity. The increased activity was dose-dependently affected and significantly inhibited by capillarisin (**Fig. 44A**). The NO level was also investigated using transfected-RAW 264.7 cells. The results demonstrated that capillarisin potently inhibited NO production in a dose-dependent manner in transfected RAW 264.7 macrophages (**Fig. 44A**).

The stimulation of macrophages with LPS triggers the activation of IKK and the concomitant phosphorylation and degradation of the IκB complex, allowing free NF-κB to translocate into the nucleus to activate genes with NF-κB binding regions. **Fig. 44A** shows that capillarisin inhibited NF-κB, which is known to activate various pro-inflammatory genes. Therefore, the Western blots were used to investigate the NF-κB signaling pathway to determine whether capillarisin blocked any signals leading to the nuclear translocation of NF-κB (**Fig. 44B**). The time course experiments show that, following LPS stimulation, the levels of IKKα/β increased with time. Treatment with capillarisin blocked the increase in IKKα/β after 15 and 30 min of LPS stimulation (**Fig. 44B**). Next, we used Western blot analysis to determine whether treatment with capillarisin caused the inhibition of

LPS-induced NF-κB activation by inhibiting IκBα phosphorylation or degradation (**Fig. 44C, 44D**). Capillarisin inhibited IκBα phosphorylation after 5 and 10 min of LPS stimulation (**Fig. 44C**). However, IκBα degradation was prevented only after 10 and 15 min as shown in **Fig. 44D**.

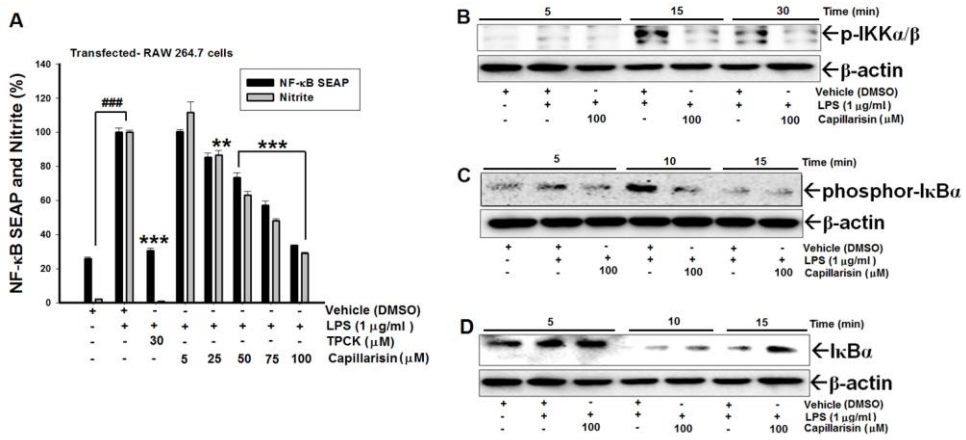

Figure 44. (**A**) Dose-dependent suppression of LPS-induced and NF-κB-dependent alkaline phosphatase (SEAP) expression (RFU= %) and nitrite production (μM= %) by capillarisin in transfected RAW 264.7 macrophages. Data were derived from three independent experiments and are expressed as the mean±S.D. (**) *P <0.01* and (***) *P <0.001* indicate a significant difference from the LPS-challenged group. $^{###}P<0.001$ indicates a significant difference from the unstimulated control group. Control (DMSO 0.2%), LPS; (LPS + DMSO)-treated cells alone; 30 μM TPCK (*N*-*p*-tosyl-L-phenylalanyl chloromethyl ketone) was used as a positive control. The effect of capillarisin on (**B**) the level of phosphorylated IKKα/β, (**C**) phosphorylated IκBα, and (**D**) IκBα protein in cytosolic extracts as determined by Western blot analysis, described in the Materials and methods.

3.4. Effect of capillarisin on NF-κB-DNA binding activity and NF-κB subunits (p65 and p50)

To further investigate the mechanism of capillarisin-mediated inhibition of pro-inflammatory mediators, NF-κB, which is a known transactive element of iNOS and COX-2, was focused [107]. We initially presumed that capillarisin inhibits the production of pro-inflammatory mediators via the NF-κB pathway. To confirm whether capillarisin affects the translocation of NF-κB, the DNA-binding activity of NF-κB was investigated by EMSA. The results demonstrated that the DNA binding activity of NF-κB was significantly reduced in nuclear extracts obtained from LPS-activated macrophages pretreated with capillarisin and parthenolide (**Fig. 45**).

To specify and indentify the particular isoform of NF-κB in RAW 264.7 macrophages, an EMSA was performed with excess amounts of unlabeled NF-κB oligonucleotide for a competition assay and with antibodies against the typical NF-κB subunits p65 and p50 for a supershift assay (**Fig. 45B**). The results indicate that the slowly migrated band observed in the EMSA is indeed NF-κB (**Fig. 45B**). Moreover, LPS-stimulated nuclear extracts with antibodies against p65 and p50 were considerably supershifted.

In addition, the level of NF-κB subunits p65 and p50 in the nuclear extracts were enhanced in the presence of LPS (1 μg/ml) alone when compared with non-stimulated cells, whereas the nuclear localization of p65 and p50 decreased in a dose-dependent manner with capillarisin treatment (**Fig. 46A, 46B**). These results suggest that capillarisin might interfere with the dissociation of IκB from the NF-κB/IκB cytosolic complex, therefore inhibiting the nuclear translocation of NF-κB.

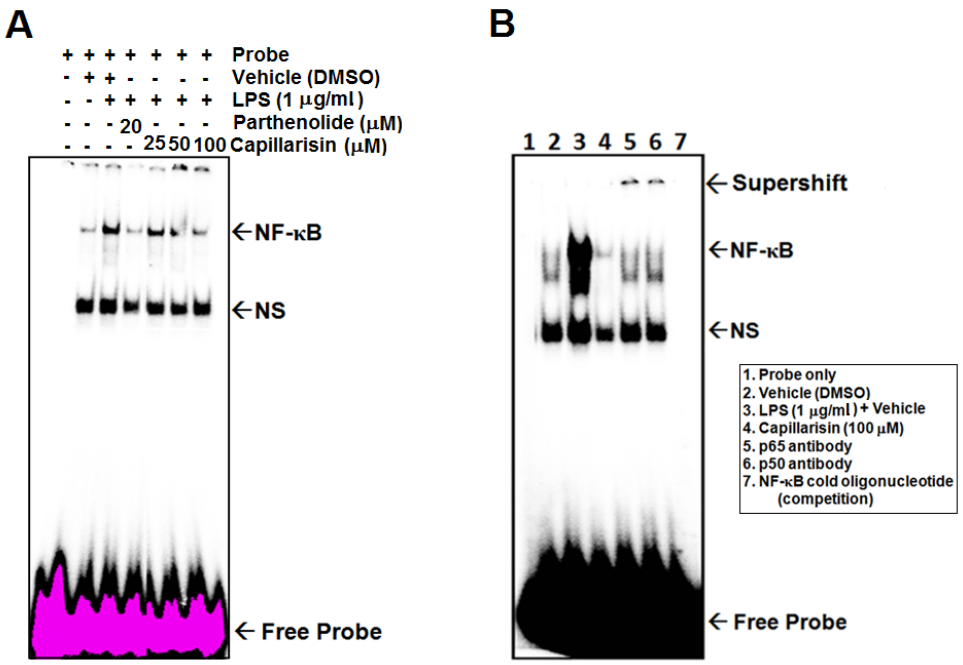

Figure 45. (**A**): Effects of capillarisin on NF-κB DNA binding activity. An electrophoretic mobility shift assay (EMSA) was performed as described in the "Material and methods" section. A representative EMSA result is shown and the NF-κB complexes, nonspecific signals (NS), and excessive probe are indicated by arrows. Parthenolide (20 μM) was used as a positive control. (**B**): Competition and supershift assays for NF-κB DNA binding using (1) probe alone, (2) the control or vehicle, (3) the LPS-stimulated nuclear extract, (4) 100 μM capillarisin, (5) p65 antibody, (6) p50 antibody, and (7) the unlabeled NF-κB oligonucleotide.

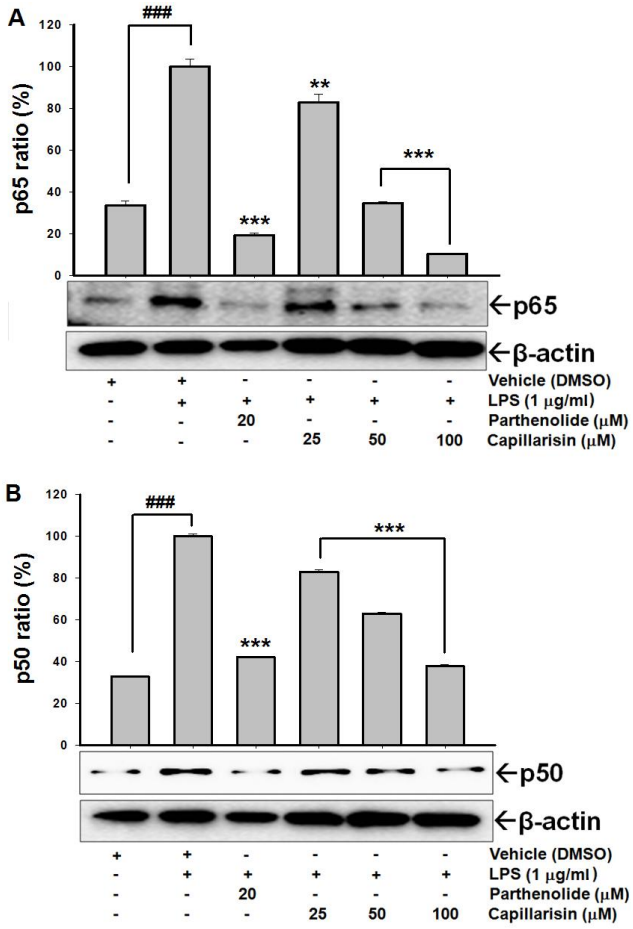

Figure 46. Effect of capillarisin on nuclear protein levels of the NF-κB subunits (**A**) p65 and (**B**) p50 using Western blot analysis as described in the "Materials and methods". Parthenolide (20 μM) was used as a positive control. Data were derived from three independent experiments and are expressed as the mean±S.D. (**) *P <0.01* and (***) *P <0.001* indicate a significant difference from the LPS-challenged group. $^{###}P<0.001$ indicates a significant difference from the unstimulated control group.

3.5. Capillarisin inhibits the LPS-induced upstream MyD88/TIRAP signaling cascade

Various adapters and signaling molecules are involved in TLR4 signaling. A time course evaluation demonstrated that the expression levels of MyD88 and TIRAP were up-regulated following stimulation with LPS (**Fig. 47A, 47B**). Treatment with capillarisin (100 μM) down-regulated the protein expression level of MyD88 after 5, 10, 15, and 30 min of LPS stimulation (**Fig. 47A**). Capillarisin suppressed the expression of the TIRAP protein after 10, 15, and 30 min of LPS stimulation as shown in **Fig. 47B**. Overall, these results indicate that capillarisin inhibits both MyD88 and TIRAP signaling triggered by LPS-activated TLR4.

3.6. Inhibitory effect of capillarisin on LPS-induced Akt and MAPKs pathways

To further scrutinize the suppressive effect of capillarisin, we investigated the effect on the Akt pathway. The phosphorylated form of Akt was evaluated by Western blotting (**Fig. 48A**). The level of p-Akt was not detected after 5 min of LPS (**Fig. 48A**). The time course experiment demonstrated that the p-Akt level is increased after 10 min stimulation with LPS, and this increase was inhibited by capillarisin after 10, 15, 30 and 60 min of LPS treatment (**Fig. 48A**). These results indicate that the suppression of LPS-induced Akt led to the inhibition of NF-κB.

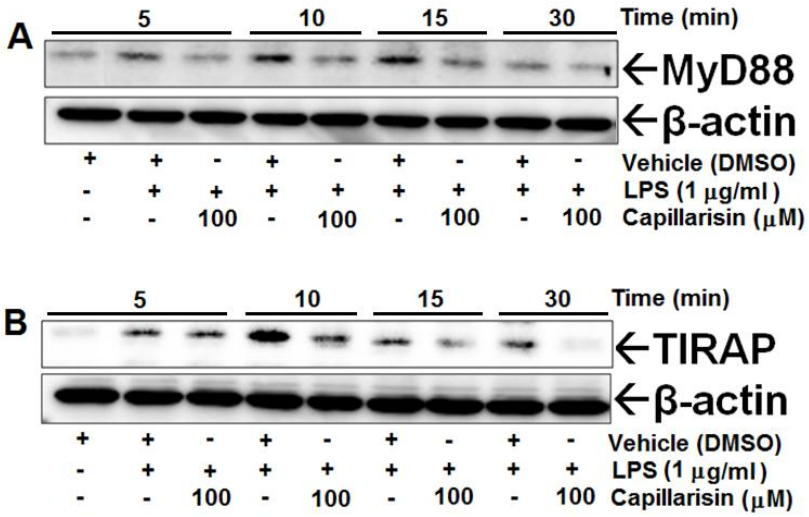

Figure 47. Effect of capillarisin on the expression of (**A**) MyD88 and (**B**) TIRAP protein in cytosolic extracts. Expression levels were determined by Western blot analysis, as described in the "Materials and methods". RAW 264.7 cells were pretreated with 100 μM capillarisin for 2 h followed by treatment with LPS (1 μg/ml) for the time periods specified.

It is well established that the MAPK pathways play a major role in LPS-stimulated iNOS and COX-2 expression levels in macrophage cells [108]. Moreover, MAPKs are also involved in the activation of NF-κB [109, 110]. To investigate whether the inhibition of NF-κB activation by capillarisin (100 μM) was mediated through the MAPK pathway, the LPS-induced phosphorylation of MAPK family proteins, especially p38 MAPK, JNK, and ERK was determined in RAW264.7 cells. As shown in **Fig. 48B, C,** and **D**, capillarisin start inhibiting the LPS-induced activation of p38 and ERK after 5 min and completely inhibited after 60 min of LPS-stimulation (**Fig. 48B**), while activation of JNK was unable to detect after 5 min of LPS. The JNK activation was partially inhibited after 10 min and completely inhibited after 15, and 30 min of LPS stimulation (**Fig. 48C**). The amounts of nonphosphorylated p38 (**Fig. 48B**), JNK (**Fig. 48C**), and ERK (**Fig. 48D**) were unaffected by either LPS or capillarisin treatment. These results indicate that MAPK phosphorylation was inhibited by pretreatment with capillarisin.

In order to further explore the signaling pathway involved in the inhibitory properties of capillarisin on LPS-induced inflammatory mediators, specific inhibitor of the NF-κB inhibitor (TPCK, 20 μM) and MAPKs (SB202190, p38 MAPK inhibitor; SP600125, JNK inhibitor; U0126, ERK inhibitor) and Akt inhibitor (LY294002) were employed (**Fig. 48E**). The pretreatment of macrophages with TPCK, SB202190, SP600125, and LY294002 significantly inhibited LPS-induced nitrite production in the media, while pretreatment of U0126 showed marginal inhibitory effect at 20 μM (**Fig. 48E**). The combination of capillarisin with TPCK, p38 inhibitor, JNK inhibitor, ERK inhibitor and Akt inhibitor profoundly augmented the inhibitory effect of capillarisin on the LPS-induced NO production (**Fig. 48E**). Takentogether, these results suggest that p38 MAPK, JNK, ERK and

Akt conjunction with NF-κB signaling pathway may contribute to the inhibitory effect of capillarisin on inflammatory mediators.

3.7. Effect of capillarisin on AP-1 DNA binding activity in LPS-stimulated macrophages

The activation of the MAPK cascade modulates AP-1 activation. One hypothesis as to the mechanism of the inhibition of MAPK signaling cascades by capillarisin is that the DNA binding ability of AP-1 was reduced through the nuclear translocation of phosphorylated MAPKs. The nuclear AP-1 DNA binding activity was significantly inhibited by treatment with capillarisin compared with non-stimulated cells and cells stimulated with LPS alone, as shown in **Fig. 49**.

3.8. Inhibitory effect of capillarisin on pro-inflammatory cytokines productions

As described above, capillarisin potently inhibited the LPS-induced production of pro-inflammatory enzymes, i.e., iNOS and COX-2. The effect of capillarisin on pro-inflammatory cytokine (TNF-α) expression was further investigated by ELISA. In response to LPS, the expression of TNF-α was markedly up-regulated and treatment with capillarisin significantly inhibited its induction by LPS (**Fig. 50**). Similarly, capillarisin showed remarbale inhibitory effect agaist mRNA levels of pro-inflammatory cytokines (TNF-α, IL-1β, IL-6) (**Fig. 51**). These data suggested that capillarisin may elicit its anti-inflammatory effects through the same transcription factor or pathway,

including NF-κB that regulates the transcription levels of these pro-inflammatory enzymes and cytokines.

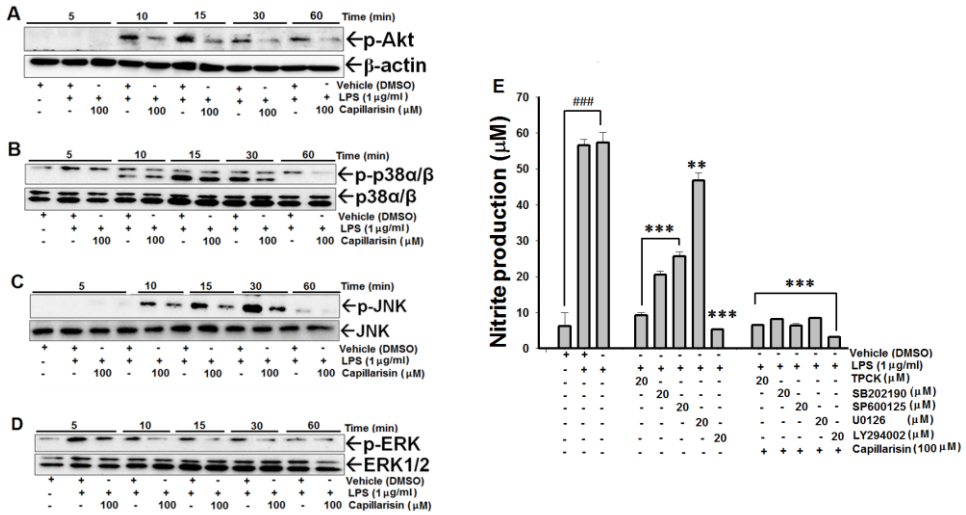

Figure 48. Effect of capillarisin on the Akt and MAPK pathways. (**A**) Phosphorylated Akt, (**B**) p-p38α/β, (**C**) p-JNK, (**D**) p-ERK proteins in cytosolic extracts were determined by Western blot analysis, as described in the "Materials and methods". (**E**) Effects of capillarisin, NF-κB inhibitor, MAPK inhibitors, and Akt inhibitor on LPS-induced nitrite production in RAW264.7 macrophages. The values are expressed as the means ± S.D. of three individual experiments. (**) P<0.05 and (***) P<0.001 indicate significant differences from the LPS-treated group. ($^{\#\#\#}$) P<0.001 indicates significant differences from the combination of LPS with capillarisin-treated group.

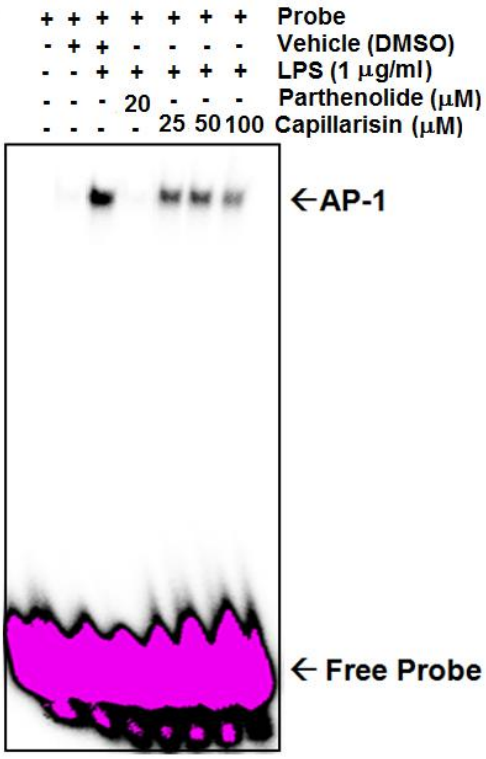

Figure 49. Effect of capillarisin on AP-1 DNA binding activity. An electrophoretic mobility shift assay (EMSA) was performed as described in the Material and methods. A representative EMSA result is shown; AP-1 complexes, nonspecific signals and excessive probe are indicated by arrows.

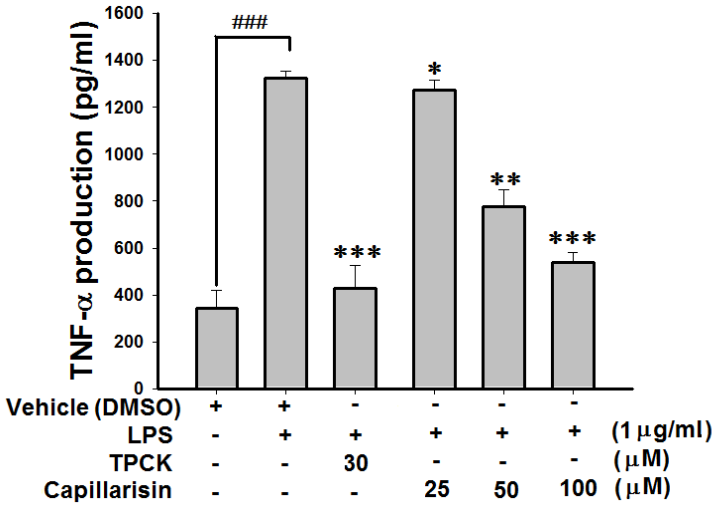

Figure 50. Inhibitory effect of capillarisin on TNF-α production in the culture medium was determined using a commercially available TNF-α ELISA kit. The data were obtained from three independent experiments and are expressed as the mean±S.D. (*) P<0.05, (**) P< 0.01 and (***) P<0.001 indicate significant differences from the LPS-treated group. ($^{###}$) P<0.001 indicates a significant difference from the unstimulated control group. Control (vehicle), LPS (LPS+ vehicle)-treated cells alone. TPCK (30 mM) was used as positive control.

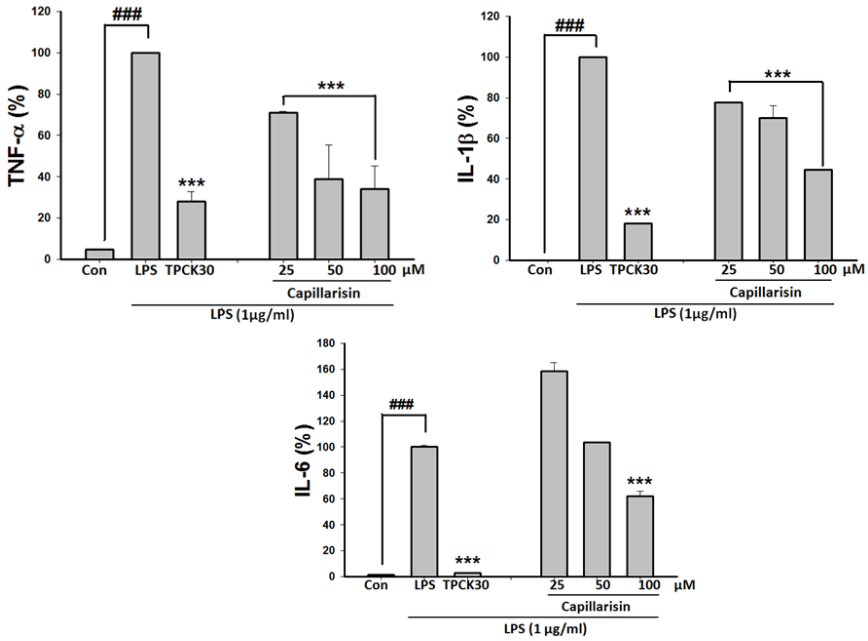

Figure 51. Inhibitory effect of capillarisin on mRNA expression levels of TNF-α, IL-1β and IL-6 were determined by qRT-PCR. The data were obtained from three independent experiments and are expressed as the mean±S.D. (***) P<0.001 indicate significant differences from the LPS-treated group. ($^{###}$) P<0.001 indicates a significant difference from the unstimulated control group. Control (vehicle), LPS (LPS+ vehicle)-treated cells alone. TPCK (30 μM) was used as positive control.

4. Discussion

Natural products have played a considerable role in drug development, especially for diseases that have existed throughout human history. The current study was undertaken to elucidate the pharmacological and biological effects of capillarisin isolated from the *A. capillaris* on the production of inflammatory mediators in LPS-stimulated macrophages and an inflammatory mouse model. Capillarisin exhibited a significant inhibitory effect on LPS-induced NO, PGE_2 and TNF-α production in RAW264.7 cells and its inhibitory effects are accompanied by a decrease in the expression of iNOS and COX-2 mRNA and protein levels in a concentration-dependent manner. This inhibition occurred in parallel with a reduction in the association of I-κB/NF-κB, and activation of MAPKs proteins, and AP-1.

Nitric oxide is recognized as a central mediator and regulator of the inflammatory response. NO is a free radical that is synthesized from *L*-arginine and is centrally involved in inflammation [111]. The production of NO and TNF-α is a critical part of the immune response to some inflammatory stimuli (excessive production of these mediators has been detected in rheumatoid arthritis, hemorrhagic shock, and artherosclerosis) [112]. Therefore, the present study demonstrated the inhibitory effects of capillarisin in terms of reducing LPS-induced NO and PGE_2 production in addition to iNOS and COX-2 expression by blocking NF-κB activation via the MyD88 and TIRAP signaling cascade. Capillarisin significantly suppressed the inflammatory mediators without altering cell viability in RAW 264.7 cells, suggesting that the anti-inflammatory effects of capillarisin were not due to cell death.

NF-κB has a central role in the regulation of the pro-inflammatory regulators inhibited by capillarisin, so it was postulated that capillarisin might suppress NF-κB activation. It was previously demonstrated that capillarisin exhibited significant pharmacological properties such as, inhibition of PMA-induced NF-κB dependent MMP-9 expression [113]. Herein, our investigation of the mechanism involved found that capillarisin inhibited the degradation and phosphorylation of IκBα and the NF-κB subunits p65 and p50. Studies have shown that the phosphorylation and acetylation of p65 plays a major role in the DNA binding and transactivation of NF-κB [114]. Further, IKK has been shown to phosphorylate p65 [115], and it is possible that capillarisin inhibits p65 and p50 through the inhibition of IKK and through cytosolic IκBα protein degradation. Moreover, capillarisin inhibited the nuclear translocation of NF-κB and its DNA binding activity. Based on this evidence, it is believed that the LPS-induced expression of the iNOS and COX-2 genes were suppressed by capillarisin through blocking NF-κB activation. These results show that capillarisin has a major effect on the anti-inflammatory response via the NF-κB pathway.

LPS-activated TLR4 induces the activation of specific intracellular pathways through receptor dimerization and the recruitment of different adaptor molecules such as MyD88 and TIRAP [116, 117]. Studies have shown that TLR4 signals through the MyD88/TIRAP pathway, leading directly to NF-κB activation [118]. These results of the time course experiment demonstrated that capillarisin significantly reduced MyD88 and TIRAP protein expression.

Few studies have directly examined alternative inflammatory signaling pathways such as MAPKs and Akt [36]. The modulation of Akt activity can affect inflammatory genes via NF-κB activation. Additionally,

the MAPKs mediate inflammatory and mitogenic signals to activate transcription factors, particularly NF-κB and AP-1, thereby inducing a battery of inflammatory genes [119]. On the other hand, MAPKs also transiently activate the expression of the iNOS and COX-2 genes in LPS-induced macrophages mediated by NF-κB activation [120]. Our time course experiment demonstrated that capillarisin inhibited the phosphorylation of Akt, p38, JNK, and ERK. Furthermore, the DNA binding ability of AP-1 was significantly reduced by capillarisin. In addition, more specific investigations by using NF-κB inhibitor, Akt inhibitor (LY294002), and specific MAPK inhibitors (SB202190, p38 MAPK inhibitor; SP600125, JNK inhibitor; U0126, ERK inhibitor) showed that the combined treatment of NF-κB inhibitor, Akt inhibitor, p38 inhibitor, JNK inhibitor or ERK inhibitor with capillarisin resulted in a profound suppression of inflammatory mediator (NO) production. Overall, the present study indicates that the inhibition of p38 MAPK, JNK, Akt and ERK phosphorylation is involved in the inhibitory effect of capillarisin on LPS-induced NO production via NF-κB and AP-1 inactivation.

The present findings suggest that pretreatment of capillarisin effectively inhibited LPS-induced TNF-α, IL-1β and IL-6 productions. A cascade of pro-inflammatory cytokines (TNF-α, IL-1β and IL-6) precedes the release of the final inflammatory mediators, i.e., prostaglandins and sympathetic amines [121]. TNF-α and IL-1β stimulates the expression of COX-2 and the subsequent release of prostaglandins [122]. Here we showed that TNF-α release was markedly inhibited by capillarisin. Because the inhibition of TNF-α release might lead to the inhibition of prostanoid production, it is possible that capillarisin acts by preventing inflammatory pain through the inhibition of the production of mediators.

PART III

Anti-nociceptive activity of anomalin and capillarisin

1. Introduction

Pain responses serve as an alert to real or imminent injury and activate appropriate protective responses [123]. Pain often extends beyond its effectiveness as an alarm system and instead becomes persistent and devastating [23, 123]. Inflammatory pain is induced by different chemical mediators released during an inflammatory process, which cause nociceptive sensitization [124]. The sensitization of primary nociceptive neurons is a common denominator for all types of inflammatory pain that lead to a state of hyperalgesia (an increased response to a stimulus that is normally painful) and allodynia (pain due to a stimulus that does not normally provoke pain) [124]. The balance between the production of pro- and anti-inflammatory mediators modulates the intensity of inflammatory hyperalgesia [121]. The inflammatory responses stimulate the release of hyperalgesic enzymes and cytokines that act directly on nociceptors and trigger the release of the final mediators responsible for inflammatory pain [125]. Moreover, the neuronal threshold is reached by the activation of various signaling pathways (NF-κB, CREB and MAPKs), and numerous other transcriptions factors [126].

Initial signaling and modification of the expression of various genes is connected through the NF-κB pathway [127]. Various stimuli such as algogenic agents (CFA and carrageenan), and pro-inflammatory enzymes and cytokines (TNF-α, IL-1β, nerve growth factor) can activate NF-κB, and NF-κB in turn regulates the expression of numerous proteins such as pro-inflammatory mediators [128]. MAPKs play essential roles in inflammatory pain sensitization. Inhibition of ERK and p-38 has been shown to have anti-nociceptive effects in several pain models. Moreover, it was found that cytokine-induced COX-2 expression is mediated via NF-κB in addition to ERK and p38 MAPK in different systems [129-131]. In addition, CREB has

been suggested to contribute to the central sensitization linked with chronic pain [132]. It has been demonstrated that ERK may be involved in the modulation of nociceptive information and central sensitization produced by intense noxious stimuli and/or peripheral tissue inflammation [133].

The previous findings led us to hypothesize that anomalin and capillarisin could produce anti-nociceptive effects via various inflammatory pain signaling pathways, suggesting that anomalin and capillarisin are good potential candidates for the relief of both acute and chronic inflammatory pain. The present work aimed to investigate the anti-nociceptive effect of anomalin and capillarisin using different models of inflammatory pain in mice. Attempts were also made to analyze the possible molecular mechanism of action through which anomalin and capillarisin exerted their effects.

2. Materials and methods

2.1. Animals

Male ICR mice (Samtako, Osan, Korea), 3-4 weeks of age, weighing 30-35 g, were used in the present study. All animal studies were performed in a pathogen-free barrier zone of the Seoul National University Animal Laboratory, according to the procedures outlined in the Guide for the Care and Use of Laboratory Animals (Seoul National University, Korea). The animals were housed at 23±0.5^{o}C with 10% humidity in a 12 h light-dark cycle. Animal care and handling procedures were followed according to the guidelines of the International Association for Study of Pain (IASP) on the use of animals in pain research [134]. Behavioral tests were done without knowing to which experimental group each mouse belonged. All behavioral tests were performed between 9:00 am and 7:00 pm, and animals were used

only once. Every effort was made to minimize the number of animals used and any discomfort. The animals were divided into six groups (control; saline with 10% DMSO, 20 mg/kg dexamethasone, 10 mg/kg anomalin, 50 mg/kg anomalin, 20 mg/kg capillarisin and 80 mg/kg capillarisin). Each group contained 5~7 mice. Anomalin, dexamethasone, and 1% carrageenan were dissolved in 10% DMSO in saline the day before starting the experiment. Drugs were administered by intraperitoneal (i.p.) or intraplantar (i.pl.) routes, and the control group received the vehicle only.

2.2. Behavioral experiments

2. 2. 1. Mechanical hyperalgesic evaluation induced by CFA or carrageenan

To produce a persistent inflammatory response, mechanical hyperalgesia was tested in mice using the Randall Selitto test, performed according previously reported methodology [122, 135, 136]. For the Randall Selitto test, the mice were placed in a quiet room 15-30 min before the beginning of the test. The Digital Randall Selitto test consisted of evoking a hind paw flexion reflex with a handheld force transducer (Digital Paw Pressure Randall Selitto Meter, IITC Life Science Inc., Woodland Hills, CA). The investigator was trained to apply the tip perpendicular to the central area of the hind paw with a gradual increase in pressure. The end point was characterized by the removal of the paw followed by clear movements. After paw withdrawal, the intensity of the pressure was recorded automatically. In order to evaluate the therapeutic effect of anomalin and capillarisin, mice received an i.pl. injection of CFA (20 µl/paw) or carrageenan (100 µg/paw) in the right hind paw. Forty minutes prior to CFA and 1 h prior to carrageenan administration, the animals received an i.p.

injection of saline, dexamethasone (20 mg/kg), anomalin (10 and 50 mg/kg) and capillarisin (20 and 80 mg/kg). To observe the acute effect of anomalin and capillarisin, mechanical nociception was evaluated at different time points (2, 4, and 6 h) using the Randall Selitto test (Digital Paw Pressure Randall Selitto Meter, IITC Life Science Inc.). To investigate the effects of long-term treatment, the development of hyperalgesia was evaluated 4 h after CFA injection from 0-5 days with interval of day four in order to interpret the possible tolerance effect as described previously [137]. The animals were tested before and after treatment. Three consecutive determinations were made at each time point, and the thresholds were averaged for statistical analysis.

2.2.2. Mechanical allodynic evaluation induced by CFA

Mechanical allodynia was analyzed using Von Frey filaments according to the methodology reported previously [138]. For the Von Frey test, mice were placed individually in a transparent plastic box with a mesh floor to allow access to the ventral surface of the hindpaw. Prior to each testing session, the animals were habituated to the testing environment for at least 30 min. Mechanical hypersensitivity was assessed using calibrated Von Frey filaments (Stoelting, USA) by those blinded to the group assignments. Each filament was applied five times to the plantar surface of the right hind paw in an ascending order of force. The withdrawal reflex on at least three of the five applications was defined as a positive response. To assess the inhibitory effects of anomalin and capillarisin on mechanical allodynia, allodynia was induced by ip.l. injection of CFA (20 µl/paw) into the right hind paw. Forty minutes prior to CFA administration, the animals received an i.p. injection of control; saline with 10% DMSO, 20 mg/kg dexamethasone, 10 and 50 mg/kg anomalin, and 20 and 80 mg/kg capillarisin. To observe the acute effect of

anomalin and capillarisin, mechanical nociception was evaluated at different time points (2, 4, and 6 h) using Von Frey test.

2.2. 3. Paw edema test in mice

To investigate the inhibitory effects of 10 and 50 mg/kg anomalin, 20 and 80 mg/kg capillarisin, inflammatory paw edema was induced by ip.l injection of CFA (20 µl/paw) and carrageenan (100 µg/paw) into the right hind paw, as described previously [106, 139, 140]. Forty minutes prior to CFA and 1 h prior to carrageenan administration, the animals received an i.p. injection of saline with 10% DMSO in saline as vehicle control, dexamethasone (20 mg/kg), anomalin (10 or 50 mg/kg), or capillarisin 20 and 80 mg/kg, paw thickness was measured using a dial thickness gauge (No. 2046F, Mitutoyo, Kawasaki, Japan) before the induction of edema and every 2 h afterwards for 6 h. In the chronic pain model, paw thickness was measured before edema induction and every 4 h after the CFA injection for 5 days with interval of day four in order to interpret the possible tolerance effect, as described previously [137].

2.3. Biochemical assays

2.3. 1. Nitric oxide determination

To evaluate the effect of anomalin and capillarisin on NO in blood plasma, all mice (vehicle control, positive control, anomalin and capillarisin groups) were sacrificed after 6 h in acute model and after day 5 in chronic model using CO_2. Blood was collected from all the mice in EDTA tubes and centrifuged at 500 ×g for 10 min at 4°C. Serum was obtained, and NO concentrations were measured using the Griess reaction [33]. Briefly, 50 µl

of blood plasma and 50 µl of saline were mixed with an equal volume of Griess reagent and incubated at room temperature for 30 min. The NO was determined according to method described previously [33].

2.3. 2. Measurements of TNF-α production in CFA-induced paw tissue

The tissue samples from all treated (vehicle, dexamethasone 20 mg/kg, anomalin 10 and 50 mg/kg, and capillarisin 20 and 80 mg/kg) groups for TNF-α determination were prepared according to the method described by de Lima et al. [18, 122, 140]. Briefly, paw skin tissues were removed from the paws four hours after the i.pl injection of CFA in mice. Tissue proteins were extracted from 100 mg tissue/ml PBS to which 0.4 M NaCl, 0.05% Tween 20, and protease inhibitors were added. The samples were homogenized and centrifuged for 10 min at 3000 g, and the supernatant was frozen at -80^{o}C for later quantification. The TNF-α production was determined using a commercially available TNF-α ELISA kit (eBioscience, Inc., San Diego, CA).

2.3. 3. Western immunoblot analysis

Western blot analysis was performed as described previously [36]. Briefly, at the end of treatment, paw skin tissues were removed, and total protein was extracted by using RIPA lyses buffer (Pierce Biotechnology, IL; 25mM Tris-HCl pH 7.6, 150mM NaCl, 1% NP-40, 1% sodium deoxycholate, 0.1% SDS) and protease inhibitors were added immediately before use. The samples were homogenized and centrifuged for 10 min at 3000 *g*, and the supernatant was frozen at -80^{o}C for later quantification. Then, ten micrograms of total protein was used for detection of iNOS, COX-2, IκBα, phosphor-IκBα, p-p38, p-ERK, and β-actin were separated by SDS-PAGE, 8% (iNOS, and COX-2) and 10% (phosphor-IκBα, IκBα p-p38, p-

ERK, and β-actin). After electrophoresis, the proteins were electrotransferred to nitrocellulose membranes (Whatman GmbH, Dassel, Germany), blocked with 5% BSA in TBS-T buffer and blotted with each primary antibody (1:1000) and its corresponding secondary antibody (1:5000) according to the manufacturer's instructions. The antibodies were detected with the WEST-SAVE Up™ luminol-based ECL reagent (LabFrontier, Seoul, Korea). The target bands were quantified using UN-SCAN-IT™ software version 6.1 (Silk Scientific Co., Orem, UT).

2.3. 4. Electrophoretic mobility shift assay (EMSA)

EMSA was performed to investigate the inhibitory effect of anomalin and capillarisin on NF-κB, CREB and AP-1 DNA binding, as described previously [33, 36]. Briefly, at the end of treatment, skin tissues were removed from the paws of mice sacrificed from each experimental group after day five of i.pl. injection of CFA. Nuclear protein extract was prepared by using Buffer A (10 mM HEPES pH 7.9, 1 M HEPES, 10 mM KCL, 0.1 mM EDTA, 0.1 mM EGTA with 1 mM DTT, 0.5 mM PMSF, and protease inhibitors added just before starting the experiment) and Buffer C (20 mM HEPES pH 7.9, 400 mM NaCl, 1 mM EDTA, 1 mM EGTA with 1 mM DTT, 0.5 mM PMSF, and protease inhibitor (PI) added just before starting the experiment). The nuclear extracts were incubated with ^{32}P-end-labeled 22-mer double-stranded NF-κB, CREB and AP-1 consensus oligonucleotides (Promega, sequences: 5′-AGT TGA GGG GAC TTT CCC AGG C-3′, 5´-AGA GAT TGC CTG ACG TCA GAG AGC TAG-3´and 5′-(CGC TTG ATG AGT CAG CCG GAA)-3′) for 30 min at room temperature. The DNA-protein complexes were then separated from the free oligonucleotides on 6% native polyacrylamide gels. The signals obtained from the dried gel were quantified with an FLA-3000 apparatus (Fuji), using the BAS reader version

3.14 and Aida version 3.22 software (Amersham Biosciences, Piscataway, NJ). The binding conditions were optimized as reported earlier [33].

2.3.5. Determination of adenosine 5'-triphosphate (ATP) in blood plasma

The ATP released was determined directly using the firefly luciferin-luciferase (L/L) assay according to Matsuka et al. [141]. At the end of the treatment, blood samples were collected from the retro-orbital plexus of the mice. Biochemical analyses were performed on serum samples obtained after centrifugation of total blood without anticoagulants at 2500 rpm for 10 min. The ATP content was measured using an ATP luminescence detection kit (Molecular Probes, Inc., OR) and a luminometer (TD-20/20, Turner Designs, Sunnyvale, CA).

2.3. 6. Analysis of liver enzymes in blood plasma

The cytotoxic assessment of anomalin and capillarisin and blood biochemical parameters (concentrations of alanine amino transferase/AST aspartate amino transferase/ALT, creatinine, total protein and albumin) was performed after acute and chronic treatment with anomalin and capillarisin. All the mice were weighed and injected daily with a single dose of anomalin (50 mg/kg, i.p.), capillarisin (80 mg/kg, i.p) or vehicle for five days with an interval on day four. At the end of treatment, blood samples were collected from the retro-orbital plexus of the mice. Biochemical analyses were performed on serum samples obtained after the centrifugation of total blood without anticoagulants at 2500 rpm for 10 min. Standardized diagnostic kits using a "FUJI DRI-CHEM 3500i" apparatus (Norderstedt, Germany) were employed in the determination of the AST, ALT, creatinine, total protein and albumin concentrations.

2.3. 7. Histological analysis

To evaluate possible effects of the daily treatment of anomalin and capillarisin on mice paw tissue, histopathological investigation of the paw tissues were performed. Mice were sacrificed using CO_2, and the inflamed paw was removed. Each paw was washed with saline after removal, fixed in 10% formalin solution, rinsed, dehydrated, and embedded in paraffin according to the method described by Khan et al., 2012 and Yen et al., 2009 [140, 142]. Paw tissue blocks were sectioned at 4 μm thickness, stained with hematoxylin-eosin, and observed by microscopy (40×). The inflamed paw sections were further analyzed by determining the number of neutrophils showing inflammation. The H & E stained paw tissue sections were quantified with ImageJ version 1.46r software, Wayne Rasband, NIH, USA.

2.3. 8. Statistical analysis

Unless otherwise stated, results are expressed as the means ± standard deviations (S.D.) from three different experiments. One-way analysis of variance (ANOVA) followed by Dunnett's *t*-test was applied to assess the statistical significance of the differences between the study groups (SPSS version 10.0, Chicago, IL). A value of $P<0.05$ was chosen as the criterion for statistical significance.

3. Results

3.1. Anomalin and capillarisin inhibit mechanical hyperalgesia and allodynia in an acute and chronic inflammatory pain models induced by CFA and carrageenan in mice

The modulatory activity of anomalin and capillarisin on different events and mediators involved in inflammatory pain was investigated in order to understand the mechanisms by which anomalin and capillarisin induces anti-nociception. The anti-nociceptive properties of anomalin and capillarisin were evaluated initially using the Randall Selitto and Von Frey tests in mice, screening tools for the assessment of analgesic properties of new substances. The i.p. administration of anomalin (10 and 50 mg/kg) and and capillarisin (20 and 80 mg/kg) produced a significant inhibition of CFA-induced mechanical hyperalgesia and allodynia in mice after 2, 4 and 6 h of CFA injection (**Fig. 52 and Fig. 53**). Dexamethasone (20 mg/kg, i.p.), a standard used as the positive control, also produced a significant inhibition of the CFA-induced mechanical hyperalgesic and allodynic responses. It is noteworthy that the anti-nociceptive effect was more remarkable after 4 h at 50 mg/kg (anomaline) and 80 mg/kg (capillarisin), respectively (**Fig. 52 and Fig. 53**). Therefore, the higher concentration of anomalin (50 mg/kg) and capillarisin (80 mg/kg) were selected for use in subsequent experiments. Next, the anti-nociceptive effect of anomalin and capillarisin was tested using different hyperalgesic stimuli, i.e., carrageenan (**Fig. 54**). Pretreatment with anomalin (50 mg/kg, i.p.), capillarisin (80 mg/kg) or the reference drug (dexamethasone; 20 mg/kg, i.p.) 1 h before the stimulus inhibited carrageenan-induced hyperalgesia remarkably (**Fig. 54**). In order to investigate the effect of anomalin and capillarisin on saline-induced hyperalgesia, another set of experiment was performed. The results

demonstrated that anomalin and capillarisin exhibited no significant effect against saline-induced hyperalgesia (**Fig. 55**).

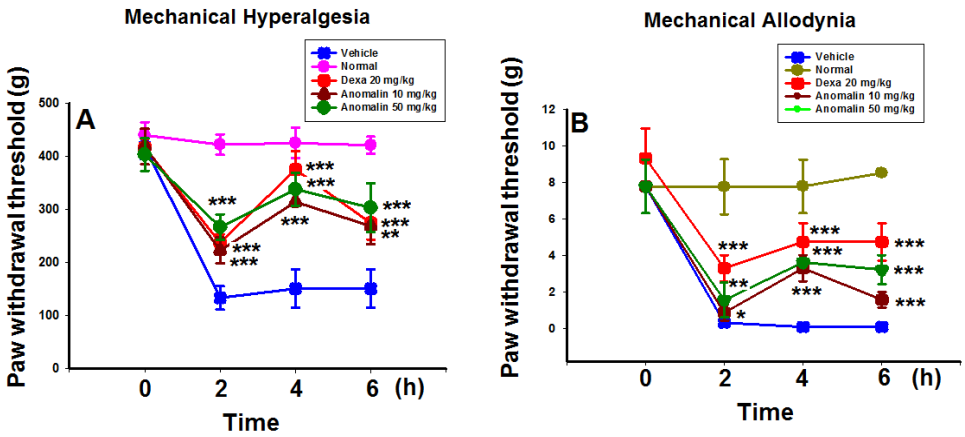

Figure 52. (**A**) Inhibition of CFA-induced mechanical hyperalgesia and (**B**) allodynia by anomalin treatment as described in "Materials and methods". The paw withdrawal effect was measured every 2 h after CFA injection until 6 h. The data obtained are expressed as the means ± S.D. (*) $P<0.05$, (**) $P<0.01$ and (***) $P<0.001$ indicate significant differences from the CFA-treated group.

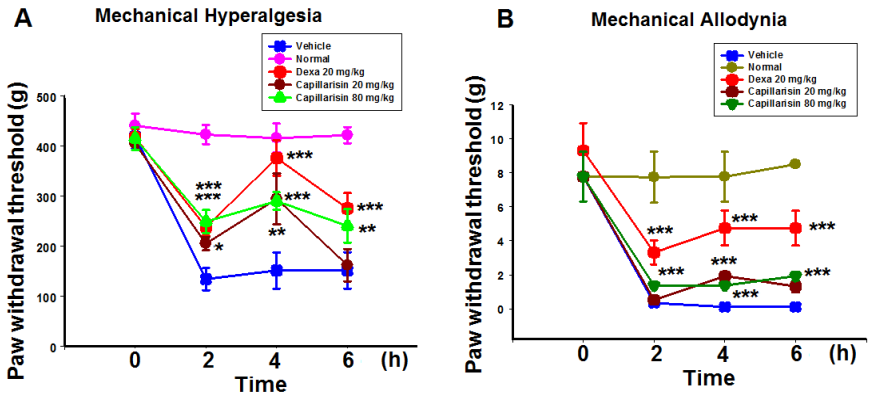

Figure 53. (A) Inhibition of CFA-induced mechanical hyperalgesia and **(B)** CFA-induced mechanical allodynia by capillarisin treatment as described in "Materials and methods". The paw withdrawal effect was measured every 2 h after CFA injection until 6 h. The data obtained are expressed as the means ± S.D. (*) $P<0.05$, (**) $P<0.01$ and (***) $P<0.001$ indicate significant differences from the CFA-treated group.

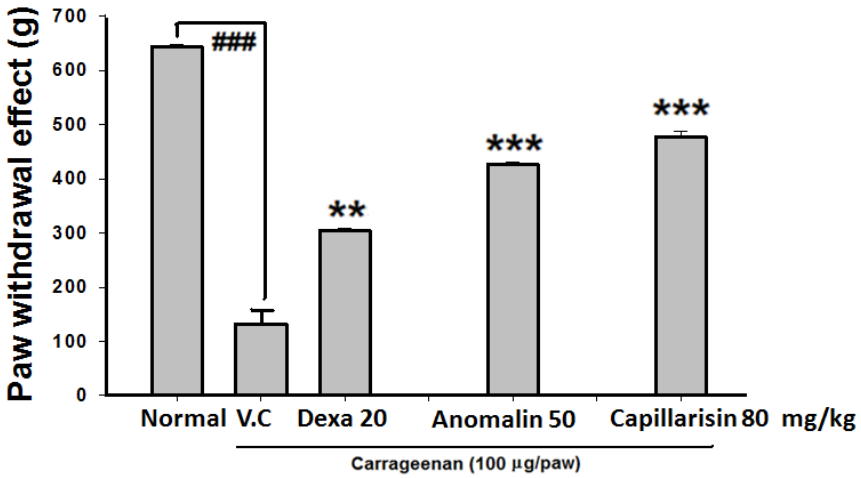

Figure 54. Effect of anomalin and capillarisin on carrageenan-induced mechanical hyperalgesia as described in the "Materials and methods" section. The paw withdrawal effect was measured 4 h after carrageenan injection. The data are reported as the means± S.D; (n= 5 mice per group). (**) $P<0.01$ indicate a significance difference from vehicle-treated group.

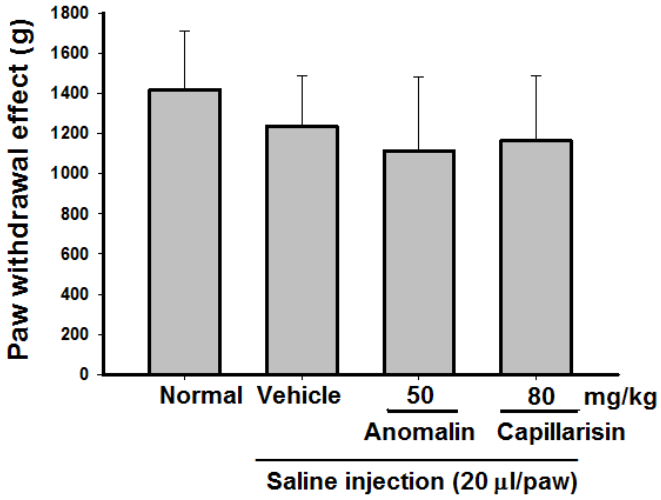

Figure 55. (**A**) Effect of anomalin and capillarisin on saline-induced hyperalgesia. The mice were treated with anomalin (50 mg/kg, i.p.), capillarisin (80 mg/kg, i.p.) or vehicle control as described in the "Materials and methods". The mechanical hyperalgesia was evaluated 4 h after the intraplantar saline injection. The data are reported as the means ± S.D; (n= 5 mice per group).

To evaluate the long-term therapeutic effect of anomalin and capillarisin, another set of experiments was performed. As demonstrated in **Fig. 56**, mice were treated once a day for five days with anomalin at 50 mg/kg and capillarisin 80 mg/kg the dose that produced the maximal anti-nociception by acute administration. Mechanical hyperalgesia induced by CFA was evaluated throughout the experimental period. Furthermore, a single daily treatment with anomalin and capillarisin decreased the paw withdrawal response significantly (**Fig. 56**). Vehicle treatment did not affect hyperalgesia, while the positive control drug dexamethasone inhibited CFA-induced hyperalgesia remarkably (**Fig. 56**).

3.2. Anomalin and capillarisin inhibited paw edema caused by short- and long-term treatment induced by CFA and carrageenan in mice

To verify the connection between the anti-inflammatory and anti-nociceptive activities of anomalin and capillarisin, the effects of anomalin and capillarisin were assessed in the CFA- and carrageenan-induced acute and chronic paw inflammation models with experimental protocols used for screening of new anti-inflammatory drugs. Administration of anomalin (10 and 50 mg/kg, i.p.) and capillarisin (20 and 80 mg/kg, i.p) 40 min before CFA and 1 h before carrageenan, significantly reduced paw edema 2, 4, and 6 h after the stimuli (**Fig. 57** and **Fig. 58**). The results obtained with the control groups supported the effects observed for anomalin and capillarisin because the vehicle (10% DMSO in saline) had no effect, whereas the positive control dexamethasone (20 mg/kg) inhibited CFA- and carrageenan-induced edema significantly (**Fig. 57** and **Fig. 58**). As described in **Fig. 57** and **Fig. 58**, the mice treated with 50 mg/kg anomalin and 80 mg/kg capillarisin showed reduced paw edema compared with the vehicle control.

This effect was observed up to five days after treatment. Edema was strongly inhibited by dexamethasone, the reference drug (**Fig. 59**).

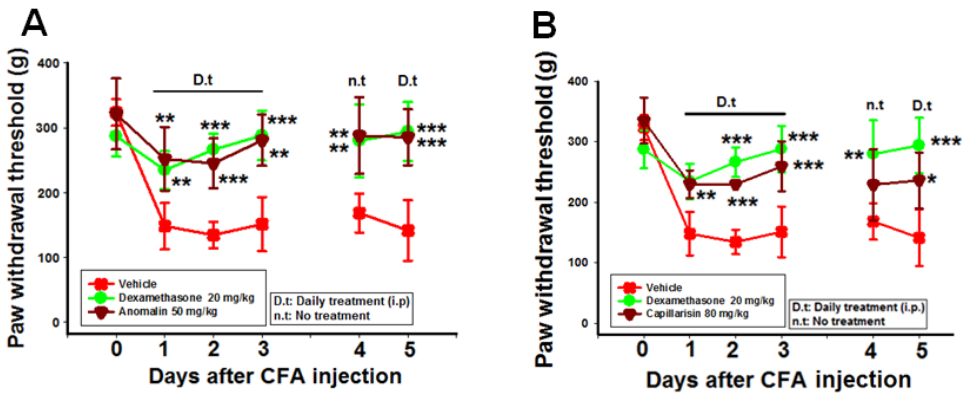

Figure 56. Inhibition of CFA-induced mechanical hyperalgesia by anomalin (**A**) and capillarisin (**B**) treatment as described in the "Materials and methods". The paw withdrawal effect was measured every 4 h after CFA injection from 0-5 days with interval of day four in order to interpret the possible tolerance effect as described in the "Materials and methods". The data are reported as the means ± S.D; (n= 7 mice per group). (*) $P<0.05$, (**) $P<0.01$ and (***) $P<0.001$ indicate significant differences from the CFA-treated group.

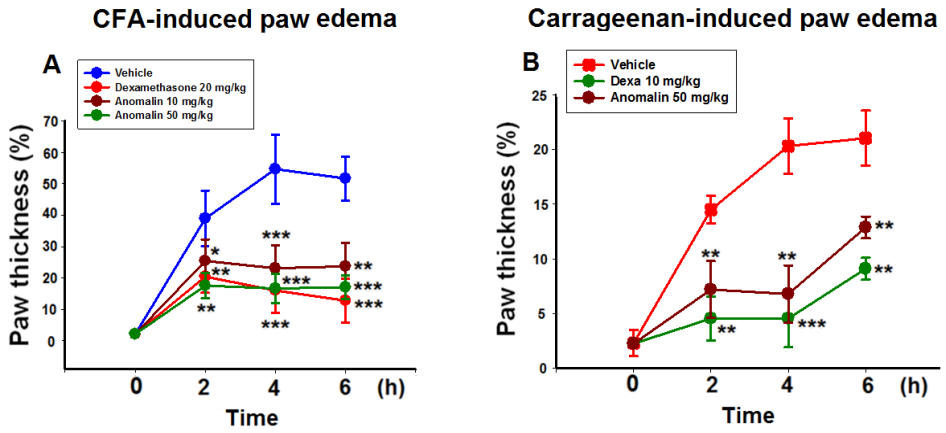

Figure 57. (**A**) Effect of anomalin on acute CFA-induced and (**B**) carrageenan-induced paw edema. The mice were treated with anomalin (i.p.), dexamethasone (10 or 20 mg/kg, i.p.) or vehicle control as described in the "Materials and methods". The paw edema was evaluated every 2 h after the CFA injection. The data are reported as the means ± S.D; (n= 5 mice per group). (*) $P<0.05$, (**) $P<0.01$ and (***) $P<0.001$ indicate significant differences from the CFA-treated group.

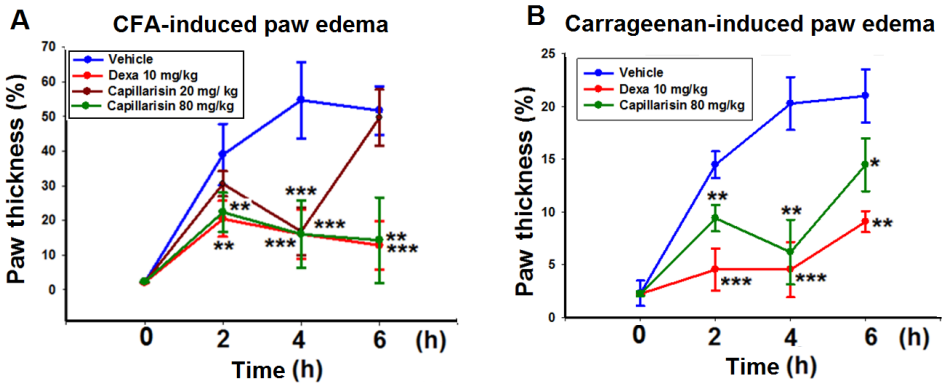

Figure 58. (**A**) Effect capillarisin on acute CFA-induced and (**B**) carrageenan-induced paw edema. The mice were treated with capillarisin (i.p.), dexamethasone (10 or 20 mg/kg, i.p.) or vehicle control as described in the "Materials and methods". The paw edema was evaluated every 2 h after the CFA injection. The data are reported as the means ± S.D; (n= 5 mice per group). (*) $P<0.05$, (**) $P<0.01$ and (***) $P<0.001$ indicate significant differences from the CFA-treated group.

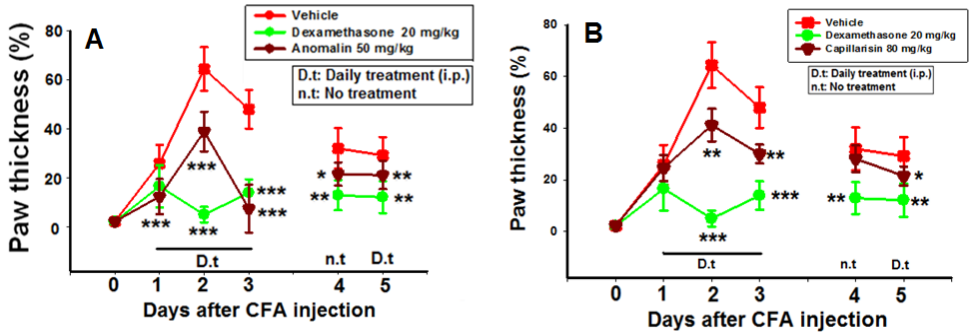

Figure 59. Effects of anomalin (**A**) and capillarisin (**B**) long-term CFA-induced paw edema. The mice were treated with anomalin (50 mg/kg, i.p.), capillarisin (80 mg/kg, i.p.), dexamethasone (20 mg/kg, i.p.) or vehicle control as described in "Materials and methods". The paw edema effect was measured every 4 h after CFA injection from 0-5 days with interval of day four in order to interpret the possible tolerance effect as described in the "Materials and methods". The data are reported as the means ± S.D; (n= 7 mice per group). (*) $P<0.05$, (**) $P<0.01$ and (***) $P<0.001$ indicate significant differences from the CFA-treated group.

3.3. Anomalin and capillarisin inhibit the release of pro-inflammatory cytokine (TNF-α) in CFA-induced treated paw tissue and reduces nitrite production in blood plasma

To further investigate the possible mechanism of the analgesic actions of anomalin and capillarisin, one of the major cytokines found in CFA-induced paw skin tissue, TNF-α, was assessed. The TNF-α level was markedly increased 6 h after CFA treatment. As shown in **Fig. 60**, pre-treatment with anomalin (10 and 50 mg/kg) and capillarisin (20 and 80 mg/kg) significantly decreased the TNF-α level in a pattern similar to the positive control, 20 mg/kg dexamethasone (**Fig. 60**).

The participation and production of nitrite in CFA-induced blood plasma was analyzed after 6 h and 5 days of treatment. The treatment of mice with CFA increased NO production considerably (**Fig. 61**). However, the increased NO production was markedly reduced by treatment with anomalin and capillarisin as observed after 6 h and 5 days of treatment (**Fig. 61**).

3.4. Inhibitory effect of anomalin and capillarisin on iNOS and COX-2 expressions during inflammatory hyperalgesia

To investigate whether iNOS and COX-2 mediate the blockage of ongoing hyperalgesia, Western blot analysis was performed in paw skin tissue. The effects of anomalin and capillarisin on iNOS and COX-2 protein expressions were determined after treatment with 50 mg/kg of anomalin and 80 mg/kg of capillarisin for 5 days. The iNOS and COX-2 protein expressions in paw tissue dramatically increased after CFA treatment (**Fig. 62** and **Fig. 63**). The increase in iNOS (**Fig. 62** and **Fig. 63**) and COX-2 (**Fig. 62** and **Fig. 63**) expressions in CFA-induced paw tissue was

significantly reduced by anomalin and capillarisin. Dexamethasone at 20 mg/kg was used as positive control (**Fig. 62** and **Fig. 63**).

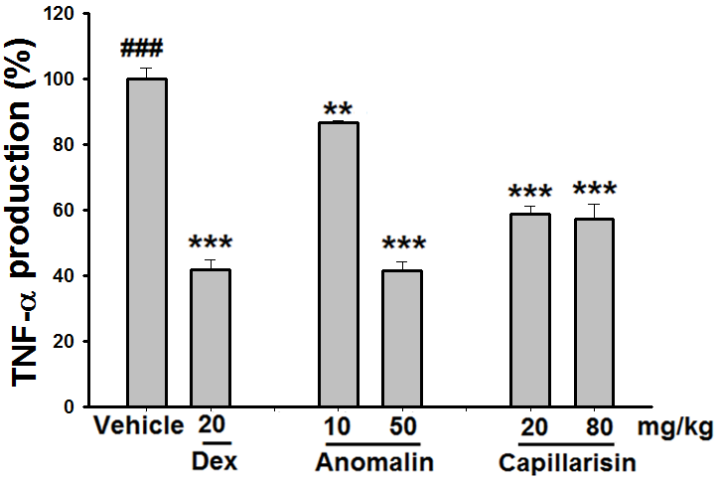

Figure 60. Effect of treatment with anomalin and capillarisin on TNF-α in paw tissue. The mice were treated with anomalin (10 and 50 mg/kg, i.p.), capillarisin (20 and 80 mg/kg, i.p.), dexamethasone (20 mg/kg, i.p.) or vehicle control as described in "Materials and methods". The TNF-α level was measured by ELISA as described in "Materials and methods". The data are reported as the means ± S.D; (n= 7 mice per group). (*) $P<0.05$, (**) $P<0.01$ and (***) $P<0.001$ indicate significant differences from the CFA-treated group. ($^{###}$) $P<0.001$ indicates a significant difference vehicle control group.

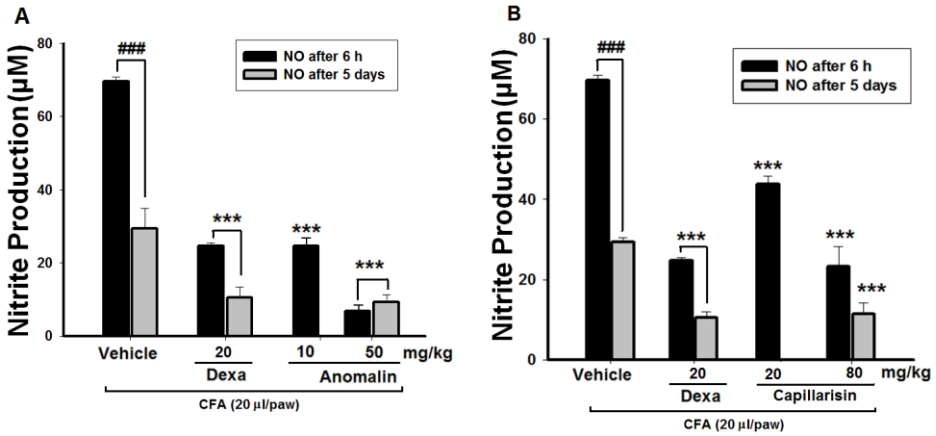

Figure 61. Effect of treatment with anomalin (**A**) and capillarisin (**B**) on nitrite (NO) production determination in blood plasma. The mice were treated with anomalin (10 and 50 mg/kg, i.p.), capillarisin (20 and 80 mg/kg, i.p.), dexamethasone (20 mg/kg, i.p.) or vehicle control as described in "Materials and methods". The NO was determined by Griess reagent as described in "Materials and methods". The data are reported as the means ± S.D; (n= 7 mice per group). (*) $P<0.05$, (**) $P<0.01$ and (***) $P<0.001$ indicate significant differences from the CFA-treated group. ($^{###}$) $P<0.001$ indicates a significant difference vehicle control group.

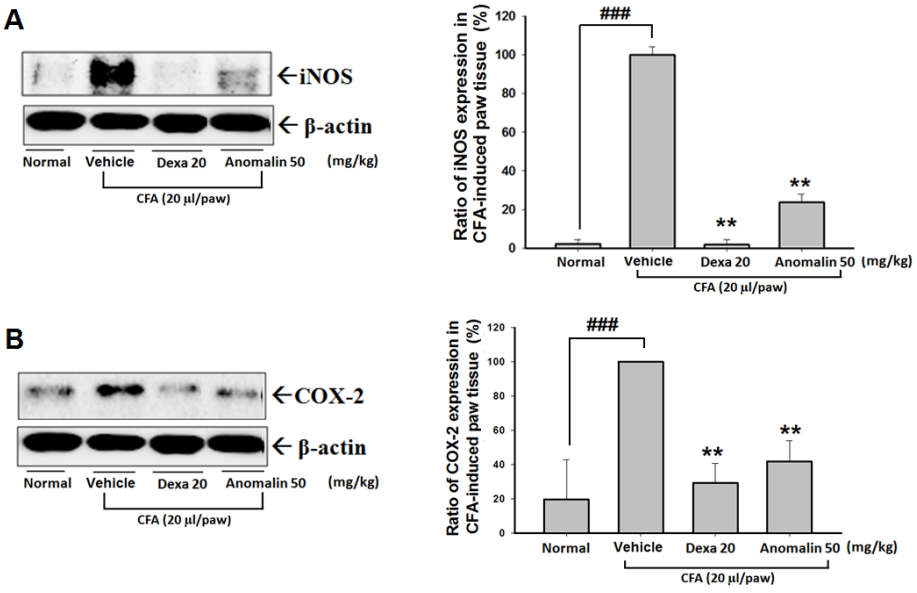

Figure 62. Down-regulation of iNOS and COX-2 expressions by anomalin in CFA-induced paw tissue using Western blotting as described in "Materials and methods". (**A**) iNOS protein expression (**B**) COX-2 protein expressions. The data are expressed as the means ±S.D. from three separate experiments. The treatment groups were as follows: normal (Not treated), vehicle control (10% DMSO in saline), anomalin (50 mg/kg, i.p.) and dexamethasone (20 mg/kg, i.p.) as a positive control. The data are reported as the means ± S.D. (**) $P<0.01$ indicate significant differences from the CFA-treated group. ($^{###}$) $P<0.001$ indicates a significant difference from the vehicle control group.

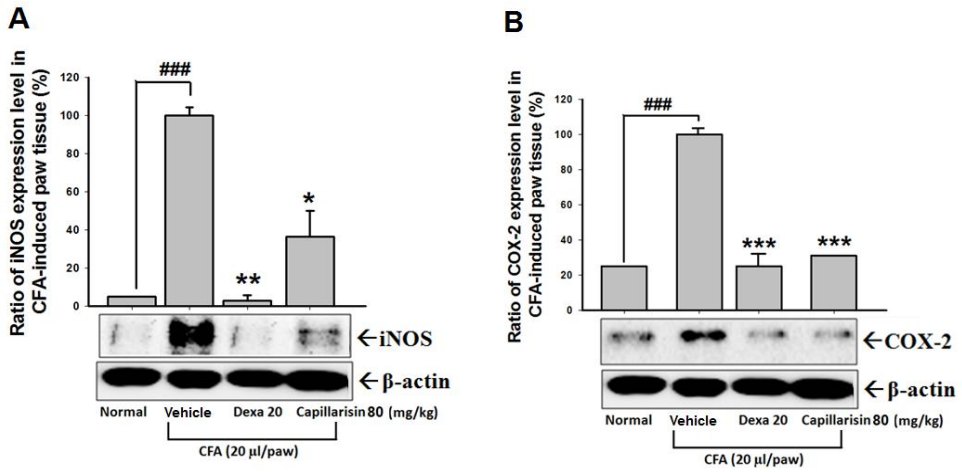

Figure 63. Down-regulation of iNOS and COX-2 expressions by capillarisin in CFA-induced paw tissue using Western blotting as described in "Materials and methods". (**A**) iNOS protein expression (**B**) COX-2 protein expressions. The data are expressed as the means ±S.D. from three separate experiments. The treatment groups were as follows: normal (Not treated), vehicle control (10% DMSO in saline), capillarisin (80 mg/kg, i.p.), and dexamethasone (20 mg/kg, i.p.) as a positive control. The data are reported as the means ± S.D. (*) $P<0.05$, (**) $P<0.01$ and (***) $P<0.001$ indicate significant differences from the CFA-treated group. ($^{###}$) $P<0.001$ indicates a significant difference from the vehicle control group.

3.5. Inhibitory effect of anomalin and capillarisin on the NF-κB signaling pathway during inflammatory hyperalgesia

NF-κB is known to modulate the expression of a variety of genes, including those encoding COX-2 and iNOS, because their respective inhibition blocked hyperalgesia, the associated induction of COX-2 and iNOS, and the increased formation of PGE_2 and NO in paw tissues [143]. Therefore, the NF-κB signaling pathway was investigated. Initially, upstream IκBα phosphorylation and degradation were evaluated by Western blotting. Compared with the normal group (vehicle), the CFA-induced group exhibited significantly higher levels of phosphorylated IκBα (**Fig. 64**). The amount of phosphorylated IκBα was markedly attenuated after i.p. injection of anomalin and capillarisin (**Fig. 64**). On the other hand, the CFA-induced group showed significantly lower levels of cytoplasmic IκBα expression when compared with the normal group (**Fig. 64**). The reduction of IκBα expression was completely protected after injection of anomalin (**Fig. 64**). Whereas, capillarisin didn't show any significant effect to protect IκBα degredation. Moreover, dexamethasone was observed to have a significant effect in both cases (**Fig. 64A and 64B**).

To more deeply explore the mechanism of NF-κB in pain sensation, a test of NF-κB-DNA binding activity was performed using EMSA. As shown in **Fig. 65**, CFA-induced mice (**Fig. 65**) were observed to have increased NF-κB-DNA binding compared with the normal group (**Fig. 65**). In contrast, the increased NF-κB-DNA binding activity was promisingly inhibited by treatment with anomalin and capillarisin (**Fig. 65**). Dexamethasone also abolished the NF-κB-DNA binding activity (**Fig. 65**).

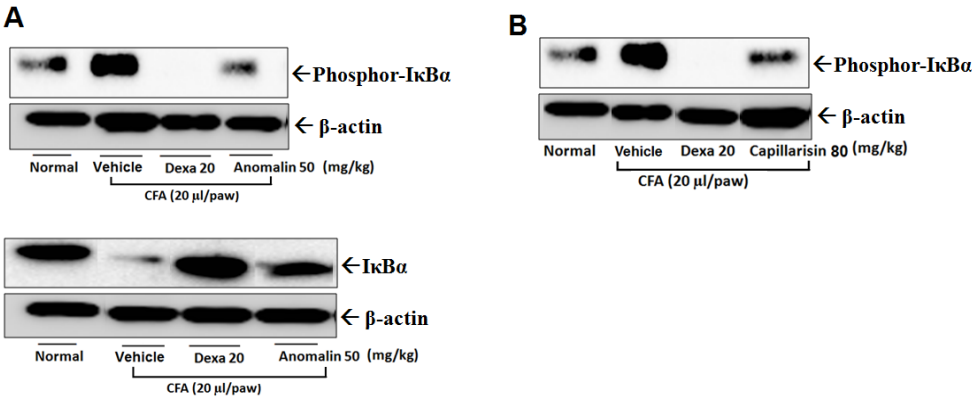

Figure 64. Effect of anomalin (**A**) and capillarisin (**B**) on p-IκBα and IκBα in CFA-induced paw tissue using Western blotting as described in "Materials and methods".

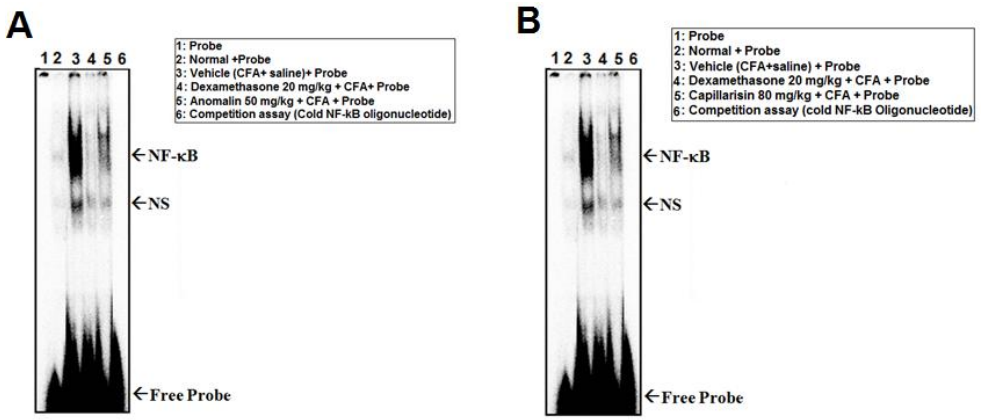

Figure 65. Effects of anomalin (**A**) and capillarisin (**B**) on NF-κB DNA binding activity. An electrophoretic mobility shift assay (EMSA) was performed as described in the "Materials and methods" section. A representative EMSA result is shown. The NF-κB complexes, nonspecific signals (NS), and excess probe are indicated by arrows.

3.6. Inhibitory effect of anomalin and capillarisin on the MAPKs signaling pathway during inflammatory hyperalgesia

MAPK pathways contribute to pain sensitization after tissue and nerve damage through various molecular and cellular mechanisms [144]. After tissue injury, ERK, p38, and JNK are differentially activated, leading to the production of pro-inflammatory and pro-nociceptive mediators, thereby enhancing and prolonging pain sensations. Therefore, we investigated the signaling mechanism of the ERK and p38 MAPKs. The results demonstrated that the CFA-induced group dramatically increased the levels of both p-p38 and p-ERK (**Fig. 66**). Treatment with anomalin (50 mg/kg) significantly reduced the p-p38 and p-ERK protein expression levels (**Fig. 66**). Capillarisin showed significant down-regulation of p-ERK, whereas, no effect was found on p-p38. Dexamethasone at 20 mg/kg exhibited a potent inhibitory effect against p-p38 and p-ERK (**Fig. 66**).

The activation of the MAPK pathway also modulates AP-1 activation. It was hypothesized that the suppression of MAPK signaling by anomalin and capillarisin could be due to the lower DNA binding capacity of AP-1 through the nuclear translocation of phosphorylated MAPKs. The results showed that anomalin and capillarisin both drastically inhibited nuclear AP-1-DNA binding activity compared with the normal and CFA-induced groups, as shown in **Fig. 67**.

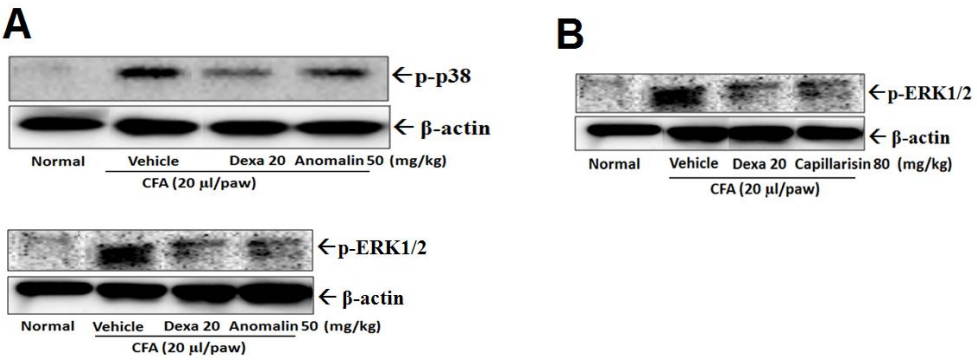

Figure 66. (A) Effect of anomalin (**A**) and capillarisin (**B**) on MAPK p-p38 and p-ERK1/2 protein levels in cytosolic extracts of CFA-induced paw tissue were determined by Western blot analysis as described in the "Materials and methods".

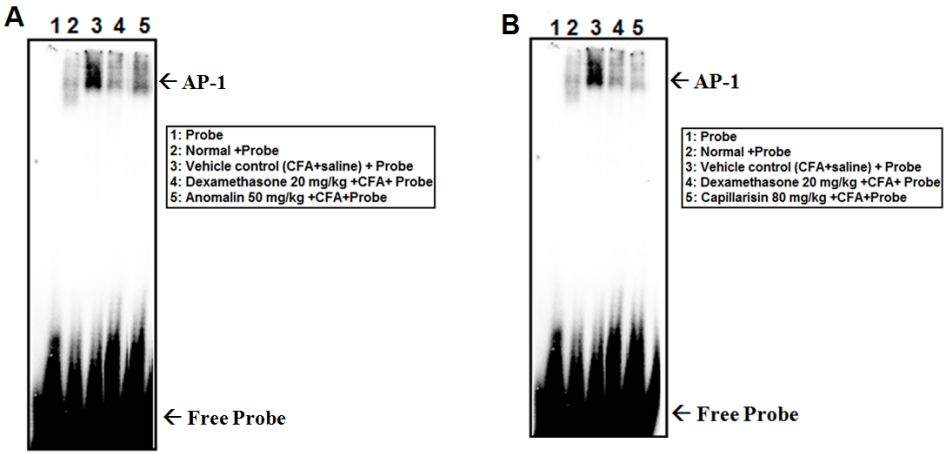

Figure 67. (A) Effect of anomalin (**A**) and capillarisin (**B**) on AP-1 DNA binding activity. An EMSA was performed as described in the "Materials and methods". A representative EMSA result is shown; CREB complexes, nonspecific signals and excess probe are indicated by arrows.

3.7. Inhibitory effect of anomalin and capillarisin on CREB signaling pathway during inflammatory hyperalgesia

We proceeded to investigate the mechanisms downstream of the MAPK pathway that specifically involved ERK and p-38. MAPK signaling transduces a wide range of extracellular stimuli into diverse intracellular responses by producing changes in the level of gene expression or transcription [145]. Activated ERK translocates from the cytosol into the nucleus and activates CREB [145]. Therefore, CREB-DNA binding activity was analyzed using EMSA. The results illustrated that CFA injection significantly increased the CREB-DNA binding activity (**Fig.68**). The increased CREB-DNA binding effect was markedly abolished by anomalin and capillarisin (**Fig.68**).

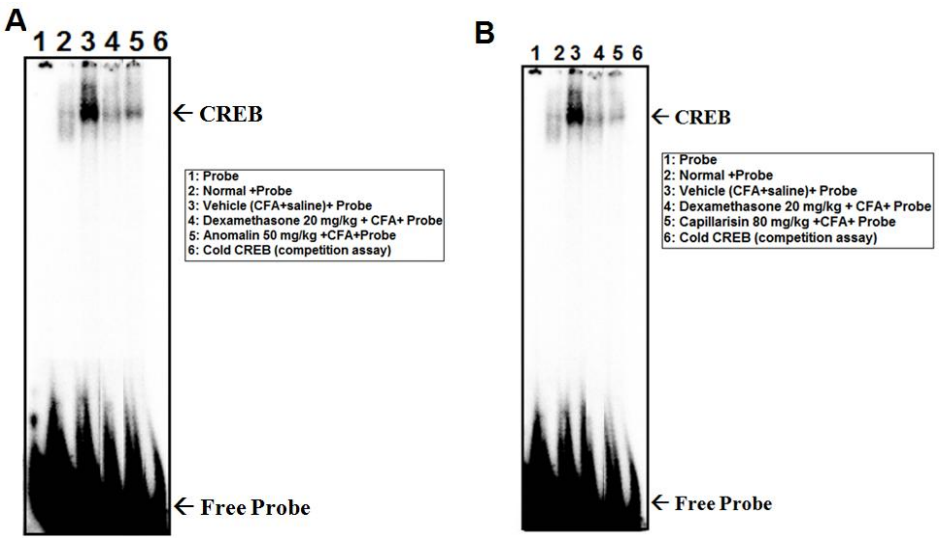

Figure 68. Effect of anomalin (**A**) and capillarisin (**B**) on CREB DNA binding activity. An EMSA was performed as described in the "Materials and methods". A representative EMSA result is shown; CREB complexes, nonspecific signals and excess probe are indicated by arrows.

3.8. Inhibitory effect of anomalin and capillarisin on CFA-induced plasma ATP and substance P in CFA-induced paw skin tissue

The hypothesis that ATP is a pain mediator might reveal important novel analgesic targets. Therefore, ATP levels were determined in the plasma of different groups of animals. As demonstrated in supplementary **Fig. 69**, ATP release was significantly increased after CFA injection. On the other hand, i.p. injection of anomalin (50 mg/kg), capillarisin (80 mg/kg) and the positive control dexamethasone (20 mg/kg) remarkably reduced the ATP level (**Fig. 69**).

Acute and chronic inflammatory pain are associated with a number of diseases, and the release of substance P plays a pivotal role in these conditions [146]. To investigate the effect of anomalin on SP, the SP in the total protein extracted from paw skin tissue was analyzed by Western blotting. The SP expression level was dramatically increased after CFA injection, as shown in **Fig. 69**. Pre-treatment with anomalin and capillarisin markedly abolished the expression level of SP. Similarly, the positive control dexamethasone was observed to have potent activity against SP induction (**Fig. 69**).

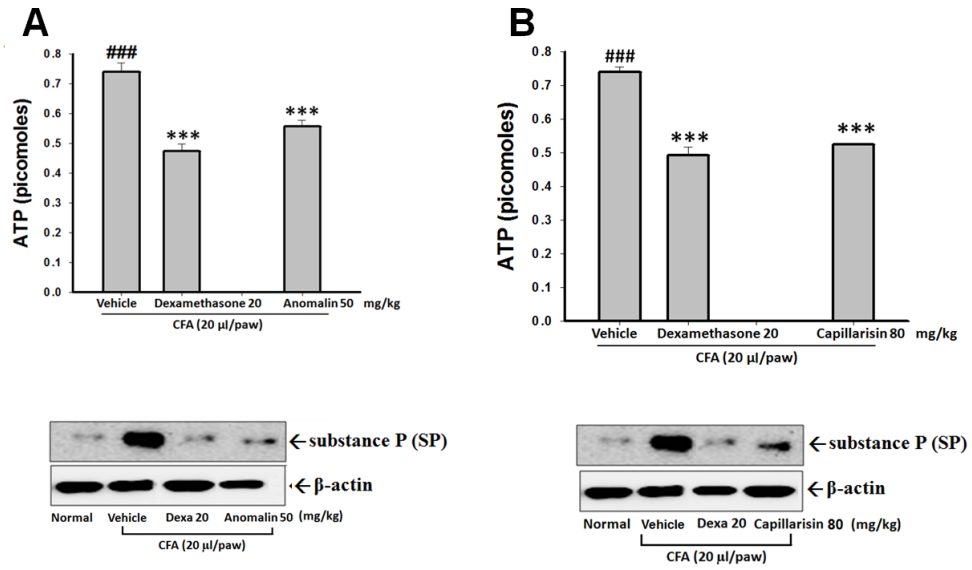

Figure 69. (**A**) Effect of anomalin and (**B**) capillarisin on ATP release in plasma and SP in CFA-induced paw tissue assessed by ELISA and Western blot analysis respectively as described in the "Materials and methods". The data are reported as the means ± S.D; (n= 7 mice per group). (***) $P<0.001$ indicate significant differences from the CFA-treated group. ($^{###}$) $P<0.001$ indicates a significant difference from the vehicle control group.

3.9. Effect of anomalin and capillarisin on immunohistological analysis

The long-term administration of the available anti-inflammatory and analgesic drugs may lead to the development of various side effects. Taking this possibility into consideration, the effects of anomalin and capillarisin were evaluated. Treatment with anomalin (50 mg/kg, i.p.) and capillarisin (80 mg/kg, i.p) in a single dose scheme over five days with an interval on day four did not induce any variations in the general appearance or toxic signs in the mice when compared to vehicle-treated mice. Furthermore, liver function was evaluated through analysis of hepatic enzymes (ALT, AST, total protein and albumin), which were not altered by treatment with anomalin or capillarisin in comparison to the vehicle control. Values obtained for the creatinine level, which is used as an indicator of renal function, did not differ from those of control mice (**Table 2**). Similarly, a microscopic evaluation of the paw showed no inflammatory cell infiltrate in mice treated daily with anomalin (**Fig. 70 and 71**).

Table 2. Effect of daily treatment with anomalin and capillarisin on biochemical parameters.

Sample	GPT/ALT(UI/L)	GOT/AST (UI/L)	Creatinine (mg/dl)	Total Protein (g/dL)	ALB(g/dL)
Vehicle	98±2.4	148±5.7	0.3±0.14	6.6 ±0.23	3.4±0.1
Anomalin 50 mg/kg	98±2.3	148±4.4	0.3±0.1	5.6 ±0.20	2.1±0.2
Capillarisin 80 mg/kg	114±1.1	198	0.3±0.11	5.0 ±2.3	2.0± 2.2

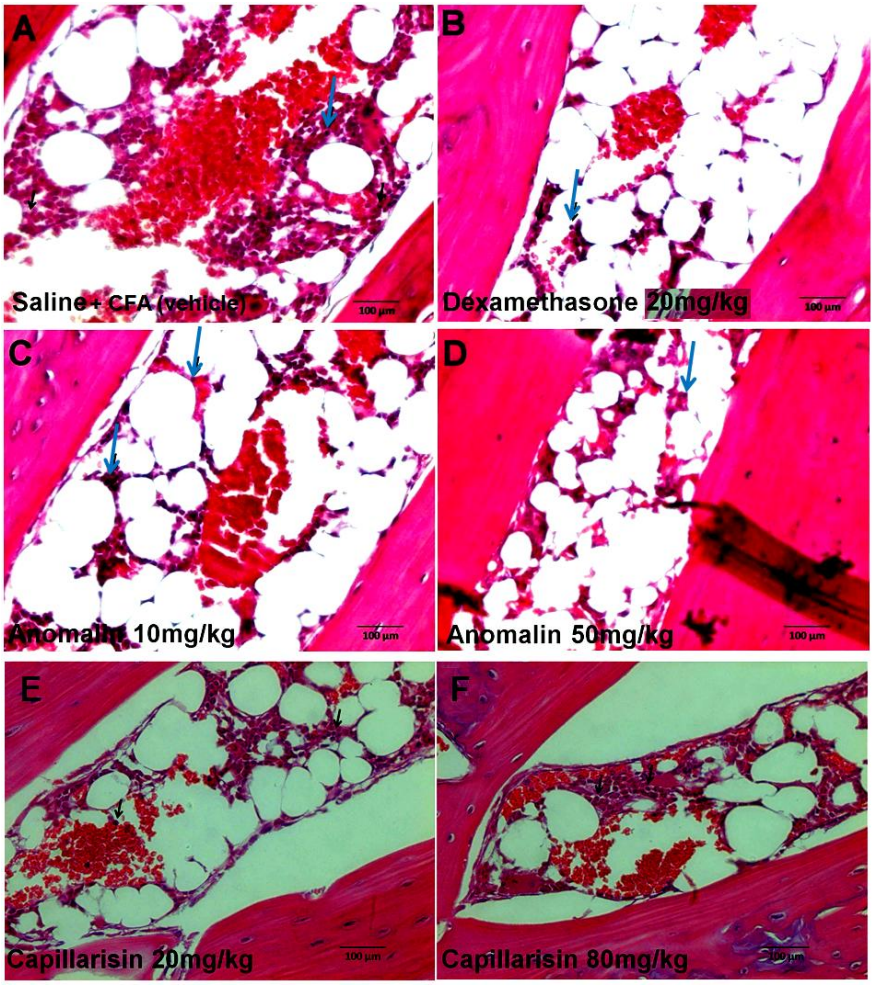

Figure 70. Histological analysis of CFA-induced inflamed paw. (**A**)Vehicle control (saline +10% DMSO), (**B**) Dexamethasone 20 mg/kg, (**C**) Anomalin 10 mg/kg and (**D**) Anomalin 50 mg/kg, (**E**) Capillarisin 20 mg/kg, (**F**) Capillarisin 80 mg/kg. Paw tissue blocks were sectioned at 4 μm thickness, stained with hematoxylin-eosin, and observed by microscopy (40×) as described in "Material and methods" section. The inflamed paw sections were further analyzed by determining the number of neutrophils (blue color arrow) showing inflammation.

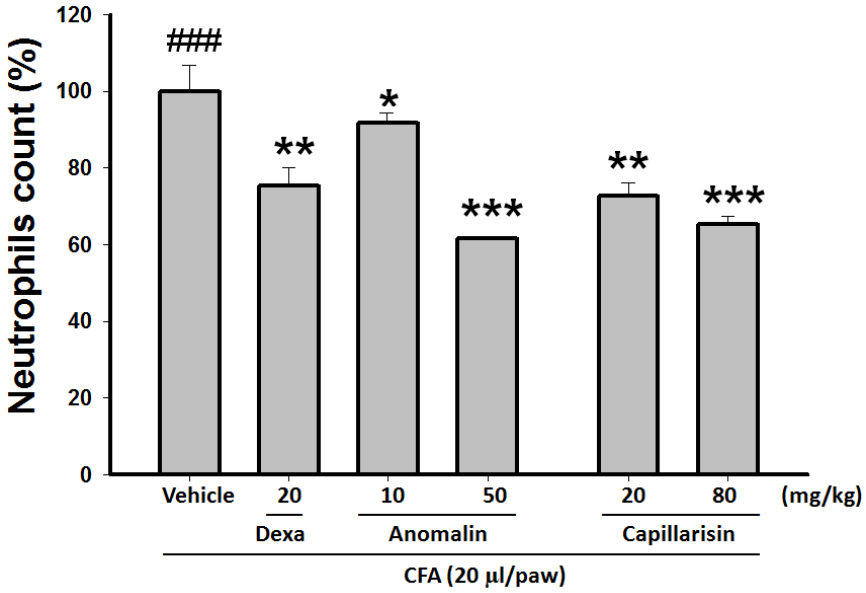

Figure 71. Quantitative analysis of histological analysis of CFA-induced inflamed paw as described in "Materials and methods". The data are reported as the means ± S.D. (*) $P<0.05$, (**) $P<0.01$ and (***) $P<0.001$ indicate significant differences from the CFA-treated group. ($^{###}$) $P<0.001$ indicates a significant difference from the vehicle control group.

4. Discussion

Inflammatory pain is a state that often becomes debilitating. Recently, therapeutic candidates have been effective in treating inflammatory pain disorders, but many of these are known for their severe side effects [147]. In this regard, the search for new compounds and potential candidates that could be applied in acute and chronic inflammatory pain therapy has been a challenge. In the current study, it was demonstrated for the first time that systemic (i.p.) administration of the pyranocoumarin derivative anomalin and chromone derivative capillarisin produced a remarkable inhibition of mechanical hyperalgesia and allodynia induced by CFA- and carrageenan-induced in both acute and chronic inflammation models in mice. It is notable that the anti-hyperalgesic and anti-allodynic effect of anomalin and capillarisin was observed after 2 h of treatment and persisted until 6 h in the acute model and until day 5 in the chronic model. Additionally, pre-treatment with anomalin and capillarisin reduced CFA- and carrageenan-induced paw edema significantly.

Previous findings have demonstrated that anomalin and capillarisin isolated from *S. divaricata* and *A. capillaris* exhibited promising inhibitory effects against NF-κB activation by suppressing iNOS and COX-2 expression levels [33, 37]. Similarly, the pro-inflammatory cytokines (TNF-α, IL-6 and IL-1β) were inhibited significantly [33, 37]. On the basis of these findings, the present study hypothesized that various inflammatory signaling pathways might be involved in modulating pain sensations. Currently, it is well understood that chronic inflammatory pain resulting from peripheral injection of CFA or carrageenan [148] leads to the release of numerous inflammatory and nociceptive mediators, resulting in increased long-lasting discharge of primary sensory fibers that modifies neuroimmune cells and

their function in the central nervous system [148]. In this context, the remarkable ability of anomalin and capillarisin to counteract CFA- and carrageenan-induced inflammatory pain is almost certainly linked with its ability to interfere in cell signaling, especially the NF-κB, MAPKs/AP-1 or CREB pathways.

Local injection of CFA produces inflammatory hyperalgesia initiated by peripheral nociceptor activation and local release of mediators, such as NO, cytokines (TNF-α) and prostanoids (PGE_2 regulated by COX-2) modulated by NF-κB, which are involved in the sensitization of the nociceptive pathway [23]. The intraplantar injection of CFA induced a significant increase of NO in plasma and TNF-α level in the paw. Pre-treatment with anomalin and capillarisin reduced nitrite production in both acute and persistent pain and reduced the TNF-α level in paw tissue. Similarly, the iNOS and COX-2 expression levels were further evaluated in CFA-induced paw tissue. The results illustrated that iNOS and COX-2 expressions were potently inhibited by anomalin and capillarisin. However, previous reports suggest that iNOS and COX-2 are both induced through the NF-κB pathway [149, 150]. It is possible that iNOS and COX-2 may mediate the process of NF-κB activation, which is involved in the activation and release of NO and PGE_2 in CFA-induced hyperalgesic mice.

The NF-κB pathway was the initial focus as the mechanism modulating anti-nociceptive action of anomalin and capillarisin. It is known that CFA induction enhances NF-κB activation [151]. Our results demonstrated that intraperitoneal treatment of anomalin and capillarisin markedly reduced IκB phosphorylation and degradation by anomalin rather than capillarisin. Similarly, the nuclear NF-κB DNA binding affinity was drastically reduced by both the phenolic compounds. Moreover, these results

indicate that the anti-nociceptive action of anomalin and capillarisin appears to be related to its ability to block the NF-κB signaling pathway and influence the production of inflammatory pain mediators.

An important role for TNF-α in inflammatory pain has been demonstrated. It is known that a signaling pathway of pro-inflammatory cytokines, which includes TNF-α as a major component, leads to the release of the final hyperalgesic mediators, i.e., prostaglandins and amines [121]. Various cytokine antagonists are able to reduce inflammatory hyperalgesia in mice, indicating that cytokine activation is an important step in the development of inflammatory pain [121]. Considering this concept, the local injection of TNF-α produces hyperalgesia due to the considerable release of PGE_2 and other pain mediators [18]. In the present study, we have shown that anomalin and capillarisin reduced the TNF-α level. Because the inhibition of TNF-α release might lead to the inhibition of prostanoid production, it is possible that anomalin and capillarisin acts to prevent nociceptive sensitization through the inhibition of the production of mediators that sensitize the nociceptor. Hence, the sensitization of nociceptors is the common denominator of different types of pain and the reduction of NO, COX-2, and TNF-α levels may be responsible for the anti-nociceptive effect of anomalin and capillarisin.

MAPKs are activated under different persistent pain conditions which lead to the induction of pain hypersensitivity through transcriptional or nontranscriptional regulation. Some reports have shown that MAPK inhibitors induce hyperalgesia and allodynia in inflammatory and neuropathic pain models, but these inhibitors have little or no effect on basal physiological pain perception, suggesting a specific role of MAPKs in the development of pain hypersensitivity following tissue and nerve injury [152].

Peripheral tissue injury and spinal cord injury activate p38 and ERK in spinal microglia [153, 154]. ERK plays a critical role, as it is activated by nociceptive activity in the spinal cord via various neurotransmitter receptors and uses different second messenger pathways to regulate central sensitization [144]. ERK activation is essential for CREB phosphorylation after noxious stimulation, which is likely to induce the transcription of NK-1 and prodynorphin as well as other pro-nociceptive genes such as COX-2 [155]. Here, it was shown that ERK phosphorylation was dramatically increased after the injection of CFA. However, i.p. administration of anomalin and capillarisin effectively reversed the activation of ERK and CREB. Similarly, systematic administration of p38 inhibitors has been shown to alleviate inflammation associated with various diseases [156]. Activated p38 is translocated to the nucleus, where it can phosphorylate transcriptional factors such as ATF-2 (a member of the AP-1 family) as well as several other inflammatory mediators (COX-2 and TNF-α), which are then upregulated by p38 [156]. The present study proved that administration of anomalin considerably downregulated the p-p38 protein level in CFA-induced paw tissue. Whereas, capillarisin exhibited no significant effect on p38 activation. Compared to ERK and p38, the role of JNK in pain regulation is not well known.

ATP is contained in all cells at millimolar concentrations, and it is released during tissue injury resulting in the activation of nociceptors. Acute tissue-damaging stimuli can also indirectly activate nociceptors. Numerous nociceptors express ionotropic (P2X purinoceptors, notably P2X3) and G-protein-coupled (P2Y, pyrimidinergic) receptors that are responsive to ATP [23]. Moreover, the release of ATP can lead to the production and release of inflammatory mediators [157].

PART IV

Neuroprotective, Anti-neuroinflammatory and Anti-neuropathic pain properties of anomalin and capillarisin

1. Introduction

Neuropathic pain is the damage of peripheral nerves which often persistent and is poorly treated by existing therapies because distinct mechanisms are triggered by neuronal injury [158]. Peripheral nerve injury due to trauma, disease, and certain toxins sometimes produces abnormal (neuropathic) pain syndromes that are chronic and refractory to analgesic agents [158]. Neuropathic pain can cause due to arise nerve damage, including diabetic neuropathy, HIV neuropathy, post-herpetic neuralgia, drug-induced neuropathy and traumatic nerve injury. In damaged peripheral nerves, macrophages are recruited by chemotactic molecules and other evidence indicates that macrophages are important in neuropathic pain models [30, 159]. Consequently, in neuron demage various mediators, such as TNF-α, IL-1β, PGE_2 and nitric oxide can release [23].

Numerous reports have demonstrated that peripheral nerve damage injury produces long-lasting, heterogeneous pain conditions referred to neuropathic pain. Experimental models of peripheral nerve injury in animals have been developed which produce behavior suggestive of mechanical allodynia and thermal hyperalgesia, corresponding to some degree, to clinically relevant neuropathic pain model [160]. It has been greatly advanced by the introduction of animal models of post-traumatic painful peripheral neuropathy with comprehensive understandings of the mechanisms that produce neuropathic pain and the ability to search for new anti-neuropathic agents. While these models are most clearly relevant to the peripheral neuropathies (e.g., causalgia), they are likely to also be related to painful peripheral neuropathies evoked by disease (e.g., diabetes) and toxins (e.g., chemotherapeutics).

The development of therapeutics for the treatment of chonic illness has been particularly challenging. Clinical trials have identified some effective drugs to treat chronic inflammation and pain [30], such as opioids, anti-epileptic agents, and anti-depressants. Interestingly, none of these agents was developed to treat chronic inflammation and pain [31, 161]. Nevertheless, up to now, all drugs available for treating chronic pain have failed with respect to the effectiveness and safety. The development and utilization of more effective anti-inflammatory and analgesic agents of natural origin are still desired and more challenging.

The results obtained previously have also demonstrated that anomalin and capillarisin inhibited the nociception induced by CFA- and carrageenan-induced animal models. The present study aimed to investigate the neuroprotective property, anti-neuroinflamamtory mechanism and effect of anomalin and capillarisin in neurophathic pain model. Therefore, sodium nitroprussid (SNP)-induced neuroblastoma cells (N2a) *in vitro* and streptozotocin (STZ)-induced diabetes mellitus animal model was followed. Moreover, attempts have also been made to analyse some of the possible mechanisms through which anomalin and capillarisin exerted their affects.

2. Material and methods

2.1. Animals

Male ICR mice (Samtako, Osan, Korea), 3-4 weeks of age, weighing 30-35 g, were used in the present study. All animal studies were performed in a pathogen-free barrier zone of the Seoul National University Animal Laboratory, according to the procedures outlined in the Guide for the Care

and Use of Laboratory Animals (Seoul National University, Korea). The animals were housed at 23±0.5^{o}C with 10% humidity in a 12 h light-dark cycle. Animal care and handling procedures were followed according to the guidelines of the International Association for Study of Pain (IASP) on the use of animals in pain research [134]. Behavioral tests were done without knowing to which experimental group each mouse belonged. Each group contained five mice. All animals were used only once. Every effort was made to minimize the number of animals used and any discomfort. The animals were divided into four groups (control; saline with 10% DMSO, 50 mg/kg celecoxib, 50 mg/kg anomalin and 80 mg/kg capillarisin).

2.2. Cell culturing, cell viability and NO assay

The mouse neuroblastoma cell line, neuro-2a (N2a), was obtained from ATCC (MD, USA) and maintained in Dulbecco's modified Eagle's medium (DMEM; Gibco BRL, NY, USA) supplemented with 10% fetal bovine serum, 100 U/ml penicillin and 100 mg/ml streptomycin in a humidified atmosphere of 5% CO_2 at 37^{o}C. Briefly, N2a cells were plated at a density of 1×10^5 per well in a 24-well plate and incubated at 37°C for 24 h. After an overnight culture, the medium was replaced with fresh medium without FBS. To induce cell injury, cells were incubated with 500 μM SNP (Sigma-Aldrich, St Louis, USA) for 20 h. In order to evaluate the effects of anomalin and capillarisin, cells were pre-incubated with anomalin and capillarisin for 24 h, and then SNP was added to the medium for an additional 24 h. After incubation for 24 h, 100 μl aliquots of the cell-free culture medium were taken for NO measurement according to the Griess reaction method and cell viability was measured as described previously [33]. TPCK 30 μM was used as a positive control.

2.3. Quantitative real-time (qRT)-PCR

RT-PCR was performed with total RNA extracted using easyBlue™, according to the manufacturer's recommendations (Sigma-Aldrich, St Louis, MO). The purity and concentrations of RNA were determined using the ND-1000 spectrophotometer (Nanodrop Technologies, Wilmington, DE). All of the RNA samples were stored at -80^{o}C until used for analysis. Total RNA (1 µg) was converted to cDNA by RT-PCR (Genius FGEN05TD, Teche, England) using iScript^{TM} cDNA Synthesis Kit (BIO-RAD, Hercules, CA) under the following conditions. 25^{o}C for 5 min, 42^{o}C for 30 min and 85^{o}C for 5 min. Quantitative real-time polymerase chain reaction (qRT-PCR) analysis was performed using an Applied Biosystems 7300 real-time PCR system and software (Applied Biosystem, Carlsbad, CA). qRT-PCR was conducted in 0.2 ml PCR tubes with forward and reverse primers and the SYBR green working solution (iTaq^{TM} Universal SYBR Green Supermix, BIO-RAD, Hercules, CA), using customer PCR master mix with following conditions: 95^{o}C for 30 min, followed by 40 cycles of 95^{o}C for 15 sec, x^{o}C for 20 sec and 72^{o}C for 35 sec. The melting point, optimal conditions and the specificity of the reaction were first determined. The sequences of the PCR primers were described preciously [69, 70].

2.3. Western immunoblot analysis

N2a cells were pre-treated with the indicated concentrations of anomalin and capillarisin for 24 h and then stimulated with SNP (500 µM) following day for 15, 30 and 60 min (phosphor-IκBα p-p38, p-ERK, and IKKα/β). Ten micrograms of total protein for phosphor-IκBα, p-p38, p-ERK, ERK, IKKα/β and β-actin were separated by SDS-PAGE, 10%. After electrophoresis, the proteins were electro-transferred to nitrocellulose membranes (Whatman GmbH, Dassel, Germany), blocked with 5% BSA in

TBS-T buffer, and blotted with each primary antibody (1:1000) and its corresponding secondary antibody (1:5000), according to the manufacturer's instructions. The antibodies were detected with the WEST-SAVE Up™ luminol-based ECL reagent (LabFrontier, Seoul, Korea). The target bands were quantified using UN-SCAN-IT™ software Version 6.1 (Silk Scientific Co., Orem, UT).

2.4. STZ-induced animal model and measurement of mechanical allodynia

Diabetic neuropathic pain was modele using the antibiotic drug streptozocin which targets and kills the pancreatic beta islet cells rendering the animals with type I diabetes. A STZ-induced neuropathic model was performed according to the methodology described previously [162]. Briefly, diabetes mellitus type I was induced by intraperitoneal injections of streptozotocin (STZ, 150 mg/kg freshly dissolved in sodium citrate buffer at pH 4.5). All animals were fasted 6 h prior to injection of STZ. 10% sucrose water was supplied overnight to avoid sudden hypoglycemia after STZ injection. Diabetes was allowed to develop and stabilize in these STZ-treated mice over a period 5~7 days. After 6~7 days the blood glucose level was measured from tail vein according to the methodology reported previously [138, 163]. Mechanical allodynia was measured according to Cho et al. [138]. In order to evaluate the effect of anomalin (50 mg/kg), capillarisin (80 mg/kg) or celecoxib (50 mg/kg) were administered by intraperitoneal (i.p.) routes daily for 5 consective days, and the control group received the vehicle only. Mechanical allodynia was measured every day after 4 h of treatment.

2.5. Statistical analysis

Unless otherwise stated, results are expressed as means ± standard deviations (S.D) from three different experiments. One-way analysis of variance (ANOVA) followed by Dunnett's *t*-test was applied to assess the statistical significance of the differences between the study groups (SPSS version 10.0, Chicago, IL). A value of $P < 0.05$ was chosen as the criterion for statistical significance.

3. Results

3.1. Effect of anomalin and capillarisin on cell cytotoxicity and nitrite production in N2a cells

In order to optimize the proper concentrations and the effect of SNP was assessed in N2a cells using various concentrations of SNP for 24 h. The results demonstrated that SNP was observed neuroprotective at low concentrations while it exhibited significant neurotoxicity at high concentrations (**Fig. 72**). In the same manner, NO production was remarkably increased (**Fig. 72**).

Similarly, N2a cells were treated with different concentrations of SNP or anomalin and capillarisin for 24 h and MTT assay was carried out to determine the cytotoxic effect of both the samples. SNP reported as neurotoxic at high concentration [164]. The cell viability was significantly affected by treatment with 500 µM SNP (**Fig. 73B, Fig. 74B**), while

anomalin and capillarisin treatment alone (15 to 50 and 25 to 100 µM respectively) did not affect the cell viability (**Fig. 73A and Fig. 74A**). As shown in **Fig. 73** and **Fig. 74**, anomalin and capillarisin treatment attenuated SNP-induced cytotoxic effects at concentrations of 15 and 100 µM and 25 to 100 µM respectively. This result indicates that the treatment of anomalin and capillarisin both possessed protective effect on neurons.

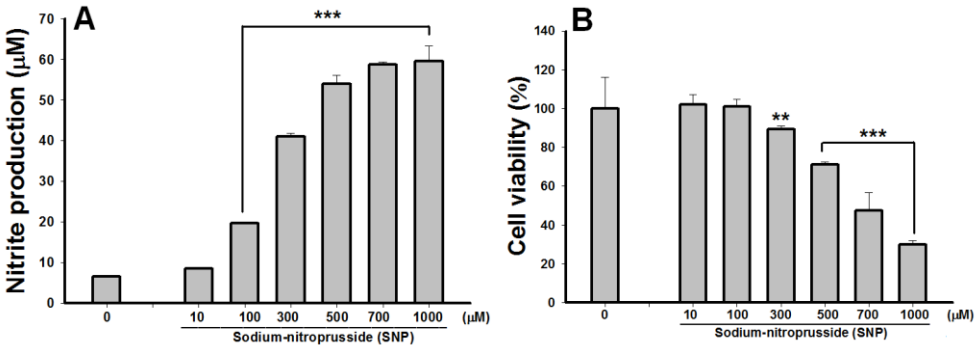

Figure 72. Effect of SNP on NO production (**A**) and cell viability (**B**) with and without SNP in N2a cells. Cells were treated for 24 h with different concentrations of SNP (0~1000 µM), and cell cytotoxicity was assessed by MTT and NO was measured by Griess reagent as described in "Materials and methods". Data were derived from three independent experiments and are expressed as the mean ± S.D. (**) *P<0.01* and *(***) P<0.001* indicate a significant difference from the SNP group. $^{###}$*P<0.001* indicates a significant difference from the unstimulated control group.

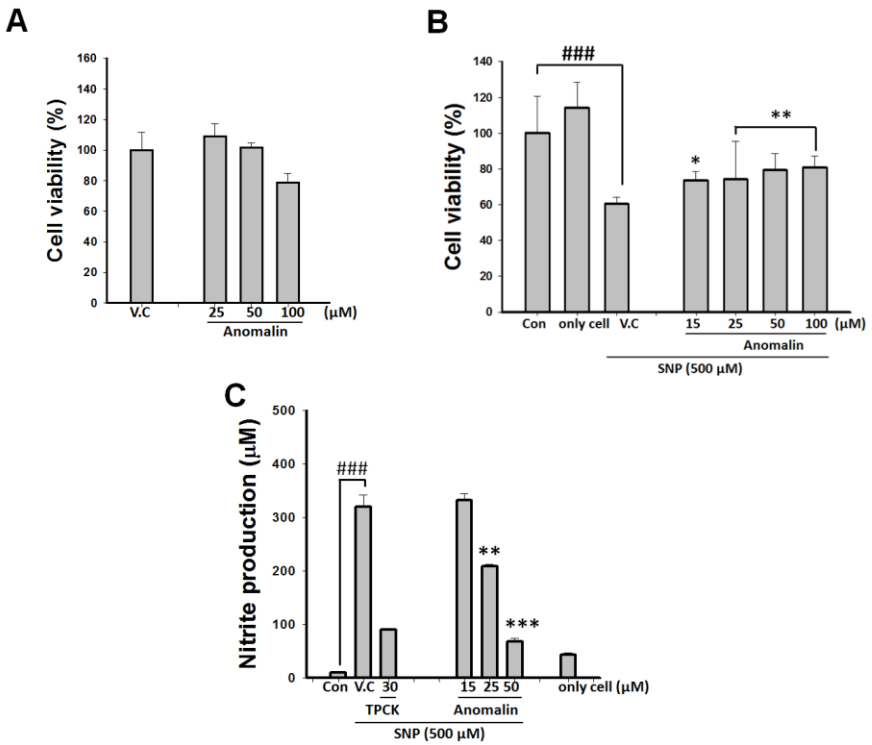

Figure 73. Effect of anomalin on cell viability in N2a cells without SNP (**A**) and with SNP treatment (**B**). Effect of anomalin on NO production in SNP-induced N2a cells (**C**). Cells were treated for 24 h with different concentrations of anomalin, and cell cytotoxicity was assessed by MTT and NO was measured by Griess reagent as described in "Materials and methods". Data were derived from three independent experiments and are expressed as the mean ± S.D. (**) *P<0.01* and *(***) P<0.001* indicate a significant difference from the SNP group. $^{###}P<0.001$ indicates a significant difference from the unstimulated control group. Control (vehicle alone), V.C; (SNP + vehicle)-treated cells alone; TPCK 30 μM, *N-p*-tosyl-L-phenylalanyl chloromethyl ketone was used as a positive control.

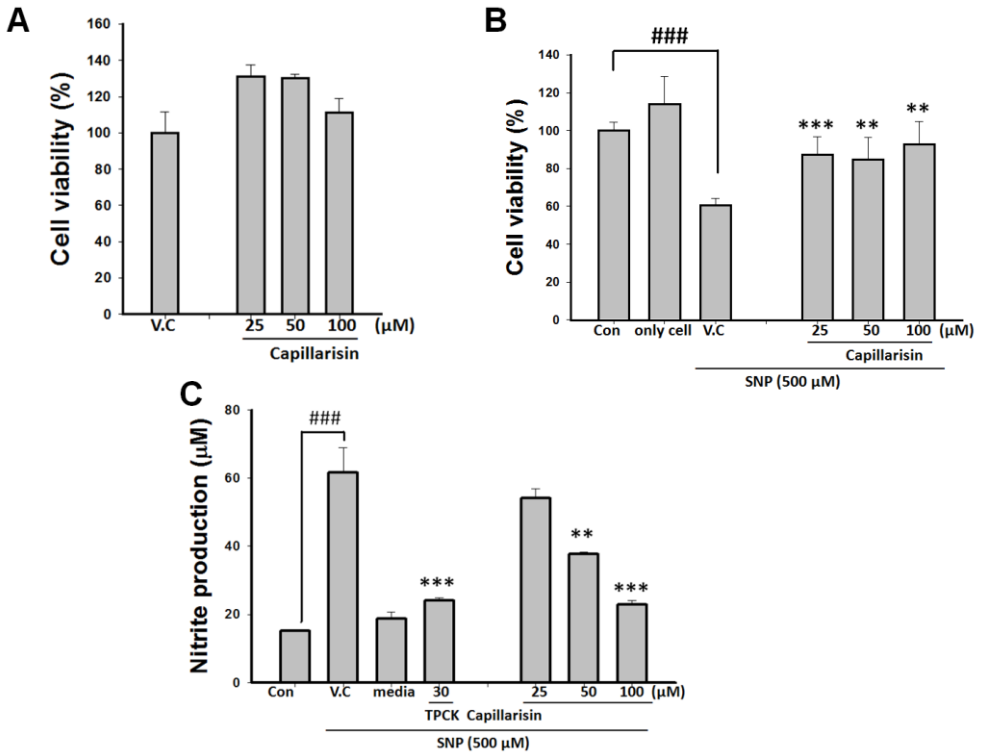

Figure 74. Effect of capillarisin on cell viability in N2a cells without SNP (**A**) and with SNP treatment (**B**). Effect of capillarisin on NO production in SNP-induced N2a cells (**C**). Cells were treated for 24 h with different concentrations of capillarisin, and cell cytotoxicity was assessed by MTT and NO was measured Griess reagent as described in "Materials and methods". Data were derived from three independent experiments and are expressed as the mean ± S.D. (**) *P<0.01* and *(***) P<0.001* indicate a significant difference from the SNP group. $^{###}$*P<0.001* indicates a significant difference from the unstimulated control group. Control (vehicle alone), V.C; (SNP + vehicle)-treated cells alone; TPCK 30 μM, *N-p*-tosyl-L-phenylalanyl chloromethyl ketone was used as a positive control.

The pro-inflammatory mediator (NO) was investigated as marker of inflammation in N2a cells. Treatment with SNP significantly increased the NO production in culture media (**Fig. 73** and **Fig. 74**). These increased production of NO remarkably reduced by anomalin and capillarisin (**Fig. 73** and **Fig. 74)**. TPCK 30 μM was used as positive for this experiment.

3.2. Effect of anomalin and capillarisin on iNOS and COX-2 mRNA expression levels in SNP-induced N2a cells

In order to determine whether anomalin and capillarisin regulates the NO with iNOS, we investigated their mRNA expression levels in SNP-induced N2a cells by quantitative-RT-PCR. SNP strongly induced the expressions of iNOS and COX-2 mRNA (**Fig. 75** and **Fig. 76**). However, in anomalin- and capillarisin-treated cells, expression of iNOS mRNA and COX-2 and were significantly decreased in a dose-dependent manner. These presenta results indicated that both the compounds (anomalin and capillarisn) could protect against NO-mediated neuronal cell injury.

3.3. Effect of anomalin and capillarisin on NF-κB and MAPKs pathway in SNP-induced N2a cells

In order to explore the molecular mechanism of anomalin and capillarisin in the signalling pathway, NF-κB and MAPKs pathways were brought under investigation by Western blotting analysis. As shown in **Fig.77** and **Fig. 78**, SNP strongly induced p-IKKα/β and p-IκBα expression levels at different time intervals. Anomalin and capillarisin down-regulated

the IKKα/β and p-IκBα expression levels in time dependent manner (**Fig.77** and **Fig. 78).**

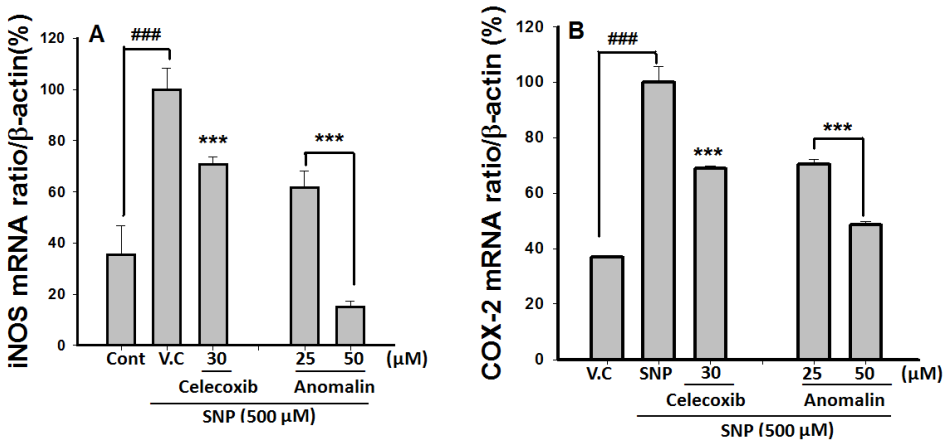

Figure 75. Effect of anomalin on iNOS (**A**) and COX-2 (**B**) mRNA expression levels in SNP-induced N2a cells. The mRNA levels were measured by qRT-PCR as described in "Materials and methods". Data were derived from three independent experiments and are expressed as the mean ± S.D. (**) *P<0.01* and *(***) P<0.001* indicate a significant difference from the SNP group. $^{###}$*P<0.001* indicates a significant difference from the unstimulated control group. Control (vehicle alone), V.C; (SNP + vehicle)-treated cells alone; Celecoxib 30 μM was used as a positive control.

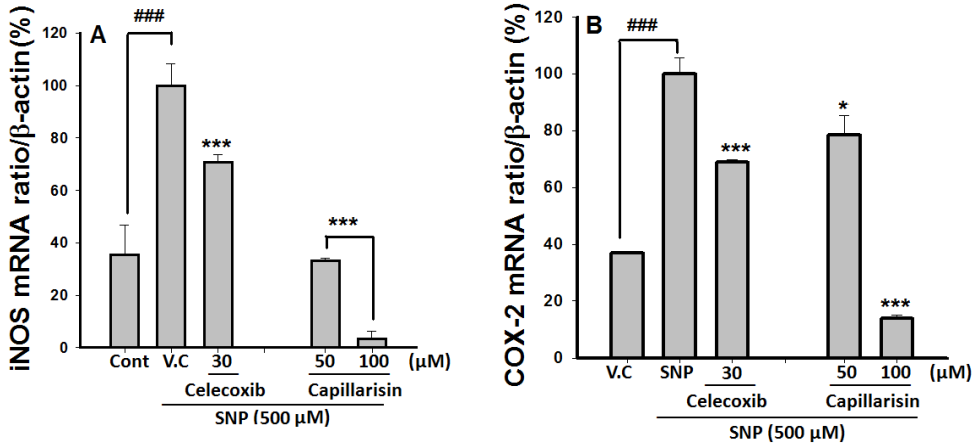

Figure 76. Effect of capillarisin on iNOS (**A**) and COX-2 (**B**) mRNA expression levels in SNP-induced N2a cells. The mRNA levels were measured by qRT-PCR as described in "Materials and methods". Data were derived from three independent experiments and are expressed as the mean ± S.D. (**) *P<0.01* and (***) *P<0.001* indicate a significant difference from the SNP group. $^{###}P<0.001$ indicates a significant difference from the unstimulated control group. Control (vehicle alone), V.C; (SNP + vehicle)-treated cells alone; Celecoxib 30 μM was used as a positive control.

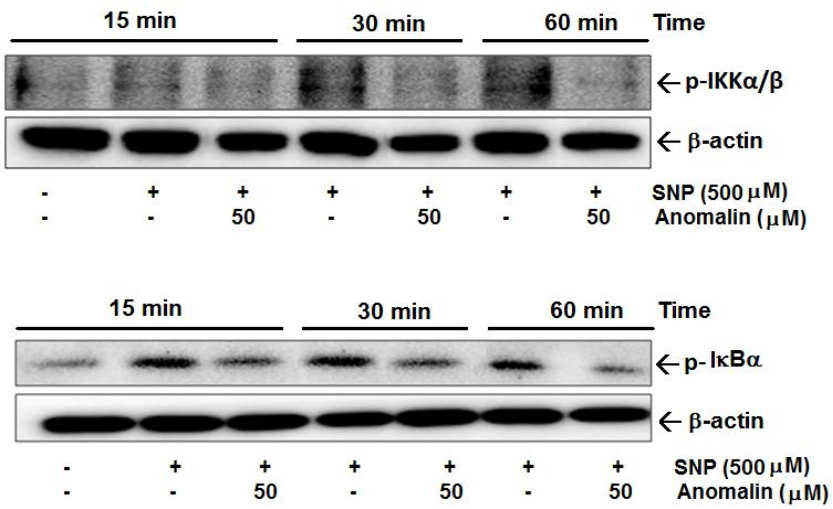

Figure 77. Effect of anomalin on phosphorylated p-IKKα/β and p-IκBα proteins in cytosolic extracts were determined by Western blot analysis, as described in the "Materials and methods". The N2a cells were pretreated with 50 μM of anomalin for 24 h and treated with SNP (500 μM) for the time periods specified.

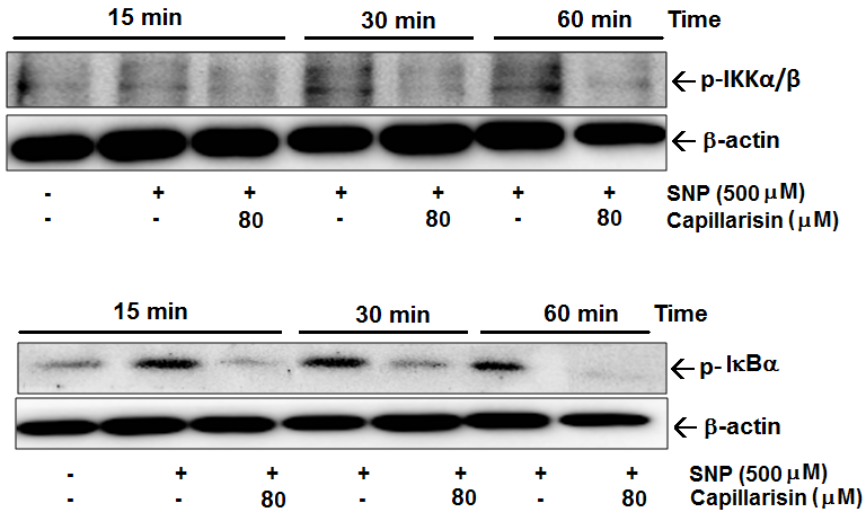

Figure 78. Effect of capillarisin on phosphorylated p-IKKα/β and p-IκBα proteins in cytosolic extracts were determined by Western blot analysis, as described in the "Materials and methods". The N2a cells were pretreated with 100 μM of capillarisin for 24 h and treated with SNP (500 μM) for the time periods specified.

Sodium nitroprusside induces NF-κB activation is implicated in MAPK's signaling [165]. Therefore, MAPK molecules were focused next by Western blotting. SNP significantly induced the phosphorylation of p-p38 and p-ERK in N2a cells (**Fig. 79** and **Fig. 80**). Anomalin and capillarisn down-regulated the increased expression levels of p-p38 and p-ERK remarkably (**Fig. 79** and **Fig. 80**).

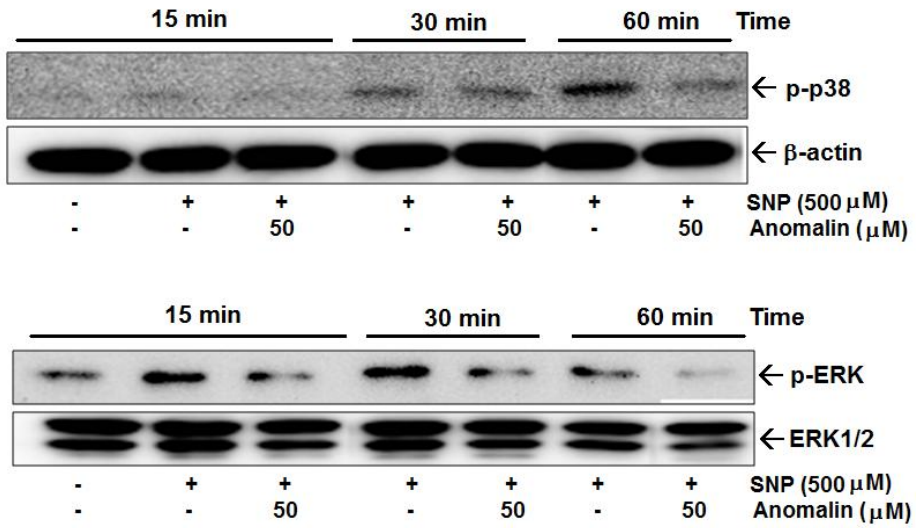

Figure 79. Effect of anomalin on phosphorylated p-p38 and p-ERK proteins in cytosolic extracts were determined by Western blot analysis, as described in the "Materials and methods". The N2a cells were pretreated with 50 μM of anomalin for 24 h and treated with SNP (500 μM) for the time periods specified.

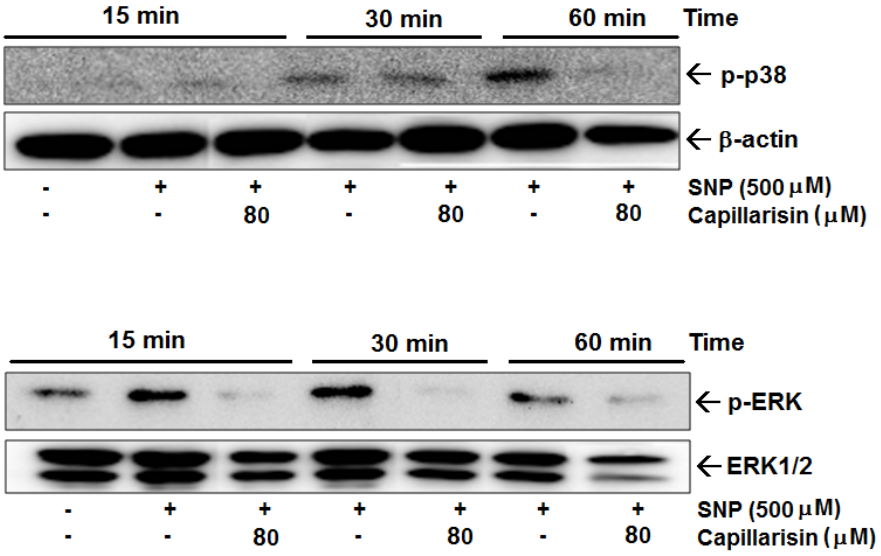

Figure 80. Effect of capillarisin on phosphorylated p-p38 and p-ERK proteins in cytosolic extracts were determined by Western blot analysis, as described in the "Materials and methods". The N2a cells were pretreated with 100 μM of capillarisin for 24 h and treated with SNP (500 μM) for the time periods specified.

3.4. Effect of anomalin and capillarisin on pro-inflammatory and pain cytokines in SNP-induced N2a cells

The levels of the pro-inflammatory cytokines (TNF-α, IL-6 and IL-1β) were significantly increased 24 h after SNP treatment (**Fig. 81**). These increase mRNA expression levels of cytokines were attenuated remarkably by anomalin and capillarisin (**Fig. 81**). Similarly, we also evaluated the effect of anomalin and capillarisin on anti-oxidant enzyme (HO-1) (data not shown).

3.5. Effect of anomalin and capillarisin on STZ-induced type I diabetic neuropathic pain model in animals

The diabetic neuropathic model is a chronic pain model designed to imitate the effects of nerve injury following chronic hyperglycemia. In the diabetic neuropathic model the mechanical withdrawal thresholds for all groups measured five days post streptozocin injection by Von Frey. **Fig. 82** illustrated that vehicle control group of mice produced significant allodynia. On the other hand, mice treated with treatment anomalin and capillarisin exhibited significant reduction in mechanical allodynia at 50 and 80 mg/ kg concentrations consecutive five days, respectively (**Fig. 82**). Interestingly, celecoxib 50 mg/kg (as positive control) effect was found less effect compared with anomalin and capillarisin (**Fig. 82**).

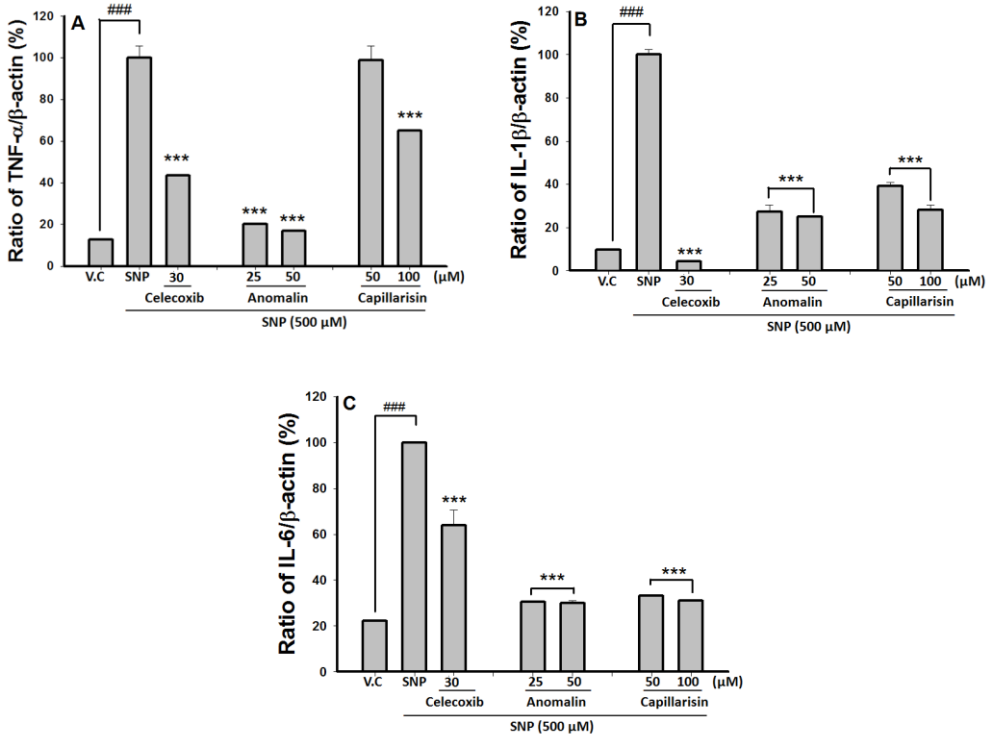

Figure 81. Inhibitory effect of anomalin and capillarisin on mRNA expression levels of TNF-α, IL-1β and IL-6 were determined by qRT-PCR. The data were obtained from three independent experiments and are expressed as the mean±S.D. (***) P<0.001 indicate significant differences from the SNP-treated group. ($^{###}$) P<0.001 indicates a significant difference from the unstimulated control group. Control (vehicle), SNP (SNP+ vehicle)-treated cells alone. Celecoxib (30 μM) was used as positive control.

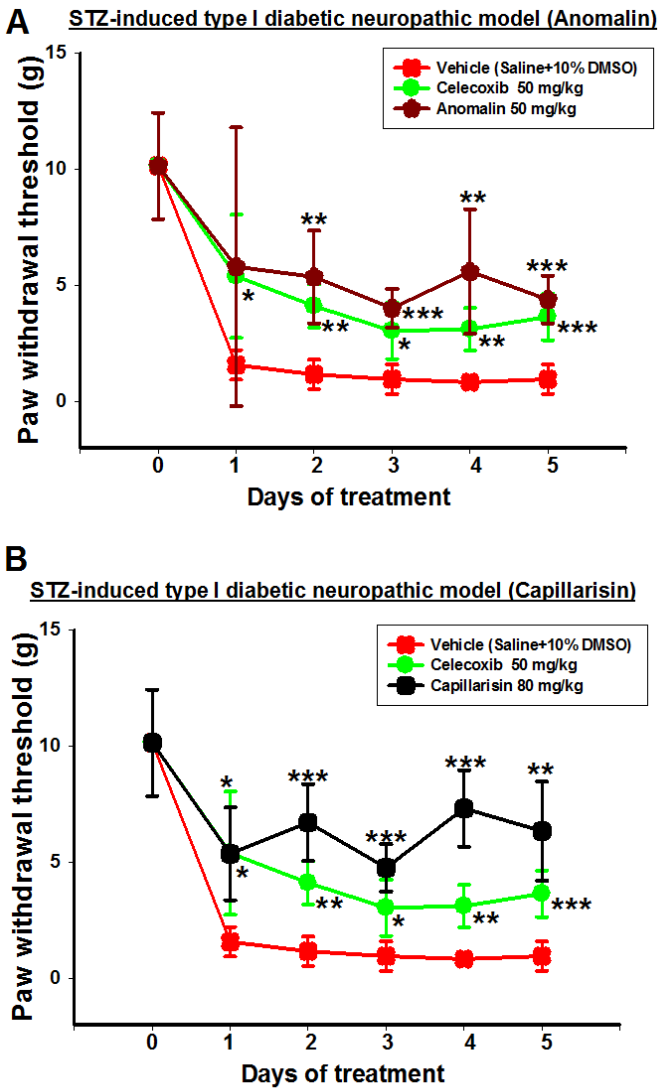

Figure 82. Inhibition of STZ-induced neuropathic pain model by anomalin (**A**) and capillarisin (**B**). Mechanical allodynia was measured by Von Frey test as described in "Materials and methods". The paw withdrawal effect was measured every day after 5 day after STZ induced diabetes. The data obtained are expressed as the means ± S.D. (*) $P<0.05$, (**) $P<0.01$ and (***) $P<0.001$ indicate significant differences from the vehicle group.

4. Discussion

Pain management and control is a major challenge specifically for patients suffering from chronic pain conditions. Regardless of the research and understanding of mechanisms of pain signaling and developing new therapeutic agents is currently no effective and successful treatment for these chronic pain conditions since decades. Hence, there is a strong need for new therapeutic agents to treat pain and to further understand the pathophysiology of chronic pain. In the present study, *in vitro* and *in vivo* pain models were performed. Although, these experimental models in *in vitro* and *in vivo* animals have limitations in their predictive capabilities they do show a robust and reproducible antihyperalgesic response to anomalin and capillarisin inhibition in all mice.

Sodium nitroprusside (SNP), $Na_2[Fe(CN)_5NO]$, SNP-is widely used in clinical and pharmacological studies as a potent antihypertensive agent, a vasodilator, and a NO donor [166]. The metabolism of SNP is shown in **Scheme 1**. The nitroprusside ion, $[Fe(CN)_5NO]^{2-}$, easily undergoes one-electron reduction to form $[Fe(CN)_5NO]^{3-}$, which releases one cyanide ligand quickly to form the paramagnetic complex $[Fe(CN)_4NO]^{2-}$. The paramagnetic species releases NO and undergoes further reactions to produce the very stable species $[Fe(CN)_6]^{4-}$ and Fe^{2+} [166]. The released cyanide can be converted to thiocyanate by rhodanese in the presence of sodium thiosulfate, a source of sulphur, and excreted in urine [166]. It is a key metabolic pathway for the detoxification of cyanide. Free cyanide readily reacts with the trivalent iron of cytochromes in mitochondria to form the cytochrome oxidase-cyanide complex. This complex inhibits cellular respiration, resulting in a reduction of ATP production. The other metabolites of SNP, $[Fe(CN)_5NO]^{3-}$ and $[Fe(CN)_4NO]^{2-}$, undergo redox

(reduction-oxidation) cycling with oxygen. O_2- formed during this cycle can produce hydrogen peroxide (H_2O_2) and oxygen (O_2) [$2O_2$- + $2H^+$ → O_2 + H_2O_2]. It has been proposed that DNA damage in cells can be triggered by the formation of reactive oxygen species, such as O_2-, H_2O_2 and OH-.[167]. These species directly induce damage in DNA [166].

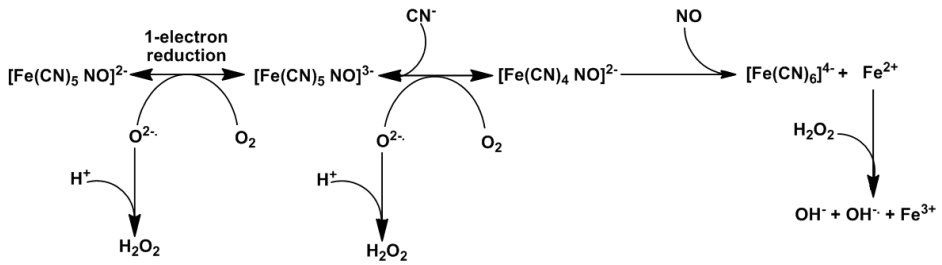

Scheme 1.

In contrast, the paramagnetic species, $[Fe(CN)_4NO]^{2-}$, releases NO. NO may result in nitrosylation of iron-sulphur centers in respiratory chain enzymes and cause metabolic inhibition, resulting in cellular toxicity. A more direct mechanism for NO-mediated cellular death has been suggested. Generation of NO under normal physiological conditions in the presence of O_2 can reproduce the chemical and mutagenic effects of NO^{2-} under acidic conditions. NO• mediates NO's neurotoxicity through an interaction with the superoxide radical (O2-•) to form peroxynitrite ($ONOO^-$). These peroxynitrite then turn to induce lipid peroxidation (LPO) linked to the disruption of cell membranes, leading to release of cell organelles. To withstand these effects, organisms have developed enzymatic and non-enzymatic antioxidant systems to alter or convert, and thus inactivate, these ROS. NO is a free radical that is physiologically produced through the *L*-

arginine/NO synthase (NOS) pathway and its overproduction can initiate neurotoxic actions under pathological conditions [168]. Production of NO is implicated in neurodegeneration in animal models and ischaemic cultured cells via stimulation of reactive oxygen species (ROS) production [168].

In order to understand the neuropathic pain, *in vitro* experimental model in SNP-induced N2a cell injury was designed. The aim of the present study was to investigate the protective effects of anomalin and capillarisin on SNP-induced cytotoxicity in mouse N2a neuronal cells and its mechanism of action in a signalling pathway. According to previous studies, the SNP is neurotoxic at higher concentrations [164]. Our result demonstrated that SNP-induced neurotoxic effect was remarbly protected by anomalin and capillarisin.

NO is an endogenous regulator of diverse cellular responses. In neurons, NO can mediate signalling but on the other hand contribute to neuronal death and brain damage in neurological disorders [169]. SNP, a NO donor, is extensively used in clinical and pharmacological studies as a potent antihypertensive agent, a vasodialator and a NO donor [166]. In N2a cells, SNP significantly produced NO in culture media. Whereas, anomalin and capillarisin, both significantly inhibited NO production of in culture media in N2a cells. Additonally, the Western blot analysis revealed that SNP-induced NO (iNOS) and PGE_2 (COX-2) regulated genes was considerably down-regulated by anomalin and capillarisin. These data indicate that anomalin and capillarisin could protect against NO-mediated neuronal cell injury. The physiological production of NO is by the *L*-arginine/NOS pathway and acts as a signal molecule in various physiological and pathological functions in brain [168]. Three isoforms of NOS, iNOS expression induced by SNP

stimulation. These results suggest that anomalin and capillarisin may prevent SNP-induced neuronal damages by preventing NO-mediated toxicity.

In order to clarify and specify the molecular mechanism of anomalin and capillarisin in SNP-induced N2a cells, NF-κB and MAPK signaling pathways were next focused. Based on the previous remarkable anti-nociceptive mechanism of anomalin and capillarisin in pain signaling, it was assumed to evaluate the effect of both the compounds on NF-κB and MAPK regulated proteins. Our results demonstrated that both the compounds exhibited significant effect on phosphorylation of IKKα/β, IκBα, p38 and ERK activations. The present study showed that anomalin and capillarisin may block the NF-κB pathway that induces neuronal cell death. The Furthermore, MAPK are essential upstream regulators of transcription factor activities, and their signaling is critical for the transduction of extracellular oxidative stress stimuli into intracellular events [170]. Therefore, blocking the MAPK pathway protects against brain injuries such as ischaemia [171].

Activation of NF-κB and MAPK contribute to the increased hyperalgesia by increasing production of various cytokines [172]. It well known that TNF-α, IL-6 and IL-1β precede the release of hyperalgesic mediators (COX-2, iNOS) which are involved with nociceptive sensitization [18]. To determine the effects of anomalin and capillarisin on SNP-induced cytokine production, qRT-PCR was performed. Herein, it was described that both the compound (anomalin and capillarisin) reduced IL-1β, IL-6 and TNF-α levels. Thus, the reduction of IL-1β IL-6 and TNF-α production can be responsible for neuronal cell damage. In addition, anomalin and capillarisin have no effect on SNP-induced anti-oxidant enzyme (HO-1) which is important for the control of cell death [173].

In order to evaluate the therapeutic effect of anomalin and capillarisin, STZ-induced diabetes type I was performed. The antibiotic drug streptozocin (STZ) which targets and kills the pancreatic beta islet cells rendering the animals with typeI diabetes [163]. Here the diabetic neuropathy model was used to address the effect of anomalin and capillarisin on allodynia after neuropathy developed. The results obtained in this study demonstrated a significant decrease in pain threshold and in the in diabetic mice by anomalin and capillarisin. Interestingly, the anomalin and capillarisin were more significant to celecoxib in reducing allodynia in the neuropathic pain model. Several other agents targeting inflammation and pain such as NSAIDs and selective COX-2 inhibitors have no established efficacy against diabetic induced-neuropathy in mice but are often used for this chronic pain [174]. Notably, the prolong use of these agents are counter indicated for patients suffering for nephropathic pain which is typical complication of diabetes. Hence, NSAIDs may offer some relief of mixed etiology pain [174]. Although, due to their severe side effects they are not suitable for moderate or severe diabetic neuropathic patients.There is currently no clear evidence of a single mechanism for diabetic neuropathic pain. It is possible that anomalin and capillarisin could decrease the pain that is implicated in the STZ-induced progressive damage to pancreatic beta cells of this diabetic neuropathic model, but this is an issue for further research.

CONCLUSION

In summary, the present study add evidences that anomalin, calipteryxin, (3´*S*,4´*S*)-3´,4´-disenecioyloxy-3´,4´-dihydroseselin, 15, 16-epoxy-3α-hydroxylabda-8,13(16),14-trien-7-one, and capillarisin exerts a significant inhibitory effects on the production of LPS-induced pro-inflammatory mediators in *in vitro*. This anti-inflammatory property of anomalin, calipteryxin, (3´*S*,4´*S*)-3´, 4´-disenecioyloxy-3´,4´-dihydroseselin), 15,16-epoxy-3α-hydroxylabda-8,13(16),14-trien-7-one and capillarisin occurs via the down-regulation of iNOS and COX-2 expressions through the inhibition of the transcription factors NF-κB and AP-1. The inhibition is caused by the suppression of IKK phosphorylation, and inhibition of IκBα phosphorylation and degradation. On the hand, MAPKs protein, including ERK, JNK and p-38 activations were significantly reduced by all the compounds. In view of the fact that NO and PGE_2 play important roles in mediating inflammatory responses, the inhibitory effects of all the compunds on iNOS and COX-2 gene expressions might be responsible for its anti-inflammatory action. Overall, the inhibition of NF-κB and AP-1 prevent the induction of the MAPK and Akt pathways, thus avoiding the pathophysiology of inflammatory disorders.

The present study provides convincing evidence that anomalin and capillarisin, naturally occurring phenolic compounds, produced significant anti-hyperalgesic and anti-allodynic effects in two models of acute and persistent inflammatory (CFA and carrageenan) pain when evaluated by the Randall Selitto and Von Frey tests in the hind paw. Additionally, both the compounds reduced CFA- and carrageenan-induced paw edema and, subsequently, the TNF-α in paw tissue and NO in blood plasma. The beneficial effect of anomalin and capillarisin appears to occur via several

molecular mechanisms, including the inhibition of NF-κB signaling, which leads to the down-regulation of iNOS, COX-2 and TNF-α, MAPKs/AP-1 and the CREB pathway.

The *in vitro* SNP-induced N2a cells experimental model showed that anomalin and capillarisin exhibited promising protective activity against SNP-induced cytotoxicity. In parallel, the NO release in the media was remarkably inhibited by both the phenolic compounds. The involvement of signaling pathways result demonstrated that anomalin and capillarisin block the NF-κB and MAPKs activation in SNP-induced N2a cells. Addionally, anomalin and capillarisin down-regulated the SNP-induced mRNA levels of TNF-α, IL-1β and IL-6 in N2a cells. Furthermore, STZ-induced diabetic neuropathic chronic pain model revealed that anomalin and capillarisin remarkably reduced mechanical allodynia in mice. It is noteworthy, that the effect of both the phenolic compounds was considerably better than celecoxib. Although, more in depth investigation are still required to elucidate the detailed mechanism, we suggest that these compounds might be more useful for treatment of chronic neuropathic pain, and the results from the present study provided base for design and interpretation of future studies on chronic neuropathic and inflammatory pain.

REFRENCES

[1] Dinarello CA. Anti-inflammatory Agents: Present and Future. Cell 2010;140:935-50.

[2] Hotamisligil GS. Inflammation and metabolic disorders. Nature 2006;444:860-7.

[3] Gaestel M, Kotlyarov A, Kracht M. Targeting innate immunity protein kinase signalling in inflammation. Nat Rev Drug Discov 2009;8:480-99.

[4] Wellen KE, Hotamisligil GS. Inflammation, stress, and diabetes. J Clin Invest 2005;115:1111-9.

[5] Gilroy DW, Lawrence T, Perretti M, Rossi AG. Inflammatory resolution: new opportunities for drug discovery. Nat Rev Drug Discov 2004;3:401-16.

[6] Nathan C. Points of control in inflammation. Nature 2002;420:846-52.

[7] Aderem A, Ulevitch RJ. Toll-like receptors in the induction of the innate immune response. Nature 2000;406:782-7.

[8] Shimazu R, Akashi S, Ogata H, Nagai Y, Fukudome K, Miyake K, Kimoto M. MD-2, a molecule that confers lipopolysaccharide responsiveness on Toll-like receptor 4. J Exp Med 1999;189:1777-82.

[9] Inohara N, Ogura Y, Chen FF, Muto A, Nunez G. Human Nod1 confers responsiveness to bacterial lipopolysaccharides. J Biol Chem 2001;276:2551-4.

[10] Inohara N, Ogura Y, Nunez G. Nods: a family of cytosolic proteins that regulate the host response to pathogens. Curr Opin Microbiol 2002;5:76-80.

[11] Hampe J, Grebe J, Nikolaus S, Solberg C, Croucher PJ, Mascheretti S, Jahnsen J, Moum B, Klump B, Krawczak M, Mirza MM, Foelsch UR, Vatn M, Schreiber S. Association of NOD2 (CARD 15) genotype with clinical course of Crohn's disease: a cohort study. Lancet 2002;359:1661-5.

[12] Tergaonkar V. NF-κB pathway: a good signaling paradigm and therapeutic target. Int J Biochem Cell Biol 2006;38:1647-53.

[13] Hayden MS, Ghosh S. Signaling to NF-κB. Genes Dev 2004;18:2195-224.

[14] Thomas KW, Monick MM, Staber JM, Yarovinsky T, Carter AB, Hunninghake GW. Respiratory syncytial virus inhibits apoptosis and induces NF-κB activity through a phosphatidylinositol 3-kinase-dependent pathway. J Biol Chem 2002;277:492-501.

[15] Brazil DP, Hemmings BA. Ten years of protein kinase B signalling: a hard Akt to follow. Trends Biochem Sci 2001;26:657-64.

[16] Hattori Y, Hattori S, Kasai K. Lipopolysaccharide activates Akt in vascular smooth muscle cells resulting in induction of inducible nitric oxide synthase through nuclear factor-κB activation. Eur J Pharmacol 2003;481:153-8.

[17] Monick MM, Hunninghake GW. Second messenger pathways in pulmonary host defense. Annu Rev Physiol 2003;65:643-67.

[18] de Oliveira CM, Nonato FR, de Lima FO, Couto RD, David JP, David JM, Soares MB, Villarreal CF. Anti-nociceptive properties of bergenin. J Nat Prod 2011;74:2062-8.

[19] Negus SS, Bilsky EJ, Do Carmo GP, Stevenson GW. Rationale and methods for assessment of pain-depressed behavior in preclinical assays of pain and analgesia. Methods Mol Biol 2010;617:79-91.

[20] Stevenson GW, Bilsky EJ, Negus SS. Targeting pain-suppressed behaviors in preclinical assays of pain and analgesia: effects of morphine on acetic acid-suppressed feeding in C57BL/6J mice. J Pain 2006;7:408-16.

[21] Argoff C. Mechanisms of pain transmission and pharmacologic management. Curr Med Res Opin 2011;27:2019-31.

[22] Woolf CJ. What is this thing called pain? J Clin Invest 2010;120:3742-4.

[23] Marchand F, Perretti M, McMahon SB. Role of the immune system in chronic pain. Nat Rev Neurosci 2005;6:521-32.

[24] Mico JA, Ardid D, Berrocoso E, Eschalier A. Anti-depressants and pain. Trends Pharmacol Sci 2006;27:348-54.

[25] Johanek L, Shim B, Meyer RA. Chapter 4 Primary hyperalgesia and nociceptor sensitization. Handb Clin Neurol 2006;81:35-47.

[26] Overington JP, Al-Lazikani B, Hopkins AL. How many drug targets are there? Nat Rev Drug Discov 2006;5:993-6.

[27] Sindrup SH, Jensen TS. Efficacy of pharmacological treatments of neuropathic pain: an update and effect related to mechanism of drug action. Pain 1999;83:389-400.

[28] Rose MA, Kam PC. Gabapentin: pharmacology and its use in pain management. Anaesthesia 2002;57:451-62.

[29] Scholz J, Woolf CJ. Can we conquer pain? Nat Neurosci 2002;5 Suppl:1062-7.

[30] Finnerup NB, Otto M, McQuay HJ, Jensen TS, Sindrup SH. Algorithm for neuropathic pain treatment: an evidence based proposal. Pain 2005;118:289-305.

[31] Vinik AI, Casellini CM. Guidelines in the management of diabetic nerve pain: clinical utility of pregabalin. Diabetes Metab Syndr Obes 2013;6:57-78.

[32] Kuo YC, Lin YL, Huang CP, Shu JW, Tsai WJ. A tumor cell growth inhibitor from *Saposhnikovae divaricata*. Cancer Invest 2002;20:955-64.

[33] Khan S, Shin EM, Choi RJ, Jung YH, Kim J, Tosun A, Kim YS. Suppression of LPS-induced inflammatory and NF-κB responses by anomalin in RAW 264.7 macrophages. J Cell Biochem 2011;112:2179-88.

[34] Hu CQ, Chang JJ, Lee KH. Anti-tumor agents, 115. Seselidiol, a new cytotoxic polyacetylene from *Seseli mairei*. J Nat Prod 1990;53:932-5.

[35] Romero-Gonzalez RR, Avila-Nunez JL, Aubert L, Alonso-Amelot ME. Labdane diterpenes from *Leonurus japonicus* leaves. Phytochemistry 2006;67:965-70.

[36] Khan S, Shehzad O, Jin HG, Woo ER, Kang SS, Baek SW, Kim J, Kim YS. Anti-inflammatory mechanism of 15,16-epoxy-3α-hydroxylabda-8,13(16),14-trien-7-one via inhibition of LPS-induced multicellular signaling pathways. J Nat Prod 2012;75:67-71.

[37] Khan S, Choi RJ, Shehzad O, Kim HP, Islam MN, Choi JS, Kim YS. Molecular mechanism of capillarisin-mediated inhibition of MyD88/TIRAP inflammatory signaling in *in vitro* and *in vivo* experimental models. J Ethnopharmacol 2013;145:626-37.

[38] Patel SA, Heinrich AC, Reddy BY, Rameshwar P. Inflammatory mediators: Parallels between cancer biology and stem cell therapy. J Inflamm Res 2009;2:13-9.

[39] Smolen JS, Steiner G. Therapeutic strategies for rheumatoid arthritis. Nat Rev Drug Discov 2003;2:473-88.

[40] Novotny NM, Markel TA, Crisostomo PR, Meldrum DR. Differential IL-6 and VEGF secretion in adult and neonatal mesenchymal stem cells: role of NF-κB. Cytokine 2008;43:215-9.

[41] Medzhitov R. Toll-like receptors and innate immunity. Nat Rev Immunol 2001;1:135-45.

[42] van Den Brink GR, ten Kate FJ, Ponsioen CY, Rive MM, Tytgat GN, van Deventer SJ, Peppelenbosch MP. Expression and activation of NF-κB in the antrum of the human stomach. J Immunol 2000;164:3353-9.

[43] Takeda K, Kaisho T, Akira S. Toll-like receptors. Annu Rev Immunol 2003;21:335-76.

[44] Mattson MP. NF-κB in the survival and plasticity of neurons. Neurochem Res 2005;30:883-93.

[45] Sun XF, Zhang H. NF-κB and NF-κBI polymorphisms in relation to susceptibility of tumour and other diseases. Histol Histopathol 2007;22:1387-98.

[46] Sarada S, Himadri P, Mishra C, Geetali P, Ram MS, Ilavazhagan G. Role of oxidative stress and NF-κB in hypoxia-induced pulmonary edema. Exp Biol Med (Maywood) 2008;233:1088-98.

[47] Kang J, Zhou L, Sun JH, Ye M, Han J, Wang BR, Guo DA. Three new compounds from the roots of *Saposhnikovia divaricata*. J Asian Nat Prod Res 2008;10:971-6.

[48] Hradilek A, Fuchs O, Neuwirt J. Inhibition of heme synthesis decreases transferrin receptor expression in mouse erythroleukemia cells. J Cell Physiol 1992;150:327-33.

[49] Yoshikawa M, Nishida N, Ninomiya K, Ohgushi T, Kubo M, Morikawa T, Matsuda H. Inhibitory effects of coumarin and acetylene constituents from the roots of *Angelica furcijuga* on D-galactosamine/lipopolysaccharide-induced liver injury in mice and on nitric oxide production in lipopolysaccharide-activated mouse peritoneal macrophages. Bioorg Med Chem 2006;14:456-63.

[50] Ahn KS, Noh EJ, Zhao HL, Jung SH, Kang SS, Kim YS. Inhibition of inducible nitric oxide synthase and cyclooxygenase II by *Platycodon grandiflorum* saponins via suppression of nuclear factor-κB activation in RAW 264.7 cells. Life Sci 2005;76:2315-28.

[51] Shin EM, Zhou HY, Guo LY, Kim JA, Lee SH, Merfort I, Kang SS, Kim HS, Kim S, Kim YS. Anti-inflammatory effects of glycyrol isolated from *Glycyrrhiza uralensis* in LPS-stimulated RAW264.7 macrophages. Int Immunopharmacol 2008;8:1524-32.

[52] Collins T, Cybulsky MI. NF-κB: pivotal mediator or innocent bystander in atherogenesis? J Clin Invest 2001;107:255-64.

[53] Lee FS, Peters RT, Dang LC, Maniatis T. MEKK1 activates both IκB kinase α and IκB kinase β. Proc Natl Acad Sci USA 1998;95:9319-24.

[54] Lee SJ, Bai SK, Lee KS, Namkoong S, Na HJ, Ha KS, Han JA, Yim SV, Chang K, Kwon YG, Lee SK, Kim YM. Astaxanthin inhibits nitric oxide production and inflammatory gene expression by suppressing IκB kinase-dependent NF-κB activation. Mol Cells 2003;16:97-105.

[55] Surh YJ, Chun KS, Cha HH, Han SS, Keum YS, Park KK, Lee SS. Molecular mechanisms underlying chemopreventive activities of anti-inflammatory phytochemicals: down-regulation of COX-2 and

iNOS through suppression of NF-κB activation. Mutat Res 2001;480-481:243-68.

[56] Aggarwal BB, Shishodia S. Molecular targets of dietary agents for prevention and therapy of cancer. Biochem Pharmacol 2006;71:1397-421.

[57] Han Z, Boyle DL, Manning AM, Firestein GS. AP-1 and NF-κB regulation in rheumatoid arthritis and murine collagen-induced arthritis. Autoimmunity 1998;28:197-208.

[58] Naureckiene S, Edris W, Ajit SK, Katz AH, Sreekumar K, Rogers KE, Kennedy JD, Jones PG. Use of a murine cell line for identification of human nitric oxide synthase inhibitors. J Pharmacol Toxicol Methods 2007;55:303-13.

[59] Van Assche G, Rutgeerts P. Physiological basis for novel drug therapies used to treat the inflammatory bowel diseases. I. Immunology and therapeutic potential of antiadhesion molecule therapy in inflammatory bowel disease. Am J Physiol Gastrointest Liver Physiol 2005;288:G169-74.

[60] Chambers CD, Tutuncu ZN, Johnson D, Jones KL. Human pregnancy safety for agents used to treat rheumatoid arthritis: adequacy of available information and strategies for developing post-marketing data. Arthritis Res Ther 2006;8:215.

[61] Yamamoto Y, Gaynor RB. Therapeutic potential of inhibition of the NF-κB pathway in the treatment of inflammation and cancer. J Clin Invest 2001;107:135-42.

[62] Kimball SR. Eukaryotic initiation factor eIF2. Int J Biochem Cell Biol 1999;31:25-9.

[63] Sweet MJ, Hume DA. Endotoxin signal transduction in macrophages. J Leukoc Biol 1996;60:8-26.

[64] Hoffmann A, Levchenko A, Scott ML, Baltimore D. The IκB-NF-κB signaling module: temporal control and selective gene activation. Science 2002;298:1241-5.

[65] Ghosh S, Karin M. Missing pieces in the NF-κB puzzle. Cell 2002;109 Suppl:S81-96.

[66] Lee HJ, Maeng K, Dang HT, Kang GJ, Ryou C, Jung JH, Kang HK, Prchal JT, Yoo ES, Yoon D. Anti-inflammatory effect of methyl dehydrojasmonate (J2) is mediated by the NF-κB pathway. J Mol Med (Berl) 2011;89:83-90.

[67] Aggarwal BB, Shishodia S, Sandur SK, Pandey MK, Sethi G. Inflammation and cancer: how hot is the link? Biochem Pharmacol 2006;72:1605-21.

[68] Kupeli E, Tosun A, Yesilada E. Anti-inflammatory and antinociceptive activities of *Seseli* L. species (Apiaceae) growing in Turkey. J Ethnopharmacol 2006;104:310-4.

[69] Choi RJ, Ngoc TM, Bae K, Cho HJ, Kim DD, Chun J, Khan S, Kim YS. Anti-inflammatory properties of anthraquinones and their relationship with the regulation of P-glycoprotein function and expression. Eur J Pharm Sci 2013;48:272-81.

[70] Pan MH, Lai CS, Wang YJ, Ho CT. Acacetin suppressed LPS-induced up-expression of iNOS and COX-2 in murine macrophages and TPA-induced tumor promotion in mice. Biochem Pharmacol 2006;72:1293-303.

[71] Rhoades KL, Golub SH, Economou JS. The regulation of the human tumor necrosis factor-α promoter region in macrophage, T cell, and B cell lines. J Biol Chem 1992;267:22102-7.

[72] Gomez PF, Pillinger MH, Attur M, Marjanovic N, Dave M, Park J, Bingham CO, 3rd, Al-Mussawir H, Abramson SB. Resolution of

inflammation: prostaglandin E_2 dissociates nuclear trafficking of individual NF-κB subunits (p65, p50) in stimulated rheumatoid synovial fibroblasts. J Immunol 2005;175:6924-30.

[73] Takamata A. Effect of vagotomy on cardiovascular adjustment to hyperthermia in rats. Jpn J Physiol 1992;42:641-52.

[74] Greenhough A, Smartt HJ, Moore AE, Roberts HR, Williams AC, Paraskeva C, Kaidi A. The COX-2/PGE_2 pathway: key roles in the hallmarks of cancer and adaptation to the tumour microenvironment. Carcinogenesis 2009;30:377-86.

[75] Liu SF, Malik AB. NF-κB activation as a pathological mechanism of septic shock and inflammation. Am J Physiol Lung Cell Mol Physiol 2006;290:L622-L45.

[76] Karin M, Lawrence T, Nizet V. Innate immunity gone awry: linking microbial infections to chronic inflammation and cancer. Cell 2006;124:823-35.

[77] Lawrence T, Bebien M. IKKα in the regulation of inflammation and adaptive immunity. Biochem Soc Trans 2007;35:270-2.

[78] Dolcet X, Llobet D, Pallares J, Matias-Guiu X. NF-κB in development and progression of human cancer. Virchows Arch 2005;446:475-82.

[79] Li Q, Verma IM. NF-κB regulation in the immune system. Nat Rev Immunol 2002;2:725-34.

[80] Karin M, Takahashi T, Kapahi P, Delhase M, Chen Y, Makris C, Rothwarf D, Baud V, Natoli G, Guido F, Li N. Oxidative stress and gene expression: the AP-1 and NF-κB connections. Biofactors 2001;15:87-9.

[81] Madrid LV, Mayo MW, Reuther JY, Baldwin AS, Jr. Akt stimulates the transactivation potential of the RelA/p65 Subunit of NF-κB

through utilization of the IκB kinase and activation of the mitogen-activated protein kinase p38. J Biol Chem 2001;276:18934-40.

[82] Carter AB, Knudtson KL, Monick MM, Hunninghake GW. The p38 mitogen-activated protein kinase is required for NF-κB-dependent gene expression. The role of TATA-binding protein (TBP). J Biol Chem 1999;274:30858-63.

[83] Moon HT, Jin Q, Shin JE, Choi EJ, Han HK, Kim YS, Woo ER. Bis-spirolabdane-type diterpenoids from *Leonurus sibiricus*. J Nat Prod 2010;73:123-6.

[84] Boalino DM, McLean S, Reynolds WF, Tinto WF. Labdane diterpenes of *Leonurus sibiricus*. J Nat Prod 2004;67:714-7.

[85] Chinou I. Labdanes of natural origin-biological activities (1981-2004). Curr Med Chem 2005;12:1295-317.

[86] Traves PG, Hortelano S, Zeini M, Chao TH, Lam T, Neuteboom ST, Theodorakis EA, Palladino MA, Castrillo A, Bosca L. Selective activation of liver X receptors by acanthoic acid-related diterpenes. Mol Pharmacol 2007;71:1545-53.

[87] Xu J, Liu C, Guo P, Guo Y, Jin DQ, Song X, Sun Z, Gui L, Ma Y. Neuroprotective labdane diterpenes from *Fritillaria ebeiensis*. Fitoterapia 2011;82:772-6.

[88] Rigano D, Aviello G, Bruno M, Formisano C, Rosselli S, Capasso R, Senatore F, Izzo AA, Borrelli F. Anti-spasmodic effects and structure-activity relationships of labdane diterpenoids from M*arrubium globosum* ssp. libanoticum. J Nat Prod 2009;72:1477-81.

[89] Scio E, Ribeiro A, Alves TM, Romanha AJ, Dias de Souza Filho J, Cordell GA, Zani CL. Diterpenes from *Alomia myriadenia* (Asteraceae) with cytotoxic and trypanocidal activity. Phytochemistry 2003;64:1125-31.

[90] Chiou WF, Sung YJ, Liao JF, Shum AY, Chen CF. Inhibitory effect of dehydroevodiamine and evodiamine on nitric oxide production in cultured murine macrophages. J Nat Prod 1997;60:708-11.

[91] Zhang JY, Jin H, Wang GF, Yu PJ, Wu SY, Zhu ZG, Li ZH, Tian YX, Xu W, Zhang JJ, Wu SG. Methyl-1-hydroxy-2-naphthoate, a novel naphthol derivative, inhibits lipopolysaccharide-induced inflammatory response in macrophages via suppression of NF-κB, JNK and p38 MAPK pathways. Inflamm Res 2011;60:851-9.

[92] Moon KY, Hahn BS, Lee J, Kim YS. A cell-based assay system for monitoring NF-κB activity in human HaCat transfectant cells. Anal Biochem 2001;292:17-21.

[93] Decker K. Biologically active products of stimulated liver macrophages (Kupffer cells). Eur J Biochem 1990;192:245-61.

[94] Yam MF, Asmawi MZ, Basir R. An investigation of the anti-inflammatory and analgesic effects of Orthosiphon stamineus leaf extract. J Med Food 2008;11:362-8.

[95] Kim HS, Whang SY, Woo MS, Park JS, Kim WK, Han IO. Sodium butyrate suppresses interferon-γ-, but not lipopolysaccharide-mediated induction of nitric oxide and tumor necrosis factor-alpha in microglia. J Neuroimmunol 2004;151:85-93.

[96] Alexander C, Rietschel ET. Bacterial lipopolysaccharides and innate immunity. J Endotoxin Res 2001;7:167-202.

[97] Datla P, Kalluri MD, Basha K, Bellary A, Kshirsagar R, Kanekar Y, Upadhyay S, Singh S, Rajagopal V. 9,10-dihydro-2,5-dimethoxyphenanthrene-1,7-diol, from *Eulophia ochreata*, inhibits inflammatory signalling mediated by Toll-like receptors. Br J Pharmacol 2010;160:1158-70.

[98] Takeda K, Akira S. TLR signaling pathways. Semin Immunol 2004;16:3-9.

[99] Verstrepen L, Bekaert T, Chau TL, Tavernier J, Chariot A, Beyaert R. TLR-4, IL-1R and TNF-R signaling to NF-κB: variations on a common theme. Cell Mol Life Sci 2008;65:2964-78.

[100] DasGupta S, Murumkar PR, Giridhar R, Yadav MR. Current perspective of TACE inhibitors: a review. Bioorg Med Chem 2009;17:444-59.

[101] Kim EK, Kwon KB, Han MJ, Song MY, Lee JH, Lv N, Choi KB, Ryu DG, Kim KS, Park JW, Park BH. Inhibitory effect of *Artemisia capillaris* extract on cytokine-induced nitric oxide formation and cytotoxicity of RINm5F cells. Int J Mol Med 2007;19:535-40.

[102] Hong JH, Hwang EY, Kim HJ, Jeong YJ, Lee IS. *Artemisia capillaris* inhibits lipid accumulation in 3T3-L1 adipocytes and obesity in C57BL/6J mice fed a high fat diet. J Med Food 2009;12:736-45.

[103] Han KH, Jeon YJ, Athukorala Y, Choi KD, Kim CJ, Cho JK, Sekikawa M, Fukushima M, Lee CH. A water extract of *Artemisia capillaris* prevents 2,2'-azobis(2-amidinopropane) dihydrochloride-induced liver damage in rats. J Med Food 2006;9:342-7.

[104] Kwon OS, Choi JS, Islam MN, Kim YS, Kim HP. Inhibition of 5-lipoxygenase and skin inflammation by the aerial parts of A*rtemisia capillaris* and its constituents. Arch Pharm Res 2011;34:1561-9.

[105] Kim YH, Lee SH, Lee JY, Choi SW, Park JW, Kwon TK. Triptolide inhibits murine-inducible nitric oxide synthase expression by down-regulating lipopolysaccharide-induced activity of nuclear factor-κB and c-Jun NH_2-terminal kinase. Eur J Pharmacol 2004;494:1-9.

[106] Shin EM, Zhou HY, Xu GH, Lee SH, Merfort I, Kim YS. Anti-inflammatory activity of hispidol A 25-methyl ether, a triterpenoid isolated from *Ponciri Immaturus* Fructus. Eur J Pharmacol 2010;627:318-24.

[107] Choy CS, Hu CM, Chiu WT, Lam CS, Ting Y, Tsai SH, Wang TC. Suppression of lipopolysaccharide-induced of inducible nitric oxide synthase and cyclooxygenase-2 by *Sanguis Draconis*, a dragon's blood resin, in RAW 264.7 cells. J Ethnopharmacol 2008;115:455-62.c

[108] Senthil Kumar KJ, Wang SY. Lucidone inhibits iNOS and COX-2 expression in LPS-induced RAW 264.7 murine macrophage cells via NF-κB and MAPKs signaling pathways. Planta Med 2009;75:494-500.

[109] Lai CS, Lee JH, Ho CT, Liu CB, Wang JM, Wang YJ, Pan MH. Rosmanol potently inhibits lipopolysaccharide-induced iNOS and COX-2 expression through downregulating MAPK, NF-κB, STAT3 and C/EBP signaling pathways. J Agric Food Chem 2009;57:10990-8.

[110] Kim HG, Yoon DH, Lee WH, Han SK, Shrestha B, Kim CH, Lim MH, Chang W, Lim S, Choi S, Song WO, Sung JM, Hwang KC, Kim TW. Phellinus linteus inhibits inflammatory mediators by suppressing redox-based NF-κB and MAPKs activation in lipopolysaccharide-induced RAW 264.7 macrophage. J Ethnopharmacol 2007;114:307-15.

[111] Jarrar D, Kuebler JF, Rue LW, 3rd, Matalon S, Wang P, Bland KI, Chaudry IH. Alveolar macrophage activation after trauma-hemorrhage and sepsis is dependent on NF-κB and MAPK/ERK

mechanisms. Am J Physiol Lung Cell Mol Physiol 2002;283:L799-805.

[112] Zhang G, Ghosh S. Molecular mechanisms of NF-κB activation induced by bacterial lipopolysaccharide through Toll-like receptors. J Endotoxin Res 2000;6:453-7.

[113] Lee SO, Jeong YJ, Kim M, Kim CH, Lee IS. Suppression of PMA-induced tumor cell invasion by capillarisin via the inhibition of NF-κB-dependent MMP-9 expression. Biochem Biophys Res Commun 2008;366:1019-24.

[114] Chen L, Fischle W, Verdin E, Greene WC. Duration of nuclear NF-κB action regulated by reversible acetylation. Science 2001;293:1653-7.

[115] Sizemore N, Lerner N, Dombrowski N, Sakurai H, Stark GR. Distinct roles of the IκB kinase α and β subunits in liberating nuclear factor κB (NF-κB) from IκB and in phosphorylating the p65 subunit of NF-κB. J Chem Biol 2002;277:3863-9.

[116] Fitzgerald KA, Palsson-McDermott EM, Bowie AG, Jefferies CA, Mansell AS, Brady G, Brint E, Dunne A, Gray P, Harte MT, McMurray D, Smith DE, Sims JE, Bird TA, O'Neill LA. Mal (MyD88-adapter-like) is required for Toll-like receptor-4 signal transduction. Nature 2001;413:78-83.

[117] Horng T, Barton GM, Medzhitov R. TIRAP: an adapter molecule in the Toll signaling pathway. Nat Immunol 2001;2:835-41.

[118] Kawai T, Takeuchi O, Fujita T, Inoue J, Muhlradt PF, Sato S, Hoshino K, Akira S. Lipopolysaccharide stimulates the MyD88-independent pathway and results in activation of IFN-regulatory factor 3 and the expression of a subset of lipopolysaccharide-inducible genes. J Immunol 2001;167:5887-94.

[119] Choi MS, Lee SH, Cho HS, Kim Y, Yun YP, Jung HY, Jung JK, Lee BC, Pyo HB, Hong JT. Inhibitory effect of obovatol on nitric oxide production and activation of NF-κB/MAP kinases in lipopolysaccharide-treated RAW 264.7cells. Eur J Pharmacol 2007;556:181-9.

[120] Kundu JK, Surh YJ. Breaking the relay in deregulated cellular signal transduction as a rationale for chemoprevention with anti-inflammatory phytochemicals. Mutat Res 2005;591:123-46.

[121] Verri WA, Jr., Cunha TM, Parada CA, Poole S, Cunha FQ, Ferreira SH. Hypernociceptive role of cytokines and chemokines: targets for analgesic drug development? Pharmacol Ther 2006;112:116-38.

[122] de Lima FO, Nonato FR, Couto RD, Barbosa Filho JM, Nunes XP, Ribeiro dos Santos R, Soares MB, Villarreal CF. Mechanisms involved in the anti-nociceptive effects of 7-hydroxycoumarin. J Nat Prod 2011;74:596-602.

[123] Kidd BL, Urban LA. Mechanisms of inflammatory pain. Br J Anaesth 2001;87:3-11.

[124] Julius D, Basbaum AI. Molecular mechanisms of nociception. Nature 2001;413:203-10.

[125] Blom N, Linnemann D. [Alzheimer's dementia and amyloid precursor-protein]. Ugeskr Laeger 1992;154:1010-5.

[126] Sachs D, Villarreal C, Cunha F, Parada C, Ferreira S. The role of PKA and PKCepsilon pathways in prostaglandin E_2-mediated hypernociception. Br J Pharmacol 2009;156:826-34.

[127] Lee KM, Kang BS, Lee HL, Son SJ, Hwang SH, Kim DS, Park JS, Cho HJ. Spinal NF-κB activation induces COX-2 upregulation and contributes to inflammatory pain hypersensitivity. Eur J Neurosci 2004;19:3375-81.

[128] Vanegas H, Schaible HG. Prostaglandins and cyclooxygenases [correction of cycloxygenases] in the spinal cord. Prog Neurobiol 2001;64:327-63.

[129] Ji RR. Mitogen-activated protein kinases as potential targets for pain killers. Curr Opin Investig Drugs 2004;5:71-5.

[130] Galan A, Cervero F, Laird JM. Extracellular signaling-regulated kinase-1 and -2 (ERK1/2) mediate referred hyperalgesia in a murine model of visceral pain. Brain Res Mol Brain Res 2003;116:126-34.

[131] Yang CM, Chien CS, Hsiao LD, Luo SF, Wang CC. Interleukin-1β-induced cyclooxygenase-2 expression is mediated through activation of p42/44 and p38 MAPKS, and NF-κB pathways in canine tracheal smooth muscle cells. Cell Signal 2002;14:899-911.

[132] Ma W, Hatzis C, Eisenach JC. Intrathecal injection of cAMP response element binding protein (CREB) antisense oligonucleotide attenuates tactile allodynia caused by partial sciatic nerve ligation. Brain Res 2003;988:97-104.

[133] Wang H, Dai Y, Fukuoka T, Yamanaka H, Obata K, Tokunaga A, Noguchi K. Enhancement of stimulation-induced ERK activation in the spinal dorsal horn and gracile nucleus neurons in rats with peripheral nerve injury. Eur J Neurosci 2004;19:884-90.

[134] Zimmermann M. Ethical guidelines for investigations of experimental pain in conscious animals. Pain 1983;16:109-10.

[135] Bannon AW, Decker MW, Kim DJ, Campbell JE, Arneric SP. ABT-594, a novel cholinergic channel modulator, is efficacious in nerve ligation and diabetic neuropathy models of neuropathic pain. Brain Res 1998;801:158-63.

[136] Resende MA, Sabino GG, Candido CR, Pereira LS, Francischi JN. Local transcutaneous electrical stimulation (TENS) effects in

experimental inflammatory edema and pain. Eur J Pharmacol 2004;504:217-22.

[137] Quintao NL, Antonialli CS, da Silva GF, Rocha LW, de Souza MM, Malheiros A, Meyre-Silva C, Lucinda-Silva RM, Bresolin TM, Filho VC. Aleurites moluccana and its main active ingredient, the flavonoid 2"-*O*-rhamnosylswertisin, have promising anti-nociceptive effects in experimental models of hypersensitivity in mice. Pharmacol Biochem Behav 2012;102:302-11.

[138] Cho H, Yang YD, Lee J, Lee B, Kim T, Jang Y, Back SK, Na HS, Harfe BD, Wang F, Raouf R, Wood JN, Oh U. The calcium-activated chloride channel anoctamin 1 acts as a heat sensor in nociceptive neurons. Nat Neurosci 2012;15:1015-21.

[139] da Silva KA, Manjavachi MN, Paszcuk AF, Pivatto M, Viegas C, Jr., Bolzani VS, Calixto JB. Plant derived alkaloid (-)-cassine induces anti-inflammatory and anti-hyperalgesics effects in both acute and chronic inflammatory and neuropathic pain models. Neuropharmacology 2012;62:967-77.

[140] Khan S, Choi RJ, Shehzad O, Kim HP, Islam MN, Choi JS, Kim YS. Molecular mechanism of capillarisin-mediated inhibition of MyD88/TIRAP inflammatory signaling in *in vitro* and *in vivo* experimental models. J Ethnopharmacol 2012.

[141] Matsuka Y, Ono T, Iwase H, Mitrirattanakul S, Omoto KS, Cho T, Lam YY, Snyder B, Spigelman I. Altered ATP release and metabolism in dorsal root ganglia of neuropathic rats. Mol Pain 2008;4:66.

[142] Yen YT, Tu PH, Chen CJ, Lin YW, Hsieh ST, Chen CC. Role of acid-sensing ion channel 3 in sub-acute-phase inflammation. Mol Pain 2009;5:1.

[143] Karin M, Ben-Neriah Y. Phosphorylation meets ubiquitination: the control of NF-κB activity. Annu Rev Immunol 2000;18:621-63.

[144] Ji RR, Gereau RWt, Malcangio M, Strichartz GR. MAP kinase and pain. Brain Res Rev 2009;60:135-48.

[145] Song XS, Cao JL, Xu YB, He JH, Zhang LC, Zeng YM. Activation of ERK/CREB pathway in spinal cord contributes to chronic constrictive injury-induced neuropathic pain in rats. Acta Pharmacol Sin 2005;26:789-98.

[146] Harrison S, Geppetti P. Substance p. Int J Biochem Cell Biol 2001;33:555-76.

[147] Calixto JB, Campos MM, Otuki MF, Santos AR. Anti-inflammatory compounds of plant origin. Part II. modulation of pro-inflammatory cytokines, chemokines and adhesion molecules. Planta Med 2004;70:93-103.

[148] Li M, Shi J, Tang JR, Chen D, Ai B, Chen J, Wang LN, Cao FY, Li LL, Lin CY, Guan XM. Effects of complete Freund's adjuvant on immunohistochemical distribution of IL-1β and IL-1RI in neurons and glia cells of dorsal root ganglion. Acta Pharmacol Sin 2005;26:192-8.

[149] Cunha TM, Souza GR, Domingues AC, Carreira EU, Lotufo CM, Funez MI, Verri WA, Jr., Cunha FQ, Ferreira SH. Stimulation of peripheral kappa opioid receptors inhibits inflammatory hyperalgesia via activation of the PI3Kγ/AKT/nNOS/NO signaling pathway. Mol Pain 2012;8:10.

[150] Wang C, Ning LP, Wang YH, Zhang Y, Ding XL, Ge HY, Arendt-Nielsen L, Yue SW. Nuclear factor-κB mediates TRPV4-NO pathway involved in thermal hyperalgesia following chronic

compression of the dorsal root ganglion in rats. Behav Brain Res 2011;221:19-24.

[151] Sun S, Yin Y, Yin X, Cao F, Luo D, Zhang T, Li Y, Ni L. Anti-nociceptive effects of Tanshinone IIA (TIIA) in a rat model of complete Freund's adjuvant (CFA)-induced inflammatory pain. Brain Res Bull 2012;88:581-8.

[152] Ji RR, Suter MR. p38 MAPK, microglial signaling, and neuropathic pain. Mol Pain 2007;3:33.

[153] Zhuang ZY, Gerner P, Woolf CJ, Ji RR. ERK is sequentially activated in neurons, microglia, and astrocytes by spinal nerve ligation and contributes to mechanical allodynia in this neuropathic pain model. Pain 2005;114:149-59.

[154] Zhuang ZY, Kawasaki Y, Tan PH, Wen YR, Huang J, Ji RR. Role of the CX3CR1/p38 MAPK pathway in spinal microglia for the development of neuropathic pain following nerve injury-induced cleavage of fractalkine. Brain Behav Immun 2007;21:642-51.

[155] Ji RR, Kawasaki Y, Zhuang ZY, Wen YR, Zhang YQ. Protein kinases as potential targets for the treatment of pathological pain. Handb Exp Pharmacol 2007:359-89.

[156] Kumar S, Boehm J, Lee JC. p38 MAP kinases: key signalling molecules as therapeutic targets for inflammatory diseases. Nat Rev Drug Discov 2003;2:717-26.

[157] Hamilton SG. ATP and pain. Pain Pract 2002;2:289-94.

[158] DeLeo JA, Tanga FY, Tawfik VL. Neuroimmune activation and neuroinflammation in chronic pain and opioid tolerance/hyperalgesia. Neuroscientist 2004;10:40-52.

[159] Le Bars D, Gozariu M, Cadden SW. Animal models of nociception. Pharmacol Rev 2001;53:597-652.

[160] Milligan ED, Watkins LR. Pathological and protective roles of glia in chronic pain. Nat Rev Neurosci 2009;10:23-36.

[161] Brill S. Managing Surgical Pain in Long-Term Opioid Patients. J Pain Palliat Care Pharmacother 2013.

[162] Wagner K, Inceoglu B, Dong H, Yang J, Hwang SH, Jones P, Morisseau C, Hammock BD. Comparative efficacy of 3 soluble epoxide hydrolase inhibitors in rat neuropathic and inflammatory pain models. Eur J Pharmacol 2013;700:93-101.

[163] Ojewole JA. Analgesic, anti-inflammatory and hypoglycaemic effects of *Securidaca longepedunculata* (Fresen.) [Polygalaceae] root-bark aqueous extract. Inflammopharmacology 2008;16:174-81.

[164] Figueroa S, Lopez E, Arce C, Oset-Gasque MJ, Gonzalez MP. SNAP, a NO donor, induces cellular protection only when cortical neurons are submitted to some aggression process. Brain Res 2005;1034:25-33.

[165] Perez-Rodriguez R, Fuentes MP, Olivan AM, Martinez-Palacian A, Roncero C, Gonzalez MP, Oset-Gasque MJ. Mechanisms of nitric oxide-induced apoptosis in bovine chromaffin cells: Role of mitochondria and apoptotic proteins. J Neurosci Res 2007;85:2224-38.

[166] Yamada M, Momose K, Richelson E. Sodium nitroprusside-induced apoptotic cellular death via production of hydrogen peroxide in murine neuroblastoma N1E-115 cells. J Pharmacol Toxicol Methods 1996;35:11-7.

[167] Sun Y. Free radicals, antioxidant enzymes, and carcinogenesis. Free Radic Biol Med 1990;8:583-99.

[168] Dawson VL, Dawson TM. Nitric oxide neurotoxicity. J Chem Neuroanat 1996;10:179-90.

[169] Culmsee C, Gerling N, Landshamer S, Rickerts B, Duchstein HJ, Umezawa K, Klumpp S, Krieglstein J. Nitric oxide donors induce neurotrophin-like survival signaling and protect neurons against apoptosis. Mol Pharmacol 2005;68:1006-17.

[170] Crossthwaite AJ, Hasan S, Williams RJ. Hydrogen peroxide-mediated phosphorylation of ERK1/2, Akt/PKB and JNK in cortical neurones: dependence on Ca(2+) and PI3-kinase. J Neurochem 2002;80:24-35.

[171] Kim Y, So HS, Youn MJ, Kim ES, Song MS, Chai KY, Woo WH, Cho KH, Moon BS, Park R. Anti-inflammatory effect of So-Pung-Tang, a Korean traditional prescription for cerebral infarction patients. J Ethnopharmacol 2007;114:425-31.

[172] Gao YJ, Ji RR. Chemokines, neuronal-glial interactions, and central processing of neuropathic pain. Pharmacol Ther 2010;126:56-68.

[173] Hwang YP, Jeong HG. Ginsenoside Rb1 protects against 6-hydroxydopamine-induced oxidative stress by increasing heme oxygenase-1 expression through an estrogen receptor-related PI3K/Akt/Nrf2-dependent pathway in human dopaminergic cells. Toxicol Appl Pharmacol 2010;242:18-28.

[174] Gore M, Dukes E, Rowbotham DJ, Tai KS, Leslie D. Clinical characteristics and pain management among patients with painful peripheral neuropathic disorders in general practice settings. Eur J Pain 2007;11:652-64.